UAB
Universitat Autònoma de Barcelona

Gait-Analysis MIoT Platform for Health Assessment

Marc Codina Barberà

Universitat Autònoma de Barcelona

Gait-Analysis MIoT Platform for Health Assessment

Ph.D. Thesis Dissertation
Electronic and Telecommunication Engineering

Author:
Marc Codina Barberà

Directors:
Jordi Carrabina Bordoll
David Castells Rufas

UNIVERSITAT AUTÒNOMA DE BARCELONA (UAB)
Department of Microelectronics and Electronic Systems (MiSE)

2024, Barcelona, Spain

Certificate of Directors

The undersigned Prof. Dr. Jordi Carrabina Bordoll and Dr. David Castells Rufas, from the Department of Microelectronics and Electronic Systems, of the Universitat Autònoma de Barcelona,

CERTIFY

That the dissertation entitled “Gait-Analysis IoT Platform for Health Assessment” has been written by Marc Codina Barberà under our supervision, in partial fulfillment of the requirements for the degree of Doctor of Philosophy.

And hereby to acknowledge the above, sign the present.

Acknowledgments

First and foremost, I want to convey my deepest gratitude to Professor Jordi Carrabina and Dr. David Castells, my directors. The guidance you provided not only imparted scientific principles and methodologies but also cultivated a research and industrial mindset within me, steering me through the challenges of the PhD journey. Your consistent encouragement and patience have infused me with the positive energy required to effectively complete both my projects and my thesis.

I would like to express my heartfelt gratitude to my colleagues at UAB: Manuel Navarrete, Ashkan Rezaee, Juan Borrego, Vinh Ngo, Borja Herranz, Arnau Casadevall and Jordi Gonzalez. Your collaboration has consistently demonstrated professionalism and productivity, significantly enhancing the progress of our shared objectives.

I extend my deepest gratitude to my parents and sister for their constant support and firm assistance in all situations. Your infinite love has remained a consistent source of strength for me.

Abstract

The integration of wearable sensors into healthcare systems has revolutionized the field of gait analysis, offering clinicians valuable insights into patients' mobility and overall health status. This research explores the potential of wearable sensor data for advanced gait and balance analysis in healthcare. The study begins with an analysis of the dynamic landscape of modern healthcare, highlighting the fusion of technology with medical practice and its impact on healthcare delivery and patient outcomes. Central to this transformation are Digital Health, Medical Internet of Things (MIoT), mHealth, eHealth, and medical platforms, which collectively redefine healthcare accessibility, efficiency, and effectiveness. The research presents a developed gait analysis and balance assessment platforms. By leveraging machine learning and artificial intelligence (AI) techniques, the study aims to develop evaluation algorithms capable of analyzing gait and balance data and improving medical diagnostics. Through an economic study, the research aims to demonstrate the efficacy of the proposed platform saving money and improving medical diagnostics.

Resumen

La integración de sensores portátiles en los sistemas sanitarios ha revolucionado el campo del análisis de la marcha, ofreciendo a los médicos valiosos datos sobre la movilidad y el estado de salud general de los pacientes. Esta investigación explora el potencial de los datos de los sensores portátiles para el análisis avanzado de la marcha y el equilibrio en la atención sanitaria. El estudio comienza con un análisis del panorama dinámico de la asistencia sanitaria moderna, destacando la fusión de la tecnología con la práctica médica y su impacto en la prestación de asistencia sanitaria y los resultados de los pacientes. En el centro de esta transformación se encuentran la salud digital, el Internet médico de las cosas (MIoT), la sanidad móvil, la sanidad electrónica y las plataformas médicas, que redefinen colectivamente la accesibilidad, la eficiencia y la eficacia de la asistencia sanitaria. La investigación presenta una plataforma desarrollada para el análisis de la marcha y la evaluación del equilibrio. Al aprovechar las técnicas de aprendizaje automático e inteligencia artificial (IA), el estudio tiene como objetivo desarrollar algoritmos de evaluación capaces de analizar los datos de la marcha y el equilibrio y mejorar los diagnósticos médicos. Mediante un estudio económico, la investigación pretende demostrar la eficacia de la plataforma propuesta para ahorrar dinero y mejorar los diagnósticos médicos.

Contents (Index)

Publication list

- **Codina, M.**, Gonzalez, J., Barroso, A., Caball, J., & Carrabina, J. (2016). Implementing the Complete Chain to Distribute Interactive Multi-stream Multi-view Real-Time Life Video Content. In Applications and Usability of Interactive TV: 4th Iberoamerican Conference, jAUTI 2015, and 6th Congress on Interactive Digital TV, CTVDI 2015, Palma de Mallorca, Spain, October 15-16, 2015. Revised Selected Papers 4 (pp. 17–25).
- Ngo, V., Casadevall, A., **Codina, M.**, Castells-Rufas, D., & Carrabina, J. (2017). A pipeline hog feature extraction for real-time pedestrian detection on FPGA. In 2017 IEEE East-West Design & Test Symposium (EWDTS) (pp. 1–6).
- Ngo, V., Casadevall, A., **Codina, M.**, Castells-Rufas, D., & Carrabina, J. (2018). A high-performance HOG extractor on FPGA. arXiv preprint arXiv:1802.02187.
- Castells-Rufas, D., Bravo-Montero, F., Quezada-Benalcazar, B., **Codina, M.**, & Carrabina, J. (2018). Automatic real-time tilt correction of DMD-based displays for augmented reality applications. In Emerging Digital Micromirror Device Based Systems and Applications X (pp. 97–107).
- Ngo, V., Casadevall, A., **Codina, M.**, Castells-Rufas, D., & Carrabina, J. (2018). A low-cost SVM classifier on FPGA for pedestrian detection. Proceedings of the Jornadas de Computacion Empotrada y Reconfigurable (JCER2018), Teruel, Spain, 10–14.
- Arndt, H., Burkard, S., Talavera, G., Garcia, J., Castells-Rufas, D., **Codina, M.**, Hausdorff, J., Mirelman, A., Harte, R., Casey, M., & others (2017). Real-Time Constant Monitoring of Fall Risk Index by Means of Fully-Wireless Insoles.. In pHealth (pp. 193–197).
- Ngo, V., Castells-Rufas, D., Casadevall, A., **Codina, M.**, & Carrabina, J. (2019). Low-power pedestrian detection system on FPGA. UCAml 2019, 35.
- **Codina, M.**, Castells-Rufas, D., Carrabina, J., Salmon, I., Ayuso, N., Guerendiain, A., & Alvarez, G. (2019). Augmented reality for emergency situations in buildings with the support of indoor localization. Multidisciplinary Digital Publishing Institute Proceedings, 31(1), 76.
- **Codina, M.**, Navarrete, M., Rezaee, A., Castells-Rufas, D., Torrelles, M., Bukard, S., Arndt, H., Drevet, S., Boudissa, M., Tonetti, J., & others (2021). Gait analysis platform for measuring surgery recovery. In Proceedings of the PHealth 2021—18th International Conference on Wearable Micro and Nano Technologies for Personalized Health (pp. 199).
- **Codina, M.**, Navarrete, M., Castells-Rufas, D., & Carrabina, J. (2022). Balance Evaluation by Inertial Measurement Unit. In International Conference on Ubiquitous Computing and Ambient Intelligence (pp. 71–76).
- **Codina, M.**, Gomez, C., Navarrete, M., Castells-Rufas, D., & Carrabina, J. (2022). Analysis and Deployment of a LoRaWAN Network at a University Campus. In

International Conference on Ubiquitous Computing and Ambient Intelligence (pp. 493–504).

- Navarrete, M., **Codina, M.**, Rezaee, A., Castells-Rufas, D., Castillejo, A., & Carrabina, J. (2022). Development of a MIot Gait Tracking Platform. In International Conference on Ubiquitous Computing and Ambient Intelligence (pp. 431–436).
- Castells-Rufas, D., Ngo, V., Borrego-Carazo, J., **Codina, M.**, Sanchez, C., Gil, D., & Carrabina, J. (2022). A Survey of FPGA-Based Vision Systems for Autonomous Cars. IEEE Access, 10, 132525–132563.
- **Codina, M.**, Torrelles, M.J., Castells-Rufas, D., Carrabina, J., (2024) Technoeconomic Analysis for the deployment of gait-oriented wearable Medical Internet-of-Things in Catalonia. Information (submitted)

List of figures

List of tables

List of acronyms

9-DoF	9 Degree of Freedom
ADC	Analog Digital Converter
AI	Artificial Intelligence
API	Application Programming Interface
BAN	Body Area Network
BLE	Bluetooth Low Energy
DAC	Digital Analog Converter
DMP	Digital Motion Processor
DPS	Degrees Per Second
EHR	Electronic Health Records
FSR	Force-Sensitive Resistor
FUOTA	Firmware Update Over-the-air
FUS	Firmware Update Service
GAP	Generic Access Protocol
GATT	Generic Attribute Profile
GPIO	General-Purpose Input/Output
I2C	Inter-Integrated Circuit
IDE	Integrated Development Environments
IMU	Inertial Measurement Unit
IoT	Internet of Things
LAN	Local Area Network
LoRa	Long Range
LPWAN	Low Power Wide Area Network
MCU	Micro Controller Unit
MEMS	Microelectromechanical Systems
MIoT	Medical Internet of Things
NFC	Near Field Communication
OTA	Over-the-Air
PAN	Personal Area Network
PCB	Printed Circuit Board
POMA	Performance-Oriented Mobility Assessment
REC	Romberg Eyes Closed
REO	Romberg Eyes Open
RFC	Romberg Foam eyes Closed
RFID	Radio Frequency Identification
RFO	Romberg Foam eyes Open
SoC	System-on-Chip
SPI	Serial Peripheral Interface
SPPB	Short Physical Performance Battery

SPS	Samples per Second
UART	Universal Asynchronous Receiver Transmitter
UCD	User-Centered Design
WAN	Wide Area Network
WHO	World Health Organization
WPAN	Wireless Personal Area Network

1. Introduction

1.1. The Addressed Problem

In the dynamic landscape of modern healthcare, the fusion of technology with medical practice has initiated a profound evolution in healthcare delivery, patient engagement, and overall health outcomes. Central to this transformation are the scopes of Digital Health, Medical Internet of Things (MIoT), mHealth, eHealth, and medical platforms, which collectively redefine the boundaries of healthcare accessibility, efficiency, and effectiveness.

Digital health, a term coined to describe non-face-to-face care strategies, represents a departure from traditional healthcare paradigms, encompassing eHealth, mHealth, telehealth, telemedicine, and telecare. Amidst the COVID-19 pandemic, digital health experienced unprecedented growth, breaking down cultural barriers and fostering connectivity between patients and medical professionals. This expansion transcends the mere digitization of health data and processes, extending to the integration of digital consumers and leveraging advanced technologies like MIoT, big data analytics, and artificial intelligence (AI) to empower patients and enhance healthcare systems.

The Internet of Things (IoT) revolution, fueled by advancements in microelectronics, has catalyzed the proliferation of connected devices across various domains, including healthcare. Wearables, home automation systems, and industrial sensors, among others, now seamlessly interface with cloud platforms, enabling the application of advanced computing techniques such as big data analytics and AI to collected health data. In the healthcare realm, IoT devices, particularly wearables, have emerged as vital tools for monitoring health parameters and facilitating remote patient care.

Moreover, the integration of telehealth, telemedicine, and telecare solutions has emerged as a cornerstone of non-face-to-face healthcare interactions, especially in the wake of the COVID-19 pandemic. These solutions, predominantly facilitated through personal computer-based platforms, enable clinicians and patients to engage in remote consultations, diagnostics, and monitoring, transcending geographical barriers and enhancing access to care.

Today's healthcare systems rely heavily on eHealth, which allows for the digital sharing of health information and services. eHealth tools, including electronic health records and telemedicine, make healthcare more efficient by automating tasks, using data to guide decisions, and putting patients in charge of their own care. mHealth apps expand eHealth's reach, allowing patients to actively engage in their healthcare and share information about specific areas.

The convergence of these technologies under the umbrella of digital health signifies a paradigm shift towards proactive, personalized healthcare delivery. By harnessing the potential of wearable devices, advanced sensors, and data analytics, healthcare stakeholders can gain invaluable insights into patient health trends, predict potential health risks, and intervene proactively to improve health outcomes.

Furthermore, digital health technologies hold promises beyond traditional clinical domains. The integration of MIoT devices enables continuous monitoring of vital health parameters, aiding in the prevention of falls among the elderly and enhancing post-surgical rehabilitation efforts. These innovations underscore the transformative potential of digital health in revolutionizing healthcare delivery and promoting holistic wellness.

With all that has been mentioned so far, we can state that, wearable sensors have become integral tools for monitoring gait patterns and movement dynamics. However, existing gait analysis platforms often lack the sophistication needed to fully utilize the wealth of data generated by these sensors.

The integration of wearable sensors offers immense potential for clinicians to gain insights into patients' mobility and overall health status, particularly among the elderly and those undergoing rehabilitation. These sensors capture various gait-related metrics, including stride length, cadence, and balance, which can provide valuable information for medical diagnostics and treatment planning.

Despite the abundance of wearable sensor data, current gait analysis platforms face challenges in effectively processing and interpreting this information. Many platforms struggle to integrate data from diverse sensor sources, leading to inconsistencies and inaccuracies in gait analysis results. Additionally, the analytical capabilities of existing platforms may be limited, hindering clinicians' ability to derive meaningful insights from the data.

To address these challenges, there is a growing need for advanced gait analysis platforms that can effectively harness wearable sensor data to improve medical diagnostics. These platforms should leverage cutting-edge technologies such as machine learning and artificial intelligence to analyze gait data accurately and efficiently. By identifying patterns and trends in the data, clinicians can gain deeper insights into patients' mobility patterns and overall health status.

Furthermore, improved gait analysis platforms should prioritize user-friendliness and seamless integration into clinical workflows. Clinicians should be able to easily access and interpret gait analysis results, enabling them to make informed decisions about patient care and treatment strategies.

1.2. Objective

The motivation behind this research is to propose new digital tools and/or offer possible improvements in the way clinical treatments are conducted in order to make better diagnoses.

The objective of this thesis is to propose, develop and validate a new MIoT framework to provide a new generation of tools to improve the way healthcare is currently managed to obtain better findings and quality of life for patients and clinicians.

To achieve this, various MIoT systems were created that include wireless sensor subsystems to monitor different aspects of patients' lives. These sensor devices centered in using miniaturized Inertial Measurement Units (IMUs) implemented on Microelectromechanical Systems (MEMS) technologies that connect via Bluetooth Low Energy (BLE) technology to a smartphone, where an application captures all data (and is also used as user interface) and send it to a cloud platform for computation and exploitation. The added value of the MIoT solution resides in providing clinically relevant parameters computed from the raw data captured. These parameters will be used by clinicians to improve their assessment. Ideally, that application-specific cloud platform should be connected to the general healthcare system platform to complement and integrate this finding with the patient's clinical and social data in a bidirectional way, thus allowing personalized medicine. At the end, the future success of this platform will depend on the change for the medical assistance from a presential clinical-centered model to a remote patient-centered one, taking also into account the socio-economic savings in providing (public) health services.

Throughout this thesis several aspects will be analyzed such as: (i) the technological complexity in building MIoT solutions; (ii) the clinical validation of those solutions (when possible) and (iii) the potential economic impact of the proposed MIoT platform in the public health system.

1.3. Structure of the dissertation

The subsequent chapters delineate the concerns and challenges expounded in this introduction:

- **Chapter 2 State of the art for eHealth & IoT i**ntroduce how the ecosystem of platforms focused on health is currently structured and the various solutions proposed in scientific literature.
- **Chapter 3 Medical IoT Platform for Gait Analysis** an introduction is made to the implementation currently used in the clinical environment, and the developed platform for gait analysis is introduced.

- **Chapter 4 Medical IoT Platform for Equilibrium Analysis** explains the expansion of the platform, adding a new parameter to analyze such as balance, showing results from a clinical study.
- **Chapter 5 Technoeconomic impact of MIoT platforms** analyzes the economic impact that the implementation of the platform can have on a public healthcare system.
- **Chapter 6 Discussion and Conclusions** summarizes the results and exposes global conclusions. Also, limitations and possible future research are discussed.

2. State of the art for eHealth & IoT

This chapter is dedicated to exploring the state of the art of IoT as technological framework and healthcare as application domain. The convergence of healthcare and IoT holds immense promise for enhancing patient care, optimizing healthcare delivery, and facilitating preventive medicine. From wearable devices monitoring vital signs to interconnected healthcare systems optimizing resource utilization, I will provide a panoramic view of the current state of healthcare IoT, offering insights into the transformative potential of these technologies for the future of healthcare.

2.1. IoT

IoT stands for the Internet of Things. It refers to the network of physical objects (or "things") embedded with sensors, software, and other technologies that enable them to connect and exchange data with other devices and systems over the internet. These objects can range from simple household items like refrigerators and thermostats to more complex industrial machinery and vehicles.

The primary goal of IoT is to enable these objects to collect and exchange data autonomously, leading to improved efficiency, accuracy, and functionality in various domains such as healthcare, agriculture, transportation, manufacturing, and smart homes.

IoT devices typically consist of sensors to gather data (Device) with a simple energy-efficient processing plus communication to a closer and more powerful but still resource-constrained component (Edge), that send it (with or without processing) to the cloud where there are “unlimited resources” of storage and computation, that allow exploiting data through Application Programming Interface (APIs) or user-interfaces. Thes components are linked through a diversity of connectivity options (such as Near Field Communication (NFC), Low Power Wide Area Network (LPWAN), Wi-Fi, Bluetooth, cellular networks, or wired connections) with different characteristics adapted to every application domain.

Author in [1] highlights IoT's potential in healthcare, focusing on medical IoT sensors, data visualization platforms, and artificial Intelligence (AI) applications, backed by a systematic review of 23 selected studies analyzing sensor circuits, Inten-sive Care Unit scenarios, device applications, and data management challenges.

2.1.1. Microelectronics paradigm

During the last two decades we have been how microelectronics have been progressively aligned with the IoT paradigm by specializing both technological processes and microelectronic chips, according to the paradigm announced by Hugo de Man in 2005 [2] that classifies the microelectronics solutions according to energy and energy efficiency, such

that sensor devices required very low energy and computation (few MIPS/MOPS), that connect to application-dependent edge devices (smartphones, smart TVs, home/industry gateways, automotive ECUs, etc.) that have still huge requirements on cost an energy but can deal with much complex computations (GOPS) and communications to finally connect to the cloud with not only “unlimited” computation (TOPS) and communication but also energy. Examples of this specialization in technology are the evolution to FinFET [3] (high performance), FDSOI (low-power) and MEMS[4] (sensor, microsystems) or in design, the lead of Intel/AMD in cloud computing chips, of ARM at edge level while the device level is still open to many competitors.

2.1.2. Devices

There is a wide variety of sensors that provide different functionalities. Specifically for the health domain, we have the capacity to monitor from a specific parameter of the body, like capture the hearth rate [5] of a patient, getting the values from gait using sensorized insoles [6], [7]; a graphite tooth sensor to diagnose infection, fracture or coughing [8] or electrodes attached to eyelids to control glucose and eye-movement to diagnose diseases associated with diabetes [9]. Moreover, to help emergency personal to find people inside a building, there are studies to provide indoor localization [10], [11].

These devices usually are personal devices and connect to edge devices (typically smartphones) through wireless personal area networks (WPAN), with low complexity, low-range and low-power consumption such as Bluetooth (specially the low power version of BLE, ANT+, Zigbee, etc. Each of these technologies offers wireless communication functionalities and profiles. Although they are different technologies, they are quite similar, mainly differing in aspects such as bandwidth, number of simultaneous devices, or energy consumption. In [12] a low complex rule engine is proposed over ZigBee. Another approach is presented in [13], this solution use BLE to transfer data from the device to the smartphone. BLE is the most popular wireless protocol in the healthcare domain while other domains that require larger ranges with lower bandwidth preferred LPWAN such as LoRaWAN, Sigfox, NB-IoT, etc.

2.1.3. Edge: Smartphone APPs & UI

The fact that smartphone devices sales overcome those of PCs/laptops is an indication of its popularity and fast and wide adoption by any kind of users.

There is a growing demand for promoting healthy behaviors in everyday consumers' routines. This led to an explosion of applications, especially for smartphones as main portable device, that are resilient, user-friendly, accessible and proficiently promote these healthy behaviors.

The connectivity from smartphones to the cloud is currently a commodity driven by the explosion of the cellular connectivity (3G, 4G, 5G and beyond) but also Wi-Fi (IEEE 802.11).

This review [14] synthesizes aspects of mobile application development, addressing issues such as poor UI/UX and user disengagement by considering factors like context, user behavior, emotions, and feedback, offering valuable insights for developers to enhance usability and user satisfaction.

For health platforms, different approaches can be found in the literature. In [15] the proposed method is to implement the ISR framework, employing various design processes aimed to comprehend the end-user's environment by identifying requirements through a sequence of focus group sessions involving stakeholders. Artifacts were generated and assessed, while the evaluation of theories and artifacts enhanced the knowledge base in design science and application domains. Alternative methods suggest developing health apps through qualitative techniques conducted over four sessions involving information technology professionals, health experts, and patients [16]. Others propose that integrating a User-Centered Design (UCD) process in the development of mHealth tools is essential for fostering user engagement, thereby ensuring the effectiveness of the app in promoting sustained behavioral change among its users [17].

2.1.4. Cloud: Back-end & Front-end

After introducing the sensor devices, the edge with its challenges in improving the user experience, and how data is extracted from the sensor to reach the internet, the last piece of the system, is the cloud. This piece of the IoT system is composed of multiple applications and components that allow tasks such as communication between systems, data reception identification and alignment, information storage, analysis, visualization and exploitation.

In [18], authors introduce the layer concept for IoT platform, sensors, network, and services. This proposed vision unifies the device and edge part in the sensor layer and the edge communication part and the cloud systems in the network layer, creating a new layer, service, where the front-end would be located. Additionally, authors in [19] present an architecture where the device and the edge become the patient front-end, and the cloud becomes the back end where data management and storage services are implemented and at the same time serves as the point of entry of data by clinicians. This paper [20], provides a qualitatively and quantitatively vision of how to implement front-end for IoT based on the challenges that bandwidth, delay applications and device heterogeneity produce.

2.2. From Health to Digital Health

Health is defined by the World Health Organization (WHO) as “a state of complete physical, mental, and social well-being and not merely the absence of disease or infirmity” [21]. Also, the word can be defined as the work of providing medical services. If we combine the two definitions, we can say that it is a balance of physical, mental, and social factors, along with proactive efforts to prevent disease and promote overall well-being.

The evolution from traditional health to eHealth represents a significant transformation in healthcare delivery, leveraging digital technologies to enhance efficiency, accessibility, and quality of care. This evolution has been driven by advancements in information technology, changing patient needs, and the increasing demand for improved healthcare services globally [22]. In [23] explores the ethical complexities of digital health innovations, encompassing AI, mobile apps, telemedicine, wearables, and IoT, emphasizing the need for robust bioethics frameworks to address confidentiality, biases, access, digital literacy, equity, privacy, and quality standards, highlighting the imperative for ongoing adaptation and readiness within health science faculties.

As the population grows and technology advances, new concepts linked to the term 'Health' have emerged. One of these concepts is Telehealth, that refers to the provision of healthcare services by healthcare professionals using information and communication technologies to overcome geographical barriers. It involves the exchange of accurate information for purposes such as diagnosis, treatment, and prevention of diseases and injuries, as well as for research, evaluation, and the ongoing education of healthcare providers, all aimed at improving the health of individuals and communities. The authors in [24] present some topics to be addressed at the training of clinical staff in telehealth. Furthermore, in [25] an introduction to key aspects of telehealth is introduced.

2.2.1. Electronic Health Records (EHR)

Since the late 70s with the implementation of the first electronic medical storage system, the digitization of healthcare systems has been on the rise, eventually leading to the elimination of paper for any health-related process. This leads to a necessity to standardize all information exchanges among the various services that make up a healthcare system. As presented in [26], two models for interconnecting the different elements of EHR systems emerge: the implementation of open standards that are easily accessible and implementable for all parties involved, or the closed standardization system, where each healthcare system is independent, and the tools developed can only be used for a single system. Authors in [27] proposes a comprehensive framework to standardize global security and privacy standards analyzing five EHR standards and pinpointing twenty essential concepts via expert evaluations.

There are proposals to implement framework to integrate medical platforms and EHR, in [28] the authors explain its Cloud-IoT solution to integrate all the health actors to share and collaborate with their data and services in a single platform. Other authors propose to create applications platform around existing EHR systems [29].

Health data is considered highly sensitive by all stakeholders despite the different health data ownership models around the world. This main fact led to a plethora of digital health platforms owned by different health organizations to manage electronic health records, usually using a whole set of standards for all data management aspects (coding, procedures, maintenance, interoperability, etc.). Furthermore, IT companies, from big players such as (e.g. google, apple, etc.) to new unicorn companies also entered such market. As in other domains that move to higher digitalization (industry, home automation, automotive, etc.), that lead to a complex ecosystem composed of many digital platforms that ideally should interact among them to provide a better service, especially with a global worldwide health view.

From the point of view of the patients is to have unified access to its own data. The way used to try solving that problem has been the use of standards (health data and procedures, pharmacy, data bases, security, privacy, etc.). Unfortunately, the large number of different standards (and its evolution) are not homogeneously adopted. This leads to a lack on interoperability among providers, organizations, borders, etc.

Few initiatives cope with that problem, such as the proposal of the International Patient Summary [30], a minimal (non-exhaustive) set of clinical data of a patient usable by all clinicians for the unscheduled country independent.

2.2.2. eHealth

Healthcare's integration with technology faces delayed adoption due to infrastructure, capacity, and political constraints, with modifications promising enhanced service efficiency and cost-effectiveness post-implementation. Despite being tested globally during the COVID-19 pandemic, eHealth systems remain in their infancy, encountering various challenges, yet technologies like cloud computing and IoT enable secure and scalable service delivery. Cloud computing and IoT are pivotal in this eHealth paradigm, as discussed in this review [31].

Key components and features of an eHealth platform usually include:

- Electronic Health Records (EHR): Centralized systems for storing and managing patients' health records digitally, allowing for easy access by authorized healthcare professionals.

- Health Information Exchange (HIE): Platforms that facilitate the secure exchange of health information among different healthcare entities, promoting interoperability and continuity of care.
- Secure Communication: Encrypted communication channels for secure and confidential exchange of information among healthcare professionals and between healthcare providers and patients.
- Patient Portals: Online platforms that empower (though web access) patients to access their health records, schedule appointments, view test results, communicate with healthcare providers, and actively participate in their own care.
- Telemedicine Services: Integration of telehealth and telemedicine capabilities, enabling remote consultations, diagnostics, and monitoring of patients.
- Remote Patient Monitoring: Systems that enable the monitoring of patients' health parameters and vital signs remotely, often using wearable devices and sensors.
- Health Analytics: Data analytics tools that process large volumes of health data to derive meaningful insights, support clinical decision-making, and identify trends or patterns.
- Decision Support Systems: Incorporation of systems that provide evidence-based information and guidance to healthcare professionals during the diagnosis and treatment planning processes, including those provided by AI algorithms.

2.2.3. mHealth

With the emergence of smartphones, new technological possibilities have opened, leading to the appearance of new tools, and making access to information even easier. This is why telemedicine has taken another step forward in the evolution towards the concept of mHealth. The Global Observatory for eHealth, a division of the WHO, provided a definition for mHealth, stating that it encompasses medical and public health practices aided by mobile devices. These devices include mobile phones, patient monitoring devices, personal digital assistants, and various other wireless devices [32].

Key features and components of mHealth platforms include:

- Mobile Applications: Development and deployment of health-related applications (apps) that run on mobile devices. These apps can cover a wide range of functions, including health monitoring, medication reminders, fitness tracking, and telemedicine services.
- Remote Monitoring Devices: Integration with wearable devices and sensors that collect real-time health data, such as heart rate, activity levels, and vital signs. This data can be transmitted to the mobile platform for analysis and interpretation.
- Health Information and Education: Provision of accessible and user-friendly health information, educational content, and resources through mobile apps, promoting health literacy and awareness.

- Medication Management: Tools to help users manage their medications, including medication reminders, dosage tracking, and prescription refill notifications.
- Fitness and Wellness Tracking: Integration with sensors and apps to monitor physical activity, sleep patterns, nutrition, and other wellness-related metrics.
- Gamification Elements: Incorporation of gamified elements within health apps to motivate and engage users in adopting healthy behaviors and lifestyle changes.

eHealth platforms and mHealth platforms play a significant role in extending healthcare services beyond traditional healthcare settings, reaching individuals in diverse locations and demographics. These platforms contribute to patient empowerment, improve healthcare access, and support preventive and proactive approaches to health management.

The categories of mHealth apps that are most pertinent for integration into clinical practice encompass [33]:

- Facilitate clinical diagnosis and/or decision-making processes.
- Enhance clinical outcomes by modifying patient behavior and promoting adherence and compliance with established treatment protocols.
- Serve as independent digital therapeutic interventions.
- Deliver educational content related to diseases.

Finally, the concept of eHealth can be defined as a concept that encompass everything mentioned above. The review conducted in the [34] study shows that the majority define eHealth as a set of diverse concepts but always focused on technology and health, and to a lesser extent on stakeholders and e-commerce. Other authors add e-training as one of the bases of eHealth [35]. One example of implementation is the deployment of an eHealth model in Catalonia during the Covid-19 outbreak [36].

2.2.4. Wearable health & wellbeing solutions

In the literature, there are many proposals of MIoT platforms or solutions that implements a unique use-case scenario with its device-edge-cloud that solve a problem. For example, the proposal in [37] introduces a platform composed of several passive Radio Frequency Identification (RFID) sensors and antennas. These sensors, placed on the body of the monitored patient, assess their behavior while sleeping and trigger an alarm in case of detecting any anomalies. Other solutions are focused on rural areas, distant from major cities, offering telemedicine systems to aid in diagnosing and treating people's ailments [38].

Moreover, during Covid-19 pandemic, there where new proposal to monitor and help people with its health. One of this proposal is a monitoring system to control and monitor people in isolation during the quarantine [39]. The system integrates a custom watch device that

captures temperature, hearth rate and oxygen saturation (SpO2) and a minicomputer to control localization of the patient and process all the data generated to send it to the cloud.

2.2.5. Digital Health and Medical IoT platforms

A MIoT platform is a technology infrastructure specifically designed for the healthcare industry that leverages stakeholders access together with user interaction, IoT devices and sensors to collect, store, analyze and exchange medical data. These platforms are part of the broader concept of digital health, integrating connected devices to enhance healthcare services and outcomes.

One of the challenges of Medical IoT is to compute and store the amount of data generate by the patient's sensors. To address this issue, there are proposal like this [40], to use the blockchain to secure a contract and payment between the health system and the patient to use commercial cloud platforms for storage and computation of the patient's data. Other researchers propose different solutions to provide security to the data stored in Cloud Service Providers (CSP) [41]. Key features of a medical IoT platform may include:

- Device Connectivity: Integration with various medical devices such as wearables, smart monitors, and sensors that gather real-time health data.
- Data Aggregation and Storage: The ability to collect and store health-related data generated by IoT devices securely.
- Interoperability: Support for data exchange and communication between different devices and systems, ensuring seamless integration into existing healthcare ecosystems.
- Data Analytics: Utilization of analytics tools to process and derive meaningful insights from the collected data, aiding in diagnosis, treatment, and preventive care.
- Continuous Remote Monitoring: Facilitation of remote patient monitoring, allowing healthcare providers to track patients' health status without requiring them to be physically present.
- Security and Compliance: Implementation of robust security measures to protect sensitive health data, and adherence to healthcare regulations and standards.
- Integration and exchange of EHR: Compatibility with existing EHR systems to ensure continuity of patient information and healthcare records.
- Alerts and Notifications: Generation of alerts or notifications for healthcare providers in case of abnormal or critical health indicators.

Medical IoT platforms contribute to the advancement of personalized medicine, improved patient outcomes, and more efficient healthcare delivery by harnessing the capabilities of interconnected devices and data analytics within the healthcare ecosystem.

Considering the European case in which public health authorities are the main health providers that integrate health data from other stakeholders, we bet on the digital ecosystem

platform interaction proposed in [42] and depicted Figure 1. Following this model, adding partner platforms is proposed as the main way to close the interaction loop between users connected to that platform with their wearable devices and clinicians connected also to the global public health platform to be able to analyze the complete patients' data.

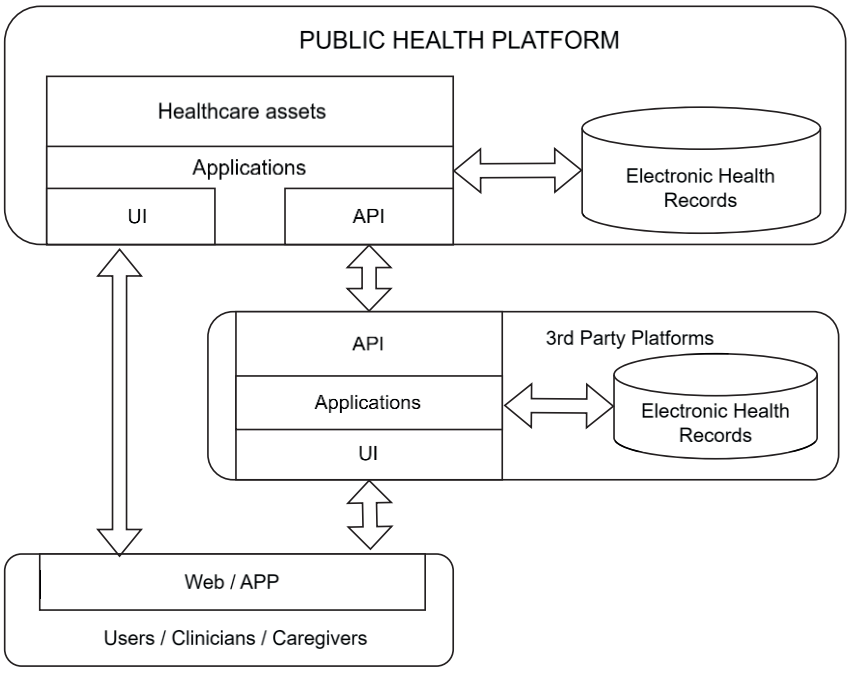

Figure 1: Platform integration model for complex ecosystems allowing new partners to add clinically relevant data to the global public heath platform.

2.3. Summary of the chapter

In this chapter, we've explored into the elementary concepts of IoT paradigm and its applications to the healthcare domain, that has been transformed from a traditional clinician-patient model to a complex digital health one after going through different phases (telehealth, eHealth, mHealth), up to the Medical Internet of Things (MIoT). From wearable devices to interconnected medical systems, MIoT has revolutionized how we monitor and manage health-related data. This technology enables the continuous transmission and exchange of essential information, allowing healthcare professionals to remotely monitor patients' conditions and intervene when necessary. With MIoT, the healthcare landscape has evolved from traditional face-to-face interactions to a connected and proactive approach that is being said patient centered.

Furthermore, our exploration has highlighted the paradigm shift in healthcare delivery, moving away from conventional in-person consultations towards innovative methods of remote assistance and system integration. This transition has been facilitated by advancements in telecommunications and data analytics at the cloud, empowering both

patients and healthcare providers with real-time insights and interventions. As we navigate through various medical platforms, we gain insights into the diverse applications of MIoT in healthcare, ranging from remote patient monitoring to personalized treatment plans. Through these platforms, we witness firsthand how technology is reshaping the healthcare industry, driving efficiency, accessibility, and ultimately, improving patient outcomes.

3. MIoT Platform for Gait Analysis

This chapter introduces the development of a medical IoT platform aimed at providing a new technological framework for clinical challenges that can take profit from the capture and analysis of the parameters of gait during daily live activities or specific prepared exercises. The first section covers the two main applications targeted in this thesis related to gait aspects: Fall prevention and surgery recovery; and presents the relevant parameters of gait that can be computed from raw data coming from the sensors included in our device. Next, I introduce the medical tests focused on evaluating the patient's condition on theses aspects. Finally, I detail the platform components implemented in the framework of this research together with the results obtained.

3.1. Impact of falls

Roughly 30% of individuals aged 65 and above experience falls annually, leading to severe injuries, reduced mobility, and a decline in independence [43], [44]. Falls represent a notable public health concern worldwide, with approximately 684,000 fatal incidents occurring annually. They stand as the second most prevalent cause of unintentional trauma-related deaths globally, ranking just below traffic accidents. The highest mortality rates associated with falls are observed among individuals aged 60 and over across all geographical regions.

In the United States, expenditures attributed to falls reached $28.9 billion for Medicare, $8.7 billion for Medicaid, and $12.0 billion from other payment sources. In 2015, total healthcare spending associated with falls exceeded $49.5 billion [45]. The average cost of falls varied depending on the denominator utilized, ranging from US $3,476 per faller to US $10,749 per injurious fall, and US $26,483 per fall necessitating hospitalization [46]. A 2000 study in the USA identified 10,300 fatal and 2.6 million non-fatal fall-related injuries that year. Direct medical costs for these injuries were estimated at $200 million for fatal falls and $19 billion for non-fatal ones [47]. Moreover, research indicated that 12% of older adults who experienced falls subsequently required long-term nursing home care [48].

A study in China estimated 2,990 falls among individuals aged over 60, primarily due to slipping or tripping outdoors while engaged in activities like walking or relaxing, often because of previous falls. About 70% of cases reported injuries. The annual fall rate among the over-60 population was 8.7%, lower than the 13.89% seen in other ethnic groups. The study's fall rate matches the 7.9-16.2% range reported in European countries over six months [49]. Other studies in China found fall-related injuries ranging from 0.6% to 19.5%, with significant risk factors including older age, female gender, use of walking aids, living environment, chronic illnesses, medication usage, visual impairment, and falls in non-forward directions. Fall-related injury costs per person ranged from US$16 to US$3,812, underscoring the significant public health concern among older Chinese individuals [50].

Annually, within the European Union, 58% of emergency department visits among the elderly are attributed to falls. For every fall-related fatality, there are 40 hospitalizations and 65 emergency room consultations, amounting to 36,000 deaths, nearly 1.5 million hospital admissions, and 2.3 million emergency room visits annually. The associated costs are estimated at 25 billion euros per year. With the aging population projected to increase by 60% by 2050, it is anticipated that fall-related deaths will reach 60,000 annually. This demographic shift will also result in a rise in emergency room visits and hospital admissions. Most fall-related injuries occur within the home environment, primarily in the living room or bedroom (56%), followed by the bathroom/toilet (15%), and lastly on stairs (14%). The remaining incidents take place in other or unspecified areas of the home (16%) [51]. In the Netherlands, a comprehensive investigation determined that the average expenses for medical and social care associated with fall-related injuries amount to 9,370 EUR per incident. Costs range from 3,880 euros per case in the 65 to 70-year-old age bracket, rising with age to 14,600 euros per incident in the 85+ age group [51], [52].

3.1.1. Fall Detection and prevention systems

As we have seen previously, falls are one of the main causes of hospital visits. That is why research is being conducted to detect falls in order to provide faster medical assistance. At the same time, efforts are being made to reduce these falls by developing prevention systems.

The author in [53] presents a non-invasive fall detection system using the Kinect device. They track the skeletal structure of the person to be monitored, and the resulting capture is sent to a machine learning algorithm. Other authors [54] present a multi camera system using Kinect to monitor different rooms and present a three-state transition between standing, sitting, and falling. In [55], authors present a study to detect ADL and falls using surface EMG attached to the legs of the volunteer. Although different sensors are used to detect falls, the accelerometer has been presented as the most popular sensor for its ease of integration, low cost, and good results for several years now [56], [57], [58].

Detecting falls offers the possibility of providing prompt assistance, but the real objective to reduce the percentage of falls and, at the same time, decrease the associated cost is to be able to accurately predict falls and offer a solution before they occur. Authors in [59] present a system to analyze the minimum toe clearance to prevent falls. This system has multiple Time of flight sensors installed on the shoes and all the data is send to a central unit placed at the back of the patient. In [60] authors present a similar system attaching a frequency-modulated continuous-wave radar in front of the patient's shoe to detect the distance information between the radar and surrounding objects. An alternative method for fall prevention involves the use of cameras, in [61] a study presents a system that analyze the body joints using a Kinect camera. Using this data, they create a virtual area where the feet should be during walking. If a foot is outside this area, they estimate that there is a possibility of a fall.

Gait analysis is one of the most common ways to detect potential problems that may lead to a fall. There are various solutions available, such as pressure-sensitive mats for gait assessment [62], sensor insoles with external electronics ([63], [64], [65]), or devices that analyze movement by being placed on the outside of the shoe [66]. Various systems exist for monitoring fall risk [67], [68], although none have achieved widespread deployment.

3.1.2. The WIISEL project

In 2012, a European project was initiated involving various universities, research centers, and companies to develop a platform aimed at preventing falls among the elderly. This project, called Wireless Insole for Independent and Safe Elderly Living (WIISEL) [69], [70], developed an initial version of fully wireless smart insoles that integrated pressure sensors and inertial measurement units (Figure 2). All generated data were transmitted via Bluetooth to a smartphone. This device featured an information display screen indicating the patient's fall risk status, and the data were sent to a cloud server for analysis. During the project 180 insoles were manufactured (in different phases), 22 Smartphones were used (Nexus 4) together with 35 inductive chargers with an estimate cost for the WIISEL pair of insoles of 800€. They were tested by 15 subjects during pilot studies and 39 subjects during validation. Usability/ergonomics was evaluated by 16 experts and data was calleted for 657 hours.

Figure 2: Images of the components and structure of the WIISEL insoles and APP.

In addition to creating the platform consisting of the insoles, the mobile application, and the analysis server, the cultural component in the user experience was studied by creating a mobile application using programmers from one country and then distributing the application among different European countries [71]. All devices, apps and web went through a user-centered design approach in which several stakeholders evaluated the prototypes for improvement before its deployment ([72], [73], [74]). Finally, the solution was validated by conducting various clinical tests in different countries, in the lab and at home, where patients over 65 years old tested the insoles and the application for 1 month [75] This platform had several hardware and cost problems, Figure 3 shows the detected problems with this first version. These insoles incorporated 14 capacitive sensors distributed over the entire surface of the foot. This type of sensors has a high cost making the price of the device totally dependent on the incorporation of so many sensors. At the end, the analysis related to the relevance of the parameters captures from those sensors, revealed that most of them were producing redundant gait information even the fact that they were designed by biomechanical engineers. Another problem was the size of the electronics. In order to be able to fit the whole system, 2 rigid Printed Circuit Board (PCB) were created with a semi-rigid connection between them to facilitate the positioning of all the elements. The location of the QI antenna in the heel area, together with the battery, caused failures as it was in a high impact position. The Bluetooth antenna used a simple wire model what lead to device disconnections to the smartphone. Furthermore, the mechanical finishing led to a solution that was neither comfortable nor rigid enough, what also led to many failures [76]. Therefore, since the concept was interesting enough, we planned to build a new version of the system to overcome those problems.

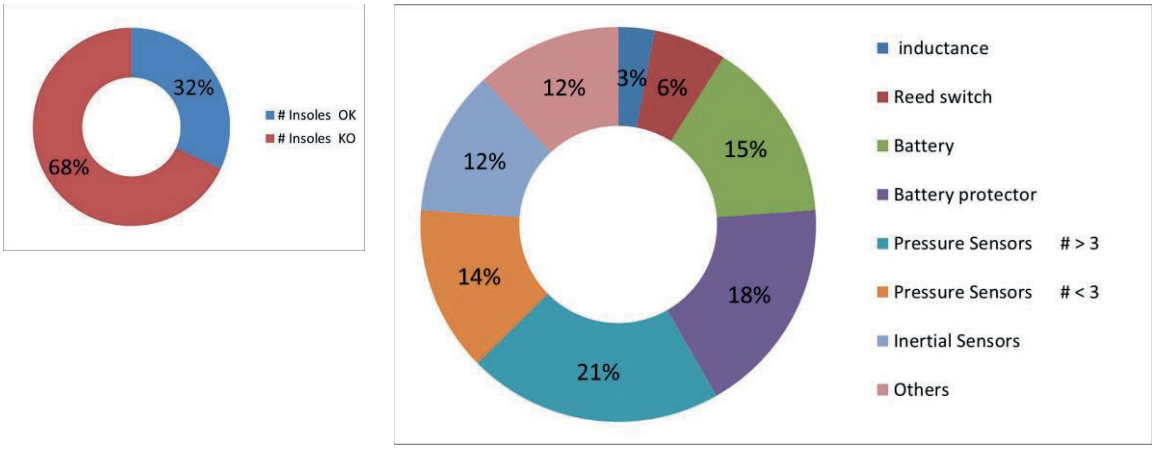

Figure 3: Failure statistics of the WIISEL insoles.

Since the WIISEL project partners could get further funding to continue the research, the UAB team decided to look for opportunities to evolve this proof of concept what was one of the starting points of this research.

3.2. Gait Analysis

One of the main issues in health for elderly people, starting from 65 years old, is falls. It is estimated that each year there are 684,000 deaths due to falls, placing as the second most prevalent cause of unintentional death globally, after traffic accidents [77]. Falls leave serious consequences depending on their severity, including death. From minor bruises that only require primary care medical assistance to hospital admissions for femur, hip, or pelvic fracture surgeries. The latter cases are the most serious (excluding death). Studies show that 50% of patients who undergo surgery to fix a bone fracture after the age of 65 are twice as likely to suffer another fall in the following 12 months, and there are studies establishing a direct relationship between falls and death. Furthermore, the recovery from these types of interventions for older people is not always satisfactory. The estimate is that 60% of patients may regain walking ability, of these, 40% may be having an autonomous live and 30% of patients do not recover and end up needing admission to a nursing home.

3.2.1. Fall detection and prevention

In recent years, several devices have emerged to help with falls and offer an emergency alarm system in case of detecting a fall. These systems initially appear in the form of a collar with a button; in case of the patient falling, they can press the button, which sends an alarm to the emergency system, and a medical team is dispatched. This initial system evolved no new collars, bracelets or smartwatches that perform the same function autonomously; in case of detecting a fall, an alert is automatically sent to the emergency system, or an emergency call is activated to request help. These current systems can make life easier for many people and improve response time to a fall accident, but to reduce the number of falls, we must address the problem at its root: it is necessary to know the causes of falls to prevent them, and not just detect them when they occur. That is why in recent times, various studies are being conducted to understand the cause of falls, how they occur, and which elements may be involved in them. There are different types of falls, those caused by external elements, such as a hole in the ground, a step, or a slip caused by water or ice, and there are falls that originate due to a person's health problem. It is in these latter cases where corrections can be made to try to mitigate them. If there is sufficient data on people's gait activity, it is possible to estimate the risk of a fall and find a solution before it happens.

Numerous research studies have endeavored to construct models for predicting falls among the elderly. Consequently, stimulated by advancements in technology, one prominent opportunity of current investigation aims to monitor fall risk in older adults through the utilization of wireless sensors that transmit data to an online platform.

The emergence of wearable devices in recent times has opened a multitude of possibilities across various medical domains. Specifically, the integration of this technology into gait studies has proven to be an invaluable resource. Through the data collected, valuable insights

into the kinematics of specific movements can be gleaned. Activities like walking or running can be dynamically assessed during their execution, presenting new opportunities for diagnosing and treating gait-related issues and identifying patterns in motion. Additionally, the evaluation of certain disabilities or motor disorders becomes feasible through gait analysis.

3.2.2. Surgery recovery

The measurement of recovery after surgery of the hip or femur involves a comprehensive assessment of various physical, physiological, and functional aspects to evaluate the patient's progress and overall well-being.

A significant component of recovery assessment involves evaluating pain levels and management strategies. Pain after hip or femur surgery can significantly impact the patient's comfort and mobility, thereby influencing the pace and quality of recovery. Healthcare providers use standardized pain scales to assess the intensity and frequency of pain reported by the patient. Based on this assessment, appropriate pain management interventions, including medication administration, physical therapy modalities, and positioning techniques, are implemented to alleviate discomfort and promote healing.

Mobility and functional status are critical aspects of recovery measurement after hip or femur surgery. Physical therapists conduct assessments to evaluate the patient's range of motion, strength, balance, and ability to perform activities of daily life. These assessments help gauge the patient's progress in regaining functional independence and identify areas requiring targeted rehabilitation interventions. Early mobilization protocols are often initiated to prevent complications such as muscle atrophy, joint stiffness, and venous thromboembolism, while promoting circulation and tissue healing.

Surgical site healing is closely monitored to assess wound integrity and identify any signs of infection, inflammation, or delayed healing. Healthcare providers routinely inspect the surgical incision site for redness, swelling, drainage, and other indicators of surgical site complications. In some cases, diagnostic tests such as wound cultures or imaging studies may be performed to evaluate the extent of tissue damage and guide treatment decisions. Proper wound care techniques, including dressing changes, wound irrigation, and infection control measures, are implemented to optimize healing outcomes and minimize the risk of surgical site infections.

To measure the recovery after surgery of the hip or femur encompasses a multidimensional assessment of physical, physiological, functional, and psychosocial factors. By systematically evaluating various aspects of the patient's recovery process and implementing personalized interventions, healthcare providers can optimize outcomes, minimize complications, and support the patient's journey toward restored health and well-being.

3.2.3. Gait parameters

Gait analysis parameters comprehend a full set of metrics used to evaluate various aspects of human locomotion. These parameters are vital in understanding biomechanical patterns and identifying abnormalities or deficiencies in gait. They typically include temporal, spatial, and kinematic measurements [78].

Temporal parameters refer to timing aspects of gait, such as stride time, stance time, swing time, and double support time. These metrics provide insights into the rhythm and cadence of walking.

Spatial parameters involve measurements related to the distance and displacement of body segments during gait. This includes step length, stride length, width of base of support, and step width. Spatial parameters help assess the spatial symmetry and stability of gait.

Kinematic parameters focus on joint movements and angles during walking. These include joint angles at various phases of gait, such as ankle dorsiflexion, knee flexion, and hip extension. Kinematic parameters provide detailed information about the quality of movement and can help identify deviations from normal gait patterns.

Other parameters may also be considered depending on the specific objectives of the gait analysis, such as dynamic stability, kinetic forces, and muscle activation patterns.

Overall, gait analysis parameters play a crucial role in clinical assessment, rehabilitation planning, and biomechanical research, providing valuable insights into human locomotion and aiding in the development of targeted interventions for gait-related disorders. Annex A shows a list of the gait parameters that can be calculated.

3.2.4. Surgery rehabilitation

In community-dwelling individuals with fall-related hip fractures, research indicates that between 25% and 75% fail to regain their pre-fracture level of ambulatory function or activities of daily living [79]. Femoral fractures carry a significant mortality rate, ranging from 4-7% in the first month, 13-16% at 3 months, and 24-28% at 12 months. Survivors face substantial morbidity, with only 50-60% regaining previous walking activity, 40-50% reclaiming independence in daily activities, and merely 25-30% recovering independence in instrumental activities of daily living within 6 months.

In the case of femur fracture, when quantifying rehabilitation, there is no standardized system, and multiple scales are used to validate the patient's improvement. Mostly, scales based on ADL are used, the authors in [80] conclude that there is no unified scale and recommend using different scales to validate rehabilitation.

3.3. Clinical Tests

In the geriatric healthcare and rehabilitation, assessing functional status and mobility plays a pivotal role in determining an individual's overall health, independence, and quality of life. This section details the two main tests that have been traditionally used in clinical premises, under the supervision of doctors or nurses, to evaluate balance, gait, and physical performance, offering valuable insights into an individual's functional abilities and risk of falls.

3.3.1. Tinetti/POMA Test

The Tinetti test, also known as the Tinetti Performance-Oriented Mobility Assessment (POMA) [81], is a widely used clinical tool designed to assess balance and gait in older adults. Developed by Dr. Mary Tinetti in the late 1980s, this assessment helps healthcare professionals evaluate an individual's risk of falls and functional mobility.

The Tinetti test consists of two main components: the balance assessment and the gait assessment. In the gait assessment component, the individual's walking pattern and mobility are evaluated. They are asked to walk across a room at their current pace, with or without an assistive device if they typically use one. The evaluator observes the individual's gait pattern, including step length, stride width, symmetry, and any signs of instability or difficulty. Additionally, the individual may be asked to perform specific maneuvers such as walking heel-to-toe or turning while walking to assess balance and coordination.

Scoring for the Tinetti test is defined on a scale ranging from 0 to 28, with points allocated for each of the test tasks according to the patient’s performance. Higher scores indicate better balance and mobility, while lower scores may indicate an increased risk of falls and impaired mobility.

The Tinetti test is particularly valuable in clinical settings, as it provides healthcare professionals with a standardized and systematic way to assess balance and gait function in older adults. By identifying individuals at risk of falls, healthcare providers can implement appropriate interventions and strategies to reduce the risk and improve overall mobility and quality of life. The test can also be used to monitor changes in balance and gait over time and evaluate the effectiveness of interventions aimed at improving mobility and reducing fall risk.

3.3.2. SPPB

The Short Physical Performance Battery (SPPB) test is a widely used clinical assessment tool designed to evaluate physical function and mobility in older adults [82]. Developed by researchers at the National Institute on Aging, the SPPB test is a simple yet effective measure

that helps healthcare professionals assess an individual's risk of disability, falls, and overall physical decline.

The SPPB test consists of three components: balance, gait speed, and lower extremity strength. Each component assesses different aspects of physical function and mobility, providing valuable insights into an individual's overall physical health.

In the balance component of the SPPB test, individuals are asked to perform three balance tasks: standing with their feet together in a side-by-side position, standing with their feet in a semi-tandem position (heel of one foot touching the big toe of the other foot), and standing with their feet in a full tandem position (heel of one foot directly in front of the toes of the other foot). The evaluator observes the individual's ability to maintain balance during each task and assigns a score based on their performance.

The gait speed component involves measuring the time it takes for the individual to walk 4 meters (about 13 feet) at their usual pace. The evaluator records the time taken to complete the walk and calculates the individual's gait speed in meters per second. This component provides valuable information about the individual's mobility and walking ability.

The lower extremity strength component assesses the individual's lower body strength through a timed chair stand test. Individuals are asked to rise from a seated position in a chair without using their arms, and the evaluator records the time taken to complete five chair stands. This component evaluates muscle strength, power, and functional capacity in the lower extremities.

Scoring for the SPPB test is based on a scale ranging from 0 to 12, with points allocated for each component based on the individual's performance. Higher scores indicate better physical function and mobility, while lower scores may indicate an increased risk of disability, falls, and decline in physical health.

Overall, SPPB and Tinetti are both assessment tools used to evaluate balance and gait, but they cater to slightly different needs. SPPB shines in its ability to detect subtle changes in mobility. This makes it a good choice for monitoring progress in rehabilitation or identifying early signs of decline in healthy individuals. Tinetti, on the other hand, excels at clearly differentiating between those with normal mobility and those with existing mobility issues. This strength makes it valuable for initial assessments or for situations where a clear picture of current function is needed. If it is needed to track progress or identify potential problems early on, SPPB is a better fit. However, if a clear distinction between normal and impaired mobility is crucial, Tinetti is the preferred option.

3.4. MIoT Platform

The development and implementation of the Medical Internet of Things (MIoT) platform represents a concerted effort to integrate a diverse array of features and functionalities aimed at meeting the multifaceted requirements of modern healthcare systems. With a primary focus on extending healthcare services beyond traditional clinical settings, the platform attempts to facilitate continuous connectivity and interaction between patients and healthcare providers, irrespective of geographical constraints (Figure 4).

A pivotal aspect of the MIoT platform is its ability to go beyond the confines of healthcare facilities, enabling patients to use medical devices and services from the comfort of their homes. This accessibility is made possible through the utilization of smartphones, which serve as both user interfaces for conduits and data access via dedicated applications, and in establishing connections with medical devices and from those to the cloud.

In addition to facilitating remote monitoring and data collection from medical sensors, the MIoT platform also incorporates advanced communication features, including the provision for video calls between patients and healthcare professionals. This real-time interaction sparks a greater encounter and enables physicians to provide personalized care and support to patients, thereby improving overall healthcare outcomes.

At the core of the MIoT platform lies a sophisticated cloud-based infrastructure, which orchestrates the unified integration of various components and services. Leveraging the power of cloud computing, the platform enables efficient data aggregation, analysis, and pattern recognition, thereby empowering healthcare providers with actionable insights and decision-making capabilities.

Furthermore, the MIoT platform offers robust patient and doctor management functionalities, streamlining administrative tasks and facilitating efficient coordination of care delivery processes. Through intuitive user interfaces and comprehensive data visualization tools, healthcare professionals can gain holistic insights into patient health metrics, facilitating informed diagnosis and treatment decisions.

Crucially, the MIoT platform adheres to industry standards, such as HL7 [83] and OpenEHR [84], ensuring perfect interoperability and data exchange with existing public health systems. By harmonizing data formats and protocols, the platform enables seamless integration with wider healthcare ecosystems, thereby improving data fluidity and promoting collaborative healthcare delivery models.

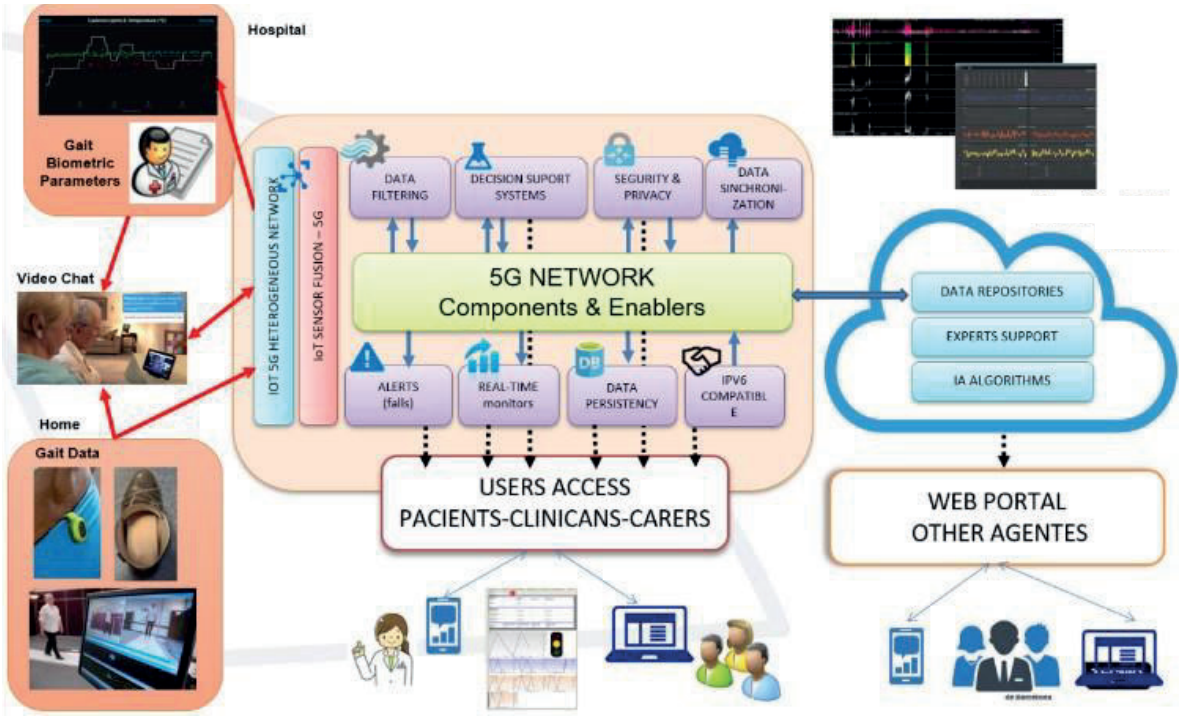

Figure 4: Example MIoT Architecture diagram on a 5G mobile network.

3.4.1. Device: Wireless Insole

Based on Wiisel's design and studying the errors that occurred in the insoles, it was decided to start designing the new insole device. The way to obtain a more reliable and cheap device includes different decisions: (1) increase the HW integration trying to place as many components as possible in the bridge of the foot to eliminate as much as possible the impacts that occur in the heel area and the torsion that originates in the metatarsus area; (2) change a large number of expensive capacitive pressure sensors by a single cheap foil with less resistive sensors; (3) improve the mechanical comfort and strength by collaborating with a professional insole manufacturer; and (4) improve wireless connectivity by using commercial antennas and include a LoRaWAN connection to produce fall detection alerts independently of the use of the smartphone.

This section provides a concise overview of the hardware design centered around an STM32 System-on-Chip (SoC) Microcontroller Unit (MCU), essential for comprehending the application firmware. Figure 5 illustrates the microelectronics hardware platform and its block diagram. The main electronic board contains the STM32WB56 (MCU+BLE) SoC, the Semtech SX1276 RF front-end for LoRa and the IMU BNO 055 plus the corresponding power, clock, and antenna sections. The board has been designed to be used for both left and right feet insoles and has dimensions of 33.38mm x 21.4mm.

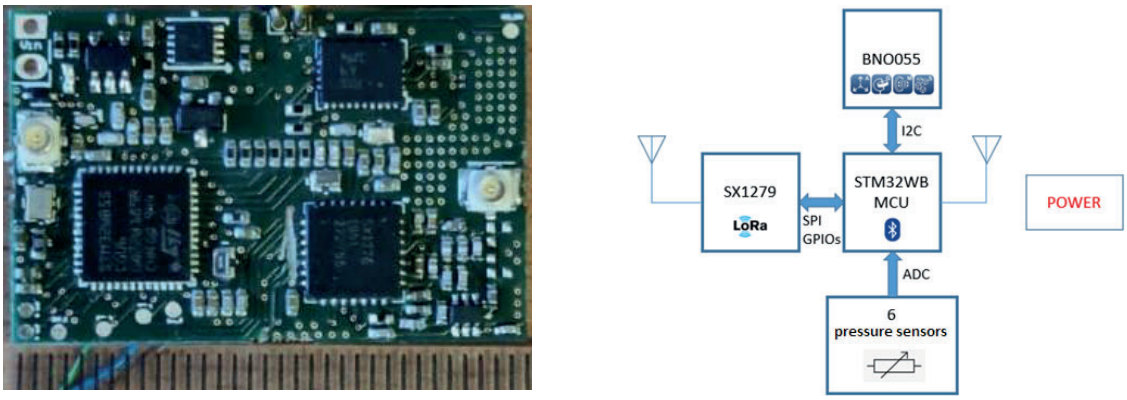

Figure 5: Core PCB and block diagram for the insole device.

3.4.1.1. IMU MEMS Sensor

The BNO055 [85] is an advanced 9 Degree of Freedom (9-DOF) absolute orientation sensor implemented in a hybrid MEMS and ASIC chip solutions that combine accelerometer, gyroscope, and magnetometer data with related computation to provide accurate orientation estimation in three-dimensional space. This highly integrated sensor module is specifically designed to simplify the implementation of motion sensing and orientation tracking applications in various fields such as robotics, virtual reality, and augmented reality.

The BNO055 features a tri-axis accelerometer capable of measuring acceleration along three axes: X, Y, and Z. With its high sensitivity (14-bits resolution) and low noise characteristics (150-190 LSB RMS µg/√Hz), the accelerometer provides reliable data for detecting changes in velocity and direction, essential for motion sensing applications.

Complementing the accelerometer is a tri-axis gyroscope that measures angular velocity along the X, Y, and Z axes, referred to the plane of the sensor chip. The gyroscope provides accurate rotational motion data (16-bit resolution), allowing for precise tracking of changes in orientation and angular velocity.

Furthermore, the BNO055 integrates a tri-axis magnetometer that measures the strength of the magnetic field along the X, Y, and Z axes. This magnetometer data is crucial for determining the device's orientation relative to the Earth's magnetic field, enabling accurate (13/15-bit resolution) heading estimation and orientation tracking.

The BNO055 also features an integrated ARM Cortex-M0 microcontroller (MCU) core, which handles sensor fusion computations and communication with external devices. This onboard microcontroller simplifies system integration and reduces the processing burden on the host microcontroller. At the MCU core, the manufacturer provides a sensor fusion algorithm that combines data from integrated accelerometer, gyroscope, and magnetometer to compute precise orientation data in real-time. This sensor fusion algorithm takes advantage

of sensor data fusion techniques to compensate for the limitations of individual sensors and provide accurate and drift-free orientation estimates in terms of either Euler angles or quaternions (Table 1).

Byte index	Type short name	Characteristic name	Unit name	Unit	Name	Description
0 to 1	Signed Short Int (2B, 16 bits)	serene.bluetooth.characteristic. IMU_packet_1.X_Accel	meters per squared second	m/s^2	X_Accel	X axis acceleration vector (gravity + linear motion)
2 to 3	Signed Short Int (2B, 16 bits)	serene.bluetooth.characteristic. IMU_packet_1.Y_Accel	meters per squared second	m/s^2	Y_Accel	Y axis acceleration vector (gravity + linear motion)
4 to 5	Singed Short Int (2B, 16 bits)	serene.bluetooth.characteristic. IMU_packet_1.Z_Accel	meters per squared second	m/s^2	Z_Accel	Z axis acceleration vector (gravity + linear motion)
6 to 7	Singed Short Int (2B, 16 bits)	serene.bluetooth.characteristic. IMU_packet_1.X_Orient	Degrees per second	dps	X_Orient	X axis of Euler Vector based on a 360º sphere
8 to 9	Singed Short Int (2B, 16 bits)	serene.bluetooth.characteristic. IMU_packet_1.Y_Orient	Degrees per second	dps	Y_Orient	Y axis of Euler Vector based on a 360º sphere
10 to 11	Singed Short Int (2B, 16 bits)	serene.bluetooth.characteristic. IMU_packet_1.Z_Orient	Degrees per second	dps	Z_Orient	Z axis of Euler Vector based on a 360º sphere
12 to 13	Singed Short Int (2B, 16 bits)	serene.bluetooth.characteristic. IMU_packet_1.X_Magn	micro Tesla	µT	X_Magn	X axis of Magnetic Field Strength Vector.
14 to 15	Singed Short Int (2B, 16 bits)	serene.bluetooth.characteristic. IMU_packet_1.Y_Magn	micro Tesla	µT	Y_Magn	Y axis of Magnetic Field Strength Vector.
16 to 17	Singed Short Int (2B, 16 bits)	serene.bluetooth.characteristic. IMU_packet_1.Z_Magn	micro Tesla	µT	Z_Magn	Z axis of Magnetic Field Strength Vector.
0 to 1	Signed Short Int (2B, 16 bits)	serene.bluetooth.characteristic. IMU_packet_2.head_Heuler	angle	Degree	Head	Head axis Euler Vector based on a 360º sphere
2 to 3	Signed Short Int (2B, 16 bits)	serene.bluetooth.characteristic. IMU_packet_2.Roll_Heuler	angle	Degree	Roll	Roll axis Euler Vector based on a 360º sphere
4 to 5	Signed Short Int (2B, 16 bits)	serene.bluetooth.characteristic. IMU_packet_2.Pitch_Heuler	angle	Degree	Pitch	Pitch axis Euler Vector based on a 360º sphere
8 to 9	Signed Short Int (2B, 16 bits)	serene.bluetooth.characteristic. IMU_packet_2.W_Quaternion		Quaternion	W_Quaternion	spatial orientations and rotations of W
10 to 11	Signed Short Int (2B, 16 bits)	serene.bluetooth.characteristic. IMU_packet_2.X_Quaternion		Quaternion	X_Quaternion	spatial orientations and rotations of X
12 to 13	Signed Short Int (2B, 16 bits)	serene.bluetooth.characteristic. IMU_packet_2.Y_Quaternion		Quaternion	Y_Quaternion	spatial orientations and rotations of Y
14 to 15	Signed Short Int (2B, 16 bits)	serene.bluetooth.characteristic. IMU_packet_2.Z_Quaternion		Quaternion	Z_Quaternion	spatial orientations and rotations of Z

Table 1: Bluetooh characteristics for IMU data

3.4.1.2. Pressure array sensor

The incorporation of piezo-resistive pressure sensor arrays implemented on a flexible surface into insole devices provides foot pressure mapping and signifies a notable progression in wearable technology, particularly in gait analysis. These custom-designed sensors, comprise of six Force-Sensitive Resistors (FSRs) located beneath the heel and metatarsal regions, assume a role in capturing and quantifying the pressure distribution exerted by the wearer's foot during motion.

This configuration of FSRs enables measurements of pressure distribution across various foot regions, offering valuable insights into gait patterns, weight distribution, and potential areas of discomfort or imbalance. While previous implementations include a higher number of sensors related to the biomechanical foot pressure points, the WIISEL project demonstrated that relevant gait and balance information was provided by this reduced set [70].

A conventional voltage divider arrangement has been employed to interface the piezo-resistive pressure sensor array with the Analog-to-Digital Converter (ADC) input channels on the STM32WB microcontroller. This setup facilitates the conversion of analog pressure signals into digital data (12 bits precision), which can subsequently be processed, evaluated, and transmitted by the microcontroller to the edge and cloud for additional analysis and visualization purposes (Table 2).

Byte index	Type (Big endian)	Characteristic name	Unit name	Unit	Description
0 to 1	uint16	care.noho.bluetooth.characteristic.A_pressure_spot	12 bits	ohm	Pressure of the sensor spot A
2 to 3	uint16	care.noho.bluetooth.characteristic.B_pressure_spot	12 bits	ohm	Sensor spot B
4 to 5	uint16	care.noho.bluetooth.characteristic.C_pressure_spot	12 bits	ohm	Sensor spot C
6 to 7	uint16	care.noho.bluetooth.characteristic.D_pressure_spot	12 bits	ohm	Sensor spot D
8 to 9	uint16	care.noho.bluetooth.characteristic.E_pressure_spot	12 bits	ohm	Sensor spot E
10 to 11	uint16	care.noho.bluetooth.characteristic.F_pressure_spot	12 bits	ohm	Sensor spot F

Table 2: Bluetooh characteristics for Pressure sensor data.

Through the analysis of data collected by these sensors, healthcare practitioners and researchers can extend their understanding of biomechanical dynamics and make informed decisions regarding aspects such as footwear design, rehabilitation methodologies, and injury prevention strategies.

3.4.1.3. BLE Wireless Communication

The BLE servers, represented by the insoles or peripheral devices containing the STM32WB, communicate with the BLE client, which is a mobile app on a phone designed to communicate with the insole (see Figure 6). They establish communication oriented to the transmission of sensor data from the insoles to the phone app and to monitor the insole behavior.

Upon system startup, both components initialize in the Generic Access Protocol (GAP). The insoles become discoverable and begin advertising for 5 minutes when they have data to transmit. Similarly, the phone app initializes in GAP and starts scanning for available devices to connect to. Upon detecting the advertising packet from the insoles, the phone app decides whether to establish a connection. Once the phone app sends a connection request to the insoles, the insoles cease advertising. The advertising packet contains information indicating to the phone app the type of data offered by the insoles, ensuring that only our custom BLE client app on the phone can detect and connect to the transmitting insoles.

Upon connection establishment, the protocol shifts from GAP to the Generic ATTribute Profile (GATT), which dictates the interaction of data exchange between the BLE devices (client and server). During this phase, the phone app queries the insoles about the services

they offer and the characteristics within those services. The phone app reads all the characteristics for each service from the insoles and configures the appropriate elements to facilitate the services' operation. Subsequently, the phone app enables notifications on the insoles.

At this juncture, an update rate timer in the insoles triggers tasks at 33 Hz, facilitating the update of IMU and pressure sensors notifications. Consequently, the sensor sampling frequency operates at 33 samples per second (sps). Depending on the specific application, the sample rate can be adjusted up to 100 sps, which is the maximum sensor fusion output data rate.

Attribute Profiles

The attribute specifies all the parameters of each service and characteristic provided by the insoles. Two distinct services, each with its characteristics, are available to the phone app.

The base feature service comprises 2 notification characteristics. These notification characteristics, denoted as IMU and Pressure, respectively, are configured using their descriptors to enable notifications, thereby transmitting relevant data to the phone app.

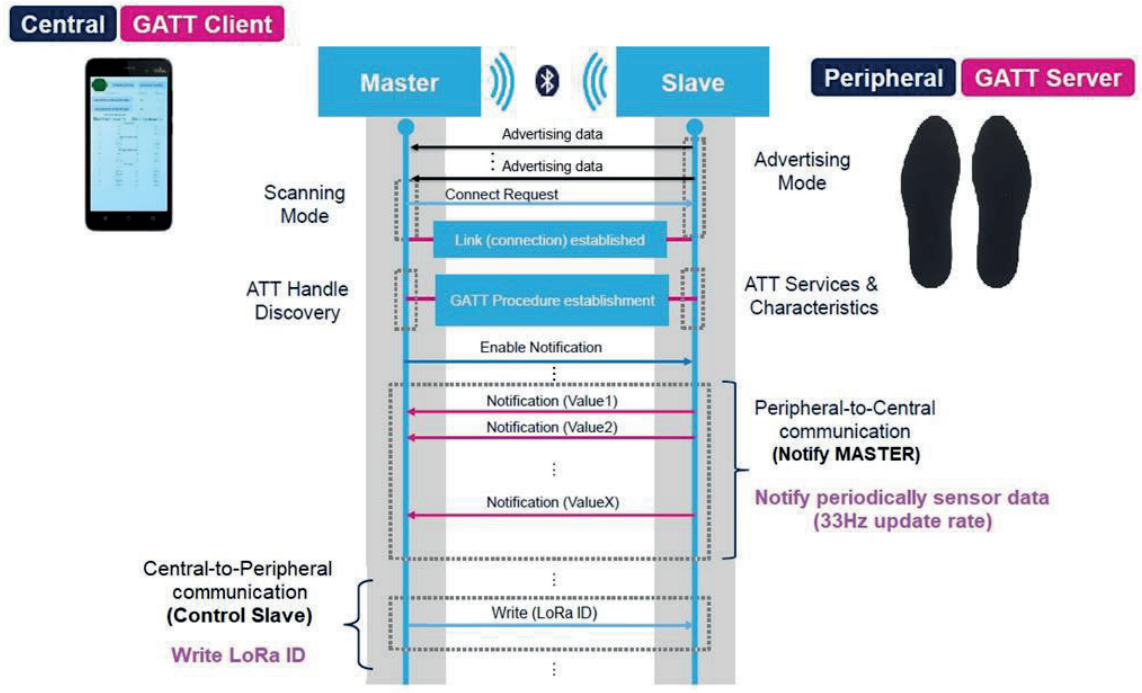

Figure 6: BLE connection negotiation.

The P2P Service encompasses the over-the-air (OTA) Reboot characteristic. This characteristic facilitates the loading of a new firmware version via OTA, enabling firmware updates remotely.

3.4.1.4. LoRa Wireless Communication

To ensure robustness in message delivery, especially during critical situations, our system incorporates a LoRa WAN module designed for wireless communication, utilizing the 868MHz frequency band. The key advantage of this technology lies in its remarkable coverage range, capable of spanning several kilometers with just a single antenna. By strategically placing a few receiving outdoor antennas throughout a city, comprehensive service coverage can be extended to all devices within the network. To provide us with LoRa WAN connectivity, the device must be registered in an application server and have coverage from one of the antennas that offers connection to that server. For this purpose, our solution is connected to The Things Network (TTN), a global initiative focused on the IoT. It provides an open-source infrastructure that utilizes LoRa WAN technology to connect devices to the internet. This network allows developers and businesses to build IoT applications at a low cost with features like high security and scalability. It also fosters a collaborative community where people can learn, experiment, and build solutions using LoRa WAN [86].

However, while LoRa WAN offers extensive coverage, it operates within a bandwidth-constrained environment. Each packet transmitted is limited to a maximum size of 222 bytes, a limitation imposed by the system and dependent on the power level at which the transmission occurs. Despite this limitation, LoRa WAN's efficient use of bandwidth ensures reliable communication even in challenging environments. Another aspect to consider when using the LoRa WAN network is the 1% duty cycle, this refers to the restriction imposed on the transmission frequency of devices within a LoRa WAN network. This restriction ensures that devices do not overwhelm the network by transmitting data too frequently, thereby avoiding interference and congestion. The duty cycle limits the amount of time a device can transmit data within a specific time window, typically defined by regulatory authorities or network operators. By adhering to the duty cycle regulations, LoRa WAN devices take turns transmitting data, allowing for efficient and fair use of network resources while maximizing battery life. If we group all the data received by the sensors (46 bytes) we can send 318 messages every hour using LoRaWAN with information from the sensors and complying with the duty cycle restrictions.

As previously highlighted, this system serves as an alternative communication channel with healthcare services, particularly in emergency situations such as when a fall occurs and is detected by the insole. In the event of a fall, the device retrieves GPS position data from the user's phone via Bluetooth Low Energy (BLE) technology. This data is then encapsulated within a LoRa message and transmitted to designated emergency systems.

This streamlined communication process eliminates the need for manual phone calls during emergencies, enabling swift and automated responses to critical incidents. By leveraging the capabilities of LoRa WAN and BLE technologies, our system ensures seamless communication between wearable devices and emergency systems, facilitating timely

intervention and assistance when it matters most. Smartphone or other devices (e.g. smartwatches) can also send this can of emergency data which should be considered complementary and redundant at the emergency services management.

3.4.1.5. SoCs

The Insole hardware chip is the STM32WB55CGU6 (UFQFPN48 7 x 7 mm). The STM32WB provides a flexible way to build solutions with a 2.4 GHz radio interface supporting Bluetooth Low Energy and 802.15.4 PHY and MAC. This device is designed to be extremely low-power; thus, it is ideal for battery-powered and power sensitive applications like this [87]. It is a dual core device, based on:

- CPU1: The high-performance Arm Cortex-M4 32-bit RISC core, on which the host application resides (application processor). It is developed with the same technology as the ultra-low power STM32L4 microcontrollers.
- CPU2: A dedicated Arm Cortex-M0+ for performing all the real-time low layer operation (network processor).

We treated this device as an STM32L4 with a Cortex-M0+, a radio and a separate DC-DC converter. There are two power supplies to choose from in dependence on the type of application: The Switch Mode Power Supply (SMPS) or the LDO.

The STM32WB peripherals need to be configured for the rest of the application:

- I²C communicates the STM32WB as a host device with the BNO055 as slave. The I²C is set with the following features: I²C Fast Mode (400 kHz speed frequency) and 7-bit address mode.
- Six ADC single-ended input ADC channels have been used for the signals coming from the pressure sensor. Calibration is performed after each power-up. ADCs are set with: Synchronous clock with system frequency divided by 4 (8 MHz); ADC 12-bit resolution; Data pre-processing: right data alignment. No per channel offset compensation. Overrun data overwritten. Scan mode for conversion of the 6 channels sequentially. Regular Conversion launched by software. 92.5 cycles sampling time per input channel. Longer sample times ensures that signals having a higher impedance are correctly converted. Conversion results are transferred by DMA into destination variable address. Interrupt generation at the end of regular conversion.

The architecture of the insole FW is based on a sequencer or simple task scheduler. Several tasks are set up that will be executed at some point. Each of these tasks will be processed and eventually reach the point where all tasks are complete. Therefore, the system will drop into Idle mode, which means it will enter a low-power mode.

3.4.1.6. Energy management

Instrumented insoles are intended to be used for the whole day and recharged at night. For that purpose, an energy saving strategy has been planned centered on de implementation of an efficient duty cycle the duty cycle refers to the ratio of time a device or system is actively consuming energy compared to the total time while the device is running and directly impacts the total energy consumption and thus battery duration related to the efficiency of devices or systems. A higher duty cycle implies that the device or system is active for a larger portion of the time, leading to increased energy consumption. Conversely, a lower duty cycle means the device or system is active for a smaller portion of the time, resulting in lower energy consumption. This technique is currently being used for most electronic devices including smartphones, laptops, and personal computers when managing computation, communication, display, etc.

In inertial sensor systems, there is no need to acquire, process and transmit data where there is not any motion detected. This scenario can either be computed by the processor core or directly notified by the sensor using data or interrupt signals. This last one is the case for the BNO055.

Furthermore, in wireless communication systems, the duty cycle determines how often the device needs to transmit or receive data. A higher duty cycle means more frequent transmissions or receptions, which in turn leads to an increase in energy consumption. Conversely, a lower duty cycle reduces the frequency of at which data is transmitted or reception is activated waiting for incoming data, at the end resulting in lower energy consumption. Building the optimal data packets, defined by the communications protocol, from incoming sensors data must be managed by the processor core and allows adjusting the duty cycle according to the operational requirements and power constraints. This strategy slows to strike a balance between functionality and energy consumption, ensuring optimal performance while conserving energy resources.

3.4.1.7. Batteries and wireless charging

Our usability goal was building a fully wireless insole avoiding the users to handle wirings and fixing external. This led us to the integration of all components inside the insole without any physical connector what could be damaged by its use.

The key components to reach that goal were the use of few smallest rigid components and the most flexible components. This leads to an integrated assembly composed by the PCB component, the Qi charger module and the battery of dimensions 79mm x 45mm that integrates all microelectronic components, the flexible pressure array sensor and two flexible antennas ([88], [89]) for Bluetooth and LoRa plus the energy storage and transmission components.

For energy storage, we selected the same semi-rigid battery used in WIISEL [90] while for energy transmission we used and updated version of the Qi standard that allows a faster and more reliable charging [91].

The Qi wireless charging standard, developed by the Wireless Power Consortium (WPC), operates based on electromagnetic induction, allowing devices equipped with Qi-compatible receivers to charge wirelessly when placed on a Qi-enabled charging pad or surface.

In the context of insoles, integrating Qi wireless charging technology offers several benefits. Firstly, it eliminates the need for cumbersome cables and connectors, speeding up the charging process and improving user comfort and mobility. Users can simply place their Qi-compatible insoles on a charging pad, desk, or any other Qi-enabled surface to initiate the charging process, without the hassle of plugging in cables or adapters.

Additionally, Qi wireless charging promotes durability and longevity by minimizing wear and tear on charging ports and connectors. Traditional charging methods often lead to degradation of connectors over time due to repeated plugging and unplugging. With wireless charging, the risk of mechanical damage to insoles is significantly reduced, resulting in extended lifespan and improved reliability.

In addition to convenience and durability, Qi technology offers versatility in charging locations. Users can recharge their insoles at home, in the office, or even in public spaces equipped with Qi charging stations, providing flexibility and convenience in various environments.

Moreover, this technology is inherently safe and efficient, employing advanced technologies to regulate power delivery and prevent overcharging, overheating, and short circuits. This ensures optimal charging performance while safeguarding the integrity of the insoles and the user's safety. The solution used in our case was the integration of the module QI Receiver click [92] (shown in Figure 7).

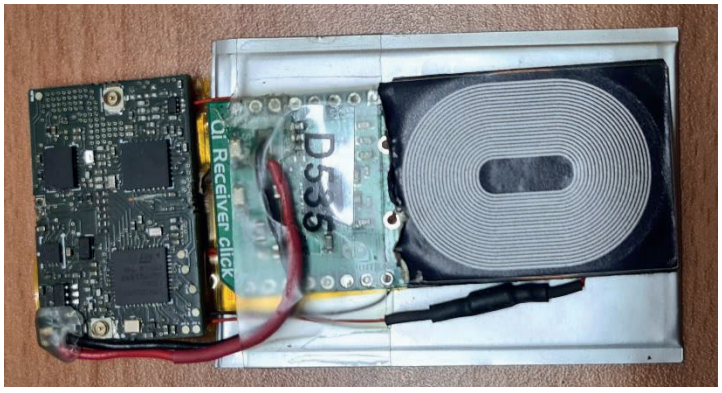

Figure 7: Integration of PCB, Qi charging module and Battery.

3.4.1.8. OTA Firmware Update

The system's implementation of OTA firmware updates for the insoles via Bluetooth communication represents a significant advancement in user convenience and device management. By eliminating the need for a physical connection between the insoles and a server, users can seamlessly initiate and complete firmware updates directly from their mobile devices or other compatible Bluetooth-enabled devices.

Through the Firmware Update OTA (FUOTA) mechanism, users gain the flexibility to independently upgrade various components of the insole system, including the insole application, the Bluetooth Low Energy (BLE) stack, and the Firmware Update Service (FUS). This modular approach to firmware updates allows for targeted improvements and optimizations to specific system functionalities without the need for comprehensive overhauls or replacements.

The ability to update the insole application via OTA firmware updates ensures that users have access to the latest features, bug fixes, and performance enhancements without the hassle of manual intervention or complex installation procedures. With each firmware update, users can expect improved stability, compatibility with new devices, and enhanced functionality tailored to their evolving needs and preferences.

Similarly, updating the BLE stack through OTA firmware updates ensures seamless compatibility with a wide range of Bluetooth-enabled devices, peripherals, and accessories. By staying current with the latest BLE specifications and protocols, the insole system can maintain robust and reliable communication channels with external devices, ensuring optimal performance and connectivity in diverse usage scenarios.

3.4.1.9. Mechanical Insole assembly

After the electronics and sensors have been developed, we proceed to create a mold of the templates to integrate the whole system. These templates are made of polyurethane and specifically designed to fit the electronics and the battery. Figure 8 (a) shows the measures that should have the insole. In Figure 8 (b) can see the 3D design to create the mold.

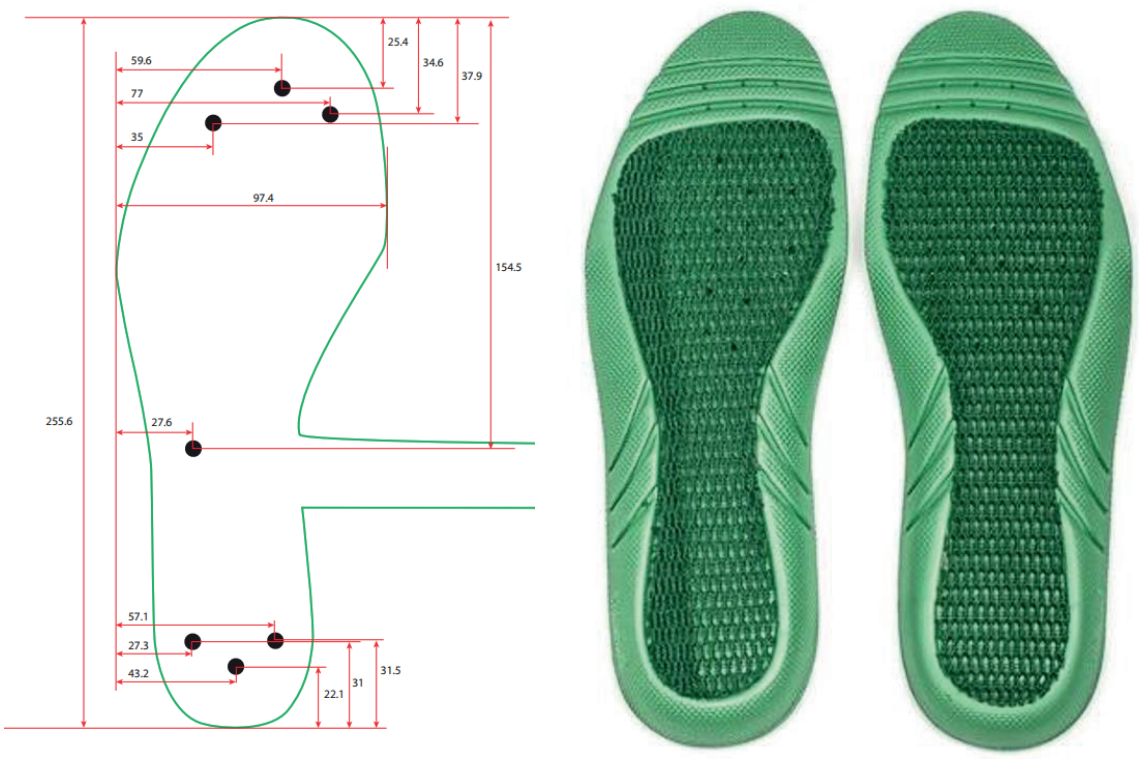

Figure 8: (a) Pression sensor measurements; (b) 3D insole desing.

In the following figure, Figure 9, can see the first integration test of the electronics inside the prototype insole before the external finishing.

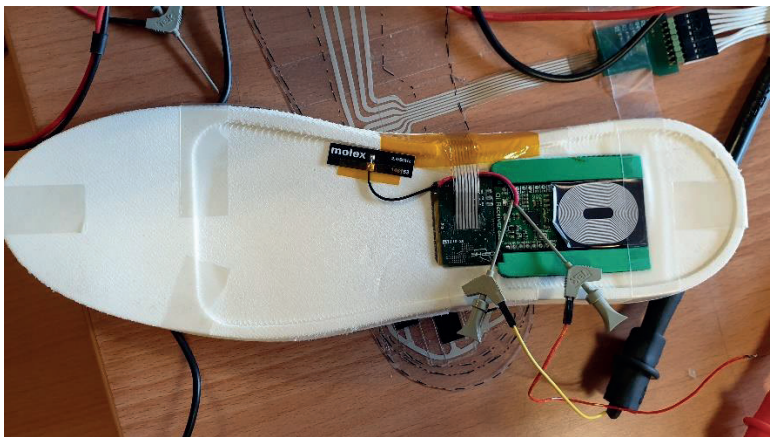

Figure 9: First electronic test with the prototype insole.

Once the electronics are integrated into the insole, it must be closed. For the upper finish, which is in contact with the foot, a leather fabric is used to withstand the humidity and heat produced during the use of the insoles.

Each insole has its own electronics with its unique identifier, which is why the identifier is engraved on the leather to easily identify which device is being used, and to make it easier for the patient to connect to the device. The Figure 10 shows the different engraving tests performed using a PC-1390 laser cutter [93].

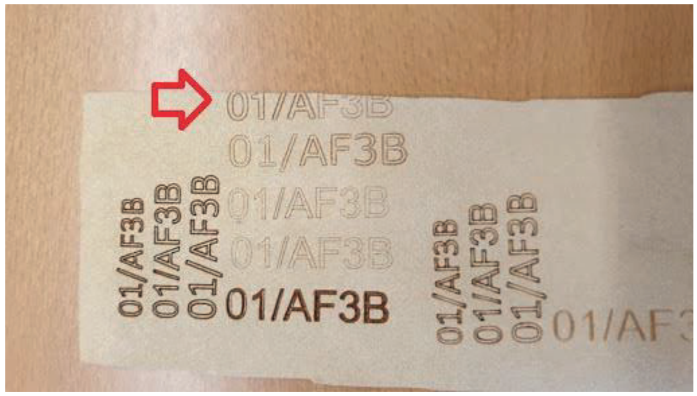

Figure 10: burn test of the IDs over the leather.

3.4.2. Smartphone APP

Smartphone applications are deployed by downloading specific programs, called APPS, either from a public repository or through specific links. The APP developed in this project contains two main features: edge data management and user interface.

3.4.2.1. Edge data management

Edge data management is the process of managing data locally, near where it is produced. This is done to lower latency and energy and save bandwidth and range by processing data closer to its source. This is mainly significant in applications where real-time processing and decision-making are essential, such as in many MIoT devices. Edge data management involves collecting, storing, processing, and analyzing information at or near this edge rather than sending it to a centralized data center or cloud for processing.

Our application gathers data from both insoles in real-time and stores it on the device. Once the process is complete, the data is transmitted to the cloud. Simultaneously, as the data is being received and stored, another process is continuously analyzing it to identify patterns that may indicate a potential fall event. When a fall is detected, the application presents an emergency screen that allows the user to seek assistance if necessary or to answer to emergency systems.

3.4.2.2. User Interface

The user-centric approach ensures that the user APP offers to the specific needs and preferences of elderly users, who may require intuitive interfaces and clear instructions for

effective interaction. By simplifying the user interface and providing comprehensive guidance, the application aims to enhance usability and accessibility, allowing older individuals to engage confidently with the testing process (Figure 11).

Furthermore, the inclusion of visual aids, such as images demonstrating correct foot placement, enhances comprehension and reinforces proper execution of the test exercises. This visual support is particularly beneficial for elderly users who may rely on visual cues for better understanding and adherence to instructions. It can also be adapted to any accessibility issues (text font size and color, audio support, etc.).

The principal goal of these design considerations is to create a user-friendly and supportive environment within the application, fostering a positive user experience and encouraging active participation in healthcare monitoring and management. Through thoughtful design and attention to user needs, the application strives to promote independence, confidence, and well-being among older individuals engaging with the testing protocol.

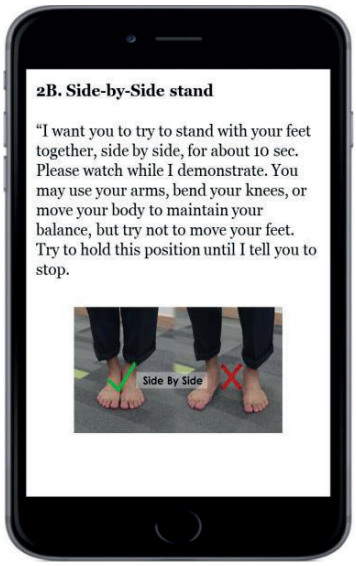

Figure 11: App capture showing Test description and image.

Figure 12 is intended to ask the users to discern whether the detected event constitutes a genuine fall or a false alarm. If the user opts for the false fall button, the application seamlessly redirects to the main screen without any further actions or consequences. Conversely, selecting the fall button navigates the user to the emergency need screen, indicating acknowledgment of a potential emergency.

A countdown timer, initialized at 30 seconds, serves as a buffer period for users to make their selection. If no response is provided within this timeframe, the application autonomously defaults to the most conservative option, assuming the occurrence of a fall. This intuitive feature ensures that potential emergency scenarios are promptly addressed, even in situations where user interaction may be delayed or unavailable.

Figure 12: APP screen during a detected fall.

Upon confirmation of a detected fall, the application navigates users to the screen depicted in Figure 13. Within this interface, users are prompted to indicate whether emergency assistance is required. Two response options are presented: "I'm Okay" and "Help". Opting for "I'm Okay" triggers the application to dispatch a text message to designated emergency contacts, containing the message "Fall without injuries" along with the user's pertinent personal information. Additionally, a call is initiated to the specified emergency contact for immediate notification.

On the other hand, selecting "Help" prompts the application to send a text message to the designated contacts, relaying the message "Fall with need for assistance" accompanied by the user's personal details. Simultaneously, a call is placed to emergency services, specifically 112, ensuring swift intervention.

In scenarios where no response is provided within the allocated 30-second window, the application automatically defaults to the most safety option, signaling the need for medical assistance.

The videocall feature enhances the telemedicine experience by fostering clear and direct communication between healthcare providers and patients. Through the video call system, clinicians can remotely assess patients' conditions in real-time, observe physical symptoms, and provide guidance on performing diagnostic tests effectively.

Figure 13: Screen for request assistance or message emergency contact.

For patients, the video call interface offers reassurance and personalized support during medical consultations. They can interact with healthcare professionals, ask questions, and receive instructions on conducting assessments or treatments at home. The ability to share real-time data from sensors further enriches the diagnostic process, allowing clinicians to make informed decisions based on comprehensive information.

Moreover, the split-screen layout optimizes the user experience by seamlessly integrating the video call interface with the testing procedure. Patients can follow instructions from clinicians while simultaneously observing their reactions and responses, fostering a sense of engagement and involvement in their healthcare journey, as shown in Figure 14.

Figure 14: Exercise screen during Videocall with clinician.

3.4.3. Cloud

The system is designed to be used in medical environments such as a hospital, where sensitive patient data is handled. To give it extra security, a double server has been implemented, giving an extra layer of security, allowing data to be inserted. from the outside and separating it from all sensitive information. It is the instance with the sensitive data that makes the data request between the secure zone and the zone exposed to the Internet.

3.4.3.1. Gait Analysis

The raw data undergo filtering to extract gait statistics such as activity time, number of steps, and distance covered. Utilizing the pressure sensors in the insoles, non-walking situations are eliminated during the filtering process. The remaining data is categorized as movement, based on the execution of steps, which excludes activities like driving a car. A step is defined as the successive contact of the heels, alternating between the left and right.

Once non-walking situations are filtered out, the data is scrutinized to identify clean walking situations. These are periods throughout the day where the patient consistently walks for at least 60 seconds on even ground. During this process, 5 seconds are trimmed from the beginning and end of each identified walking period. Clean gait is defined by ensuring that the difference in the Z axis from one step to the next remains below 1 cm, as measured by the insoles' accelerometer readings.

Gait parameters and their variations are then computed for each extracted clean walking situation. To eliminate situations where the subject encounters obstacles, clean walking

situations are excluded from the gait parameter calculation. Various constants, such as a 60-second window and a 1 cm height difference, are applied during the gait parameter extraction process.

Figure 15 displays the data collected over a selected day, presenting sensor values from pressure, acceleration, and gyroscope sensors over time. Additionally, two main overlays are depicted:

- The orange overlay indicates the times during the day when user activity was detected, used for extracting user statistics such as activity time, number of steps, and distance walked.
- The blue overlay, nested within the orange overlays, signifies periods of clean walking situations from which gait parameters are extracted.

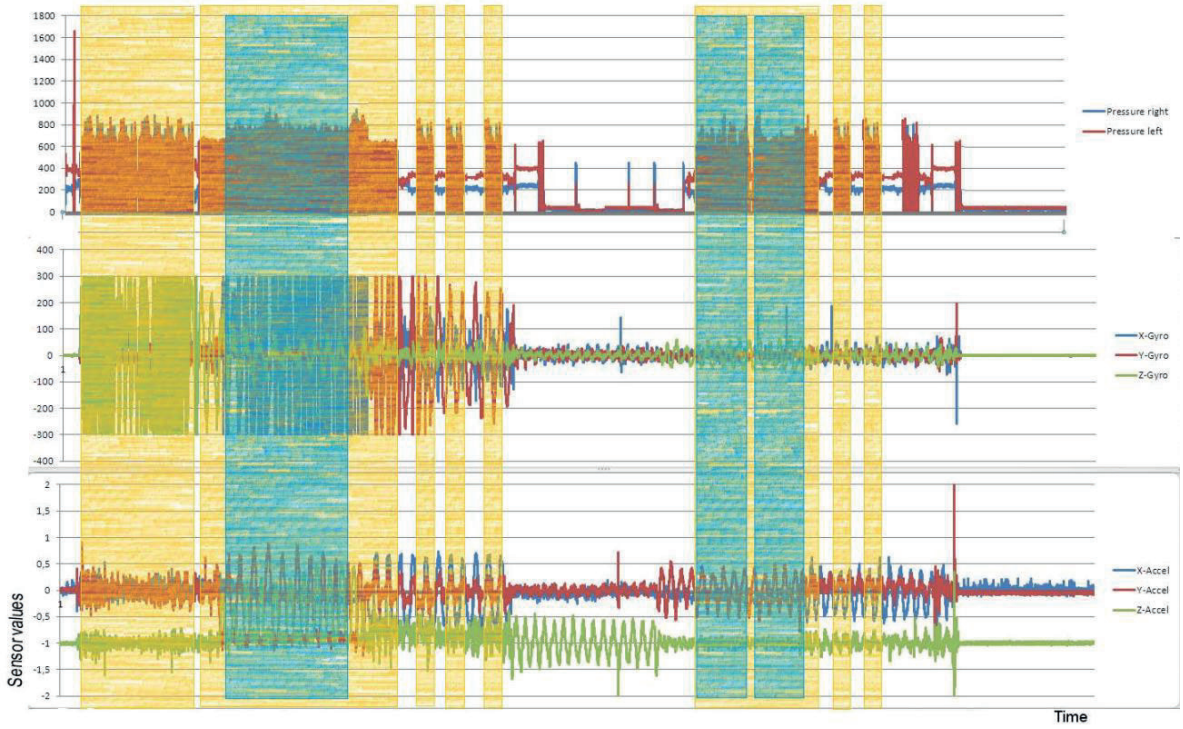

Figure 15: Visualization of raw data of all sensors.

3.4.3.2. Personalized user interface

Since each patient has different casuistic, the system must allow and offer a personalization to be able to attack the different traits that we can find. Therefore, when performing the study of each person, the system allows to select which parameters of the gait we want to use and visualize. The following image, Figure 16, shows a screen from the clinician application, that

graphs the daily data of a patient and allows us to select the sensor data we want to display and the data of the gait parameters that are displayed.

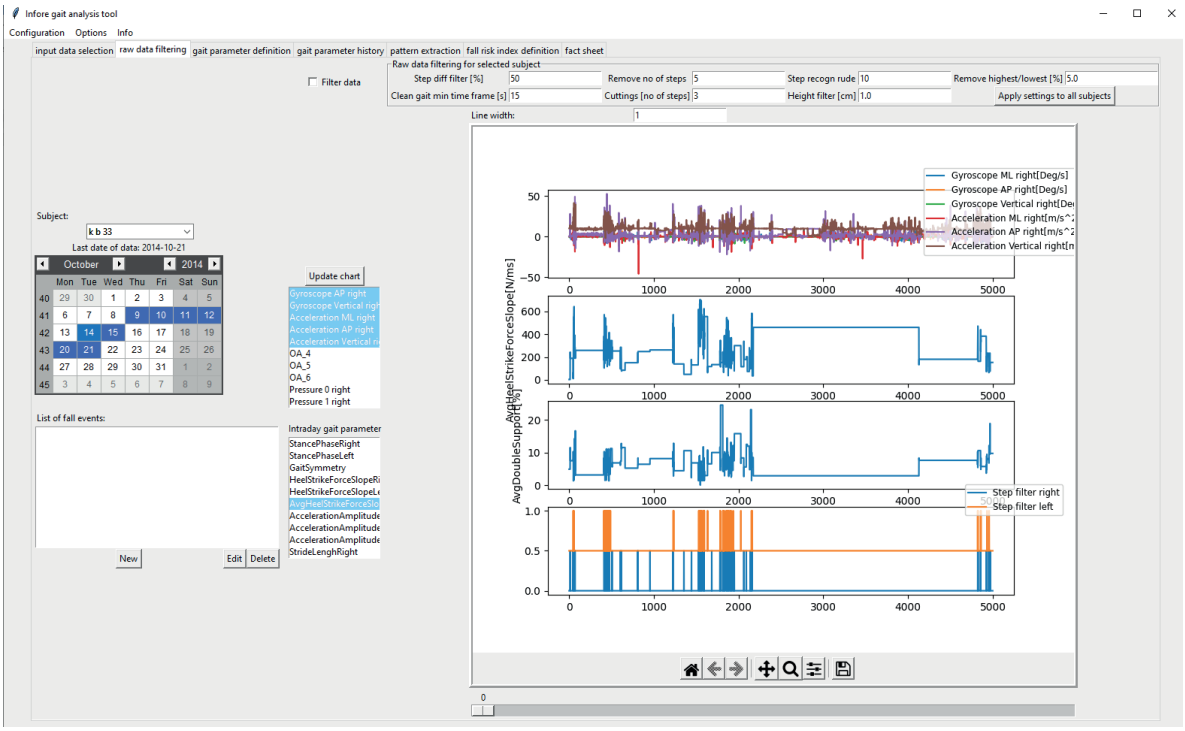

Figure 16: Screen to visualize of gait personalized parameters for each patient.

On the web application, the patient can access the reports which give gait analysis related information. Examples of reports which can be visualized are chart reporting on the number of steps and distance, chart reporting on the activity time, number of falls and simple step length and chart reporting on the Fall Risk Index and its status and step length variability (Figure 17). Annex B shows more screens of the interface.

Figure 17: Patient's report indicating the Fall Risk Index and step length variability.

3.4.3.3. Fall Risk Index and Surgery Recovery Index

The decision on the weighted combination of gait parameters into a Fall Risk Index is based on recommendations from clinicians. This index aims to furnish quantitative insights into potential gait patterns and, employing a range of thresholds, to signal whether a subject exhibits a heightened risk of falls, whether this risk evolves over time, and which corrective measures regarding gait should be pursued.

The current Fall Risk Index consists of 4 gait parameters in different weights. This combination has been found by training the system with data from fallers and non-fallers and has an accuracy (based in the available gait data) > 95% [70] for users without other disabilities:

- Stride time and its variability.
- Gait speed and its variability.

- Heel strike force and its variability.
- Double support time and its variability.

Furthermore, to exemplify the index's implementation, an initial step involves adopting a simplified method for calculating the Fall Risk Index. Initially, the index focuses solely on one parameter: stride time variability. This parameter, potentially influential, indicates a heightened risk of falls when its variability (expressed as a percentage) is high, serving as a potential marker of gait impairments. Following the calculation and testing of the fall risk index based on stride time variability, the index will be further refined and tested with the other parameters.

The Fall Risk Index is a simplified way to measure the risk of falls. It is a combination of selected gait parameters and is normalized to a range from 0 to 100.

In the range of 0 - 30, no risk of fall is expected. In the middle range from 30 to 70, a risk of fall may arise, depending on the evolution of the index. Rising values may indicate gait problems, that should be investigated. A value higher than 70 indicates a concrete risk of a fall. In this case, immediate actions should be taken to stabilize gait and to avoid a fall.

Our proposal for a Surgery recovery index is based on the same principle as the fall risk index, but instead of measuring upward evolution, it measures the improvement that occurs as the patient accumulates rehabilitation sessions that lead to an improvement of gait and normalization of its parameters.

In addition to the weight, a domination factor has been added. This means, if a single gait parameter has a worse value, while other gait parameters don’t show any abnormalities, this single gait parameter can dominate the index and set its value into a critical state.

Table 3 shows the current settings for the Fall Risk Index. If the gait parameter “Single Support” has a value of higher then 71%, the whole index has at least that value.

Gait Parameter	Weight	Domination
SingleSupport	31	71
HeelStrikeForceSlope	5	-
AvgAccelerationAmplitudeML	12	-
DoubleSupport	52	-

Table 3: Gait parameters of the Fall Risk Index and their weight

For the extraction of gait parameter and patient's statistics (activity time, no of steps, walked distance) the system considers only situations in which the subject moves. Consequently, the first step of the data processing is to filter out data in which no movement is detected. Non walking situations are defined as situations in which the subject is lying, sitting, or standing without moving. To detect the movement the system, consider data collected from both accelerometers (forward axis) on the insoles.

The step extraction is based on the values of the pressure sensors, combined with accelerometers and gyroscopes. The process of step measuring is initiated by the contact of the heel with the ground. The mean value of 3 heel pressure sensors is calculated. If the system detects that the mean value starts from a non- zero value and it increases, heel contact is confirmed. The end of the step is defined through confirmed heel contact of the other foot. If the end of a step cannot be confirmed (because no alternate heel contact appears in a defined time or a heel contact of the same foot is measured), the current step is discarded.

To be able to measure comparable gait parameters over a longer time, it is necessary to measure them under normal condition and for a certain time. Normal conditions exclude situations like walking stairs, walking on uneven ground, walking only for 5 seconds, etc. For this purpose, additional data filters have been implemented. The first filter measures the vertical movement during a step. If the altitude at the end of a step differs of more than 1 centimeter from the beginning of the step, this step is discarded. For the remaining steps, the system measures the time until the walking operation ends or the filter for the altitude is triggered. To be considered for the gait parameter calculation, the time of continuously walking needs at least 60 seconds (second filter). This guarantees that the patient is walking in a normal mode. At the end of the process, the first and the last 5 seconds of this time windows are removed, because the gait values during that time would alter the measurement.

In order to clarify the calculation of the gait parameters, the algorithm which calculates the step length is reported in the followings.

The length of an individual step is calculated by twice integrating the foots acceleration in the forward direction over time. From the first integration the velocity is found. Subsequently the velocity is integrated to obtain the distance traveled in one step. The calculation is however complicated by the fact that the angle of the insole with respect to the ground plane will change during the step. The acceleration in the steps forward direction is not equivalent to the accelerometer measurement in the insoles local forward direction that will rotate into the vertical direction and get the earth gravitational field added to the measurement. Simplified, the acceleration in the steps forward direction is the sum of the parts of the accelerometer measurements in the insoles local forward (Ay) and up/down (Az) directions that are directed in the steps forward direction. To derive this sum of vectors, the angle of the foot during the step must be derived as a function of time. This is accomplished by integrating the angular velocity measured by the gyroscope.

Angle of the foot

$$\theta(t) = \int_0^t w_x(t)dt$$

Forward velocity

$$v_y(t) = \int_0^t [\cos(\theta(t))A_y(t) - \sin(\theta(t))A_z(t)]dt$$

Step length

$$L = \int_0^t v_y(t)dt$$

The three equations above are solved numerically for each step taken. The functions $\omega x(t)$, $Ay(t)$ and $Az(t)$ are measurements from gyroscope and accelerometer that can be sampled at rates up to 50 Hz. The forward velocity, vy, can be expected to be equal to zero at the end of the step unless the user is slipping. This fact can be used to compensate for accumulation of measurement errors from gyroscope and accelerometer readouts during a step.

While gait parameters are calculated continuously on raw data, the representation, and the use of the data in the system is intended to long term trend evaluation. To this end, the gait parameters are concentrated on a daily base, having one value per day. From the intraday trend of each gait parameter, the mean value is calculated and provided as input to the gait analysis setup (which calculates the Fall Risk Index) and the pattern recognition engine. To get the measure of the intraday trend of the gait parameters, the variability of each parameter is calculated based on the highest and lowest values measured during the day. The variability is calculated with the formula (v.max – v.min)/(v.max/100), where v.max is the max value of the gait parameter during the day, v.min is the minimal value of the gait parameter during the day.

3.5. Results

The development and implementation of the MIoT platform have yielded promising results, marking significant strides in enhancing healthcare monitoring and management for elderly individuals. At the core of the platform are the innovative smart insoles, equipped with state-of-the-art technology to capture and analyze crucial movement data during daily activities and prescribed exercises. The integration of pressure sensors and an IMU within these insoles enables comprehensive monitoring of the wearer's physical condition, facilitating early detection of potential pathologies and offering valuable insights into overall health status.

The connectivity provided by BLE technology ensures efficient data extraction from the smart insoles to a smartphone interface. This real-time data transmission capability empowers users and healthcare professionals alike to monitor health metrics closely, enabling timely interventions and personalized healthcare management strategies. Moreover, the incorporation of LoRa communication technology serves as a safety net, providing an additional communication channel in emergencies and enabling prompt assistance requests when needed most.

We had produced 10 sets of insoles, with each set incurring an approximate cost of 150€. This expenditure encompasses various manufacturing expenses, including materials, labor, and any related costs associated with the production process. In Figure 18, a pair of smart insoles is showcased, exemplifying the fusion of innovative technology with user-centric design principles. These insoles represent a tangible manifestation of the platform's commitment to supporting active aging and increasing overall quality of life for elderly individuals. One of the improvements we wanted to achieve was to improve battery life. With the improvements that have been made to the templates, it has been possible to go from 6 hours of use in the version of the Wiisel project to 12 hours.

Figure 18: Developed insoles. View of electronic and sensors, and finished product.

To complement the hardware components, applications have been designed to facilitate user interactions and maximize the usefulness of the MIoT platform. The initial application serves as a conduit for connecting to the smart insoles and visualizing captured data, laying the foundation for subsequent analysis and intervention, Figure 19. Building upon this foundation, the second iteration of the application expands functionality, offering users the opportunity to engage in structured tests and even conduct video consultations with

healthcare professionals, fostering greater engagement and collaboration in healthcare management.

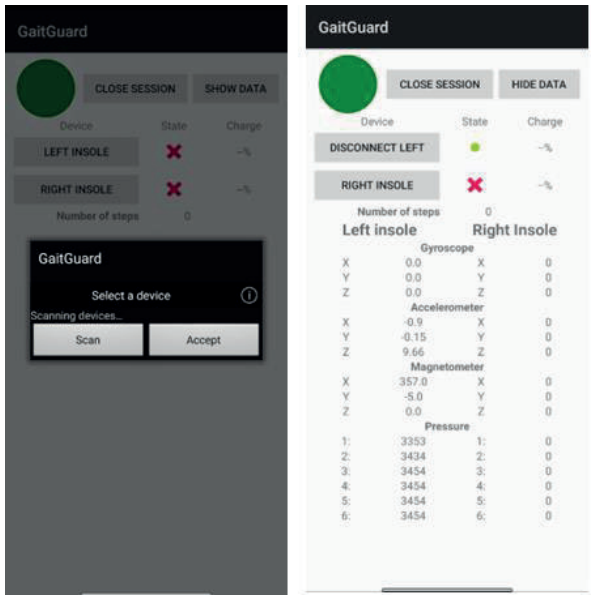

Figure 19: Android application to communicate insoles and smartphone.

Several tests were carried out to check the correct operation of the insoles and to verify the correct capture and sending of information between the insoles and the cell phone, and between the cell phone and the cloud. Walking tests were performed for several minutes with the device running and walking up and down stairs, trying to replicate a daily use of the insole. In the Figure 20 you can see one of the tests where the user is walking while using the templates, the data is displayed in the application.

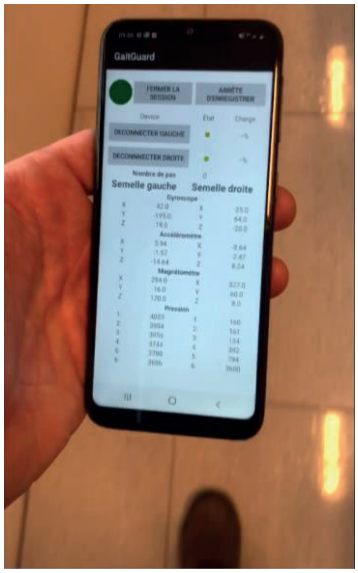

Figure 20: Insoles and App walking test.

Additionally, the cloud-based infrastructure underpinning the MIoT platform provides a robust framework for data storage, analysis, and interpretation. By leveraging sophisticated algorithms and machine learning techniques, the platform can discern patterns and trends within the collected data, generating actionable insights and facilitating informed decision-making for both patients and clinicians. The intuitive web interface, Figure 21, grants users unified access to comprehensive health metrics.

Figure 21: Interface web with multiple graphs of insoles' data.

Furthermore, the comprehensive nature of the system allows for a general approach to patient care. By leveraging the data collected from the smart insoles, healthcare professionals can gain valuable insights into the patient's mobility patterns, gait abnormalities, and overall activity levels. This information can inform personalized rehabilitation programs tailored to the specific needs and progress of each patient.

Moreover, the ability to remotely monitor patients' rehabilitation progress and activity levels through the platform facilitates timely interventions and adjustments to treatment plans as needed (Figure 22). Healthcare providers can track trends, identify potential complications,

and provide timely feedback and guidance to patients, ultimately optimizing the recovery process and improving patient outcomes.

Once the platform was developed and tested, and all hospital privacy data accomplished by implementing two different cloud solutions, a clinical study was to be carried out to test the performance of the system using patients undergoing rehabilitation following femur/hip surgery. The tests were to be carried out at the "Centre Hospitalier Universitaire de Grenoble" in mid-2020 in the framework of the SERENE-IoT project led by ST Microelectronics. Unfortunately, the outbreak of the COVID-19 pandemic made it impossible to carry out any tests as all clinical tests were cancelled.

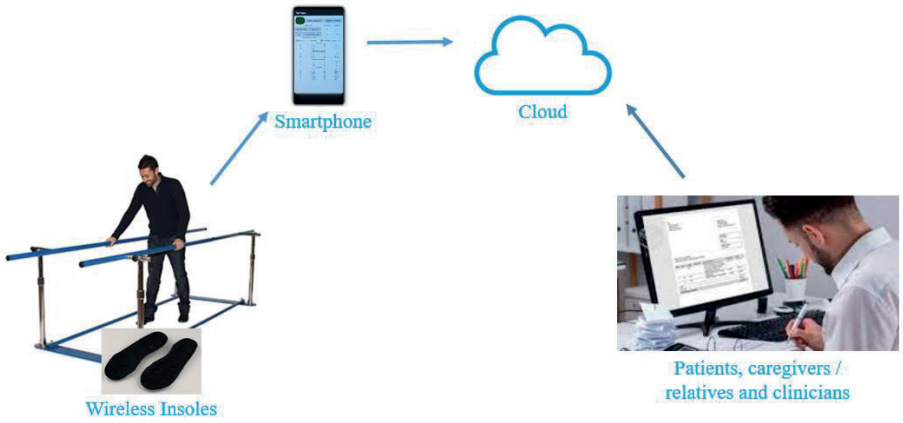

Figure 22: view of rehabilitation usage of the platform.

In essence, the MIoT platform serves as a valuable tool in the proactive management of post-surgery rehabilitation and fall prevention efforts, empowering both patients and healthcare providers with actionable insights and support throughout the recovery journey.

3.6. Summary of the chapter

This chapter introduces the MIoT platform developed for gait analysis, providing data to enhance the diagnosis of fall risk and post-lower limb surgery rehabilitation. The first section provides an overview of various studies on the detection and prevention of falls and how various systems are being worked on to reduce the number of falls or provide patient information. We introduce the insoles developed in the WIISEL European project together with the critical points that lead to a high failure rate. Based on those we implemented a new version for improve reliability (wireless connectivity and mechanical strength) and functionality (fall detection on LPWAN), and reduced cost (changing pressure sensors).

Gait monitoring can be done using different models: (1) at clinical premises or (2) patient's home in a telemedicine model and (3) by filtering continuous gate data acquired during daily life activities. We introduce the clinical tests currently used to assess fall risk by analyzing the patient's gait. These tests are used in many studies to analyze the patient's gait status,

giving a numerical assessment that help clinicians to give a better diagnosis and detect any anomaly that could end up leading to a fall. These tests have been applied in the smartphone app such that can be applied using a supervised model.

In these models, there is a direct correlation between falls risk evaluation and gait parameters evolution, categorized into spatial, temporal, and kinematic parameters. A similar model can be applied to hip and femur surgeries rehabilitation.

The components that make up the MIoT platform include the communication of the devices and integrated sensors to the cloud infrastructure and the data analysis carried out therein. Based on the data obtained in the previous design, work has been done to reduce the production cost, from €800 to €150. For this purpose, a more economical pressure sensor system has been implemented, also reducing the number of sensors from 14 to 6. As for the PCB, a small module has been created taking advantage of an SoC that includes all the communications necessary to the functioning of the system. Regarding connectivity with the smartphone, BLE technology and design techniques has been used to reduce consumption, extending the use time of the insoles from 6 to 12 hours of full continuous usage. This number has to be increased according to the duty cycle understood as the time that a person is moving compared to what is not. The mobile application has been developed from scratch incorporating screens to facilitate notification to emergency systems in the event of a fall. It also allows videoconferences with the clinician to be able to perform tests remotely without having to travel to the health center. In addition, the entire cloud service has been implemented again to easily offer the data to all the actors involved, such as patients, clinicians and the patient's family or caregivers and including hospital information system (HIS) deployment considerations on security and safety.

Unfortunately, the MIoT platform could not be validated in a clinical test for the prevention of falls due to the lack of funding but the entire system was prepared to carry out a clinical test monitoring the rehabilitation process at the Grenoble University Hospital. Unfortunately, that clinical trial was cancelled due to the emergence of the COVID-19 pandemic and consequently, once finished, the funding from the SERENE IoT project was ended.

4. Medical IoT Platform for Equilibrium Assessment

In this chapter, we introduce the work related to the development of a medical IoT platform aimed at balance/equilibrium assessment. The first section covers aspects related to equilibrium analysis. Next, we detail the medical tests focused on evaluating the patient's equilibrium-related condition and the clinical trial. Afterwards, the MIoT platform created for this purpose is explained. Finally, I discuss the results.

One of the primary risk factors for falls among the elderly is inadequate balance or equilibrium, affecting between 20% and 50% of adults aged 65 years or older. Research indicates that poor balance can lead to a threefold increase in the risk of falling. Despite this significant risk, few interventions have demonstrated effectiveness in preventing fall incidents [94]. The likelihood of fall-related injuries among elderly individuals stems from a heightened prevalence of clinical ailments such as osteoporosis, coupled with age-related physiological alterations like diminished protective reflexes, rendering even minor falls significantly perilous. According to authors in [95], gait and balance disorders or weakness are attributed to 17% of falls.

4.1. Balance/Equilibrium Analysis

In the literature, we find various proposals for conducting balance evaluation and analysis. They basically quantify different exercises to obtain a final score that serves to classify the patient. Next, the most relevant ones are presented.

4.1.1. BESTest

The BESTest, or Balance Evaluation Systems Test, is a clinical tool used to assess balance impairments in individuals [96]. It's particularly useful for evaluating balance disorders across various populations, including neurological and vestibular patients. Here's some key information about the BESTest:

It consists of 36 items organized into six sections, each targeting different aspects of balance control:

- Biomechanical Constraints: This section assesses the individual's ability to maintain balance while performing tasks that challenge their biomechanical stability.
- Stability Limits and Verticality: It evaluates the person's ability to maintain balance within their stability limits and perceive verticality.
- Anticipatory Postural Adjustments: This part focuses on the individual's ability to prepare and adjust their posture in anticipation of planned movements.
- Reactive Postural Control: It assesses how well the person can recover and regain balance following unexpected perturbations or disturbances.

- Sensory Orientation: This section examines the individual's ability to integrate sensory information from different systems (e.g., visual, vestibular, proprioceptive) to maintain balance.
- Stability in Gait: It evaluates the person's balance during various walking tasks and transitions.

Scores for each item in the BESTest are assigned according to the individual's performance, with ratings ranging from 0 (indicating severe impairment) to 3 (reflecting normal performance). Scores from all items are totaled to provide an overall balance score.

4.1.2. Berg Balance Test (BBS)

Developed by Katherine Berg in 1989, the Berg Balance Scale was designed to assess balance capabilities in older adults, with the original focus group having an average age of 73 years [97]. The primary objective of the Berg Balance Scale is to assess an individual's balance abilities and risk of falling. It helps healthcare professionals, such as physical therapists and occupational therapists, identify balance deficits and monitor changes in balance over time.

The BBS consists of 14 functional tasks that simulate daily activities requiring balance and mobility. These tasks include sitting, standing, transferring, and reaching in various directions. Each task is scored on a 5-point scale based on the individual's ability to perform it safely and independently.

The total score on the Berg Balance Scale ranges from 0 to 56, with higher scores indicating better balance and lower fall risk. The scores provide valuable information about the individual's overall balance abilities and functional mobility.

4.1.3. Tinetti

This test consists of two parts, the first of which focuses on gait, as introduced in the previous chapter. In this section, the test is introduced as part of the balance assessment, along with its specific exercises.

During the balance assessment, the individual is evaluated on their ability to maintain balance during various tasks, such as sitting, standing, and changing positions. Specific tasks may include sitting unsupported, standing up from a chair, maintaining standing balance with eyes open and closed, turning 360 degrees, and sitting down again. Each task is scored based on predefined criteria that assess the individual's stability and ability to perform the task safely.

4.1.4. Romberg

This test or trial was first presented by the German neurologist Moritz Heinrich Romberg (1795-1873) in his work "Lehrbuch der Nervenkrankheiten des Menschen" between 1840 and 1846.

The Romberg test, also known as Romberg's maneuver, is a study in clinical neurology, which assesses conscious proprioception, that is, the ability to control sudden alterations in joint position that require reflex muscle stabilization [98]. It is based on the assertion that balance is a combination of three neurological systems: vision, which adjusts where the body is at any given moment; the vestibular system, which informs the brain of the position of the head relative to the body; and proprioception, which is the knowledge of the body's position in space. In theory, even if one loses some of these faculties, a person should still be able to maintain balance.

The results of this test can help diagnose various pathologies, disorders of the vestibular system or related pathologies of the central nervous system.

4.2. Clinical Tests

In the current clinical test, the Romberg test is being utilized, which seamlessly integrates with the medical device employed for the assessment. In this context, a posturograph measures the individual's displacements during the test.

4.2.1. Test

The Romberg test is very simple to perform and does not require any type of physical or psychological preparation or the use of any equipment, although currently the posturograph platform is used to obtain numerical results that provide a quantitative conclusion about the patient's diagnosis.

The procedure is as follows:

1. The patient must stand with feet together and eyes open and maintain the posture for 30 seconds. Romberg Eyes Open (REO)
2. The patient must maintain the position for another thirty seconds but with eyes closed. Romberg Eyes Closed (REC)
3. The patient will be placed on a foam base and the two previous tests will be repeated for the same thirty seconds. Romberg Foam eyes Open (RFO) and eyes Closed (RFC)

The central nervous system, a complex network of nerves and structures within the body, plays a pivotal role in ensuring that our bodies maintain a stable position when upright. This

intricate system orchestrates a symphony of signals and responses, working tirelessly to uphold equilibrium and prevent falls or imbalance.

When we stand or sit upright, the central nervous system coordinates a delicate dance of sensory information and motor commands. It continuously processes feedback from various sources, including the inner ear, muscles, and joints, to gauge our body's position in space.

Remarkably, the balance achieved by the central nervous system can manifest in two distinct forms: dynamic and static. Dynamic balance refers to the ability to maintain stability while in motion, such as walking, running, or even dancing. On the other hand, static balance pertains to maintaining stability while at rest or in a stationary position.

To maintain balance, humans rely on three impulses to navigate the complexities of posture and movement. These impulses work harmoniously to uphold stability and grace in our everyday activities:

- Visual Impulse: a cornerstone of our perception and interaction with the world. Through visual cues, our brain gathers vital information about our surroundings, aiding in the stabilization of our posture and guiding our movements. Our eyes offer invaluable feedback to maintain equilibrium.
- Vestibular Impulse: Nestled within the labyrinthine structures of the inner ear lies the vestibular system, dedicated to the control of balance and coordination. The vestibular impulse integrates signals of motion and spatial orientation. The vestibular impulse manages our movements.
- Proprioceptive Impulse: This remarkable sense encompasses the awareness of our body's position, movement, and spatial orientation. Through proprioception, we intuitively sense the subtle nuances of joint motion, the contours of muscle tension, and the trajectory of our limbs in space.

When one of these impulses fails, the others stand ready to lend their support, forging a resilient network of compensation to preserve our balance and stability. Like skilled collaborators in a grand performance, the visual, vestibular, and proprioceptive impulses harmonize their efforts.

The Romberg test stands as a testament to the intricate interplay of these impulses. Placing the patient in a bipedal stance with eyes open, it invites scrutiny of the subtlest movements and shifts in balance. With eyes closed, the test unveils the intricate dance of compensation, revealing the resilience of the human body in its quest for equilibrium.

4.2.2. Posturograph medical device

The *Instituto Biomecánico de Valencia* (IBV) commercializes a measurement system based on dynamometric platforms (shown in Figure 23 [99]) designed to record and analyze the

reaction forces and movements performed by the subject on the ground during any type of human activity (walking, jumping, turning, standing, running, etc.).

Figure 23: Dynamometric platform.

The device (Figure 24) features a measurement area of 600x370 mm. It has a range of measurement in vertical forces of 4500 N and a range of measurement in horizontal forces of ±750 N. In terms of accuracy and repeatability in center of pressure calculation, it offers ±1 mm within the range of 0 – 40 mm and ±2 mm within the range of 40 – 200 mm.

Figure 24: Posturograph platform used for the clinical trial in the primary care medical center

NedSVE/IBV is marketed together with the sensor platform. This software is designed for the assessment and rehabilitation of balance pathologies by comparison with normal patterns. Balance function is considered to be the result of a sensory and motor complex, the purpose of which is the maintenance of posture. NedSVE/IBV detects abnormal behaviors in the maintenance of a given posture and analyzes the patient's response to alterations in visual and proprioceptive information that help him/her to achieve balance.

4.3. MIoT Platform for balance assessment

The MIoT platform developed for the evaluation of balance is introduced below. In the development of the platform, we considered the test to be carried out and which data are interesting to be able to evaluate and compare with the data obtained from the commercial system.

4.3.1. Device

The selected device offers the necessary features to be used simultaneously with the posturograph while the Romberg test is being performed. The main characteristic is that it does not disturb the patient's data collection and that these data are not altered by the presence of the device, so the device must be small, light, and easy to place on the patient's body. When it is necessary to obtain balance data, the best option is to place it on the belt, since this is the approximate point where a person's center of gravity is located. A couple of options have been tested as a sensor device such as the Garmin running pod and the creation of custom electronics with an inertial sensor.

Finally, we opted for the Nordic Thingy 52, a comprehensive IoT development kit engineered to facilitate rapid prototyping and experimentation in the Internet of Things applications. At its core lies the Nordic Semiconductor nRF52832 system-on-chip (SoC), renowned for its robust BLE connectivity and efficient performance. The Thingy 52 is equipped with a diverse array of onboard sensors, including environmental sensors such as temperature, humidity, air quality, and barometric pressure sensors, enabling precise environmental monitoring. Additionally, it features motion sensors such as an accelerometer, gyroscope, and magnetometer, facilitating motion detection and tracking functionalities. Figure 25 shown an image of the Thingy 52 device and the PCB.

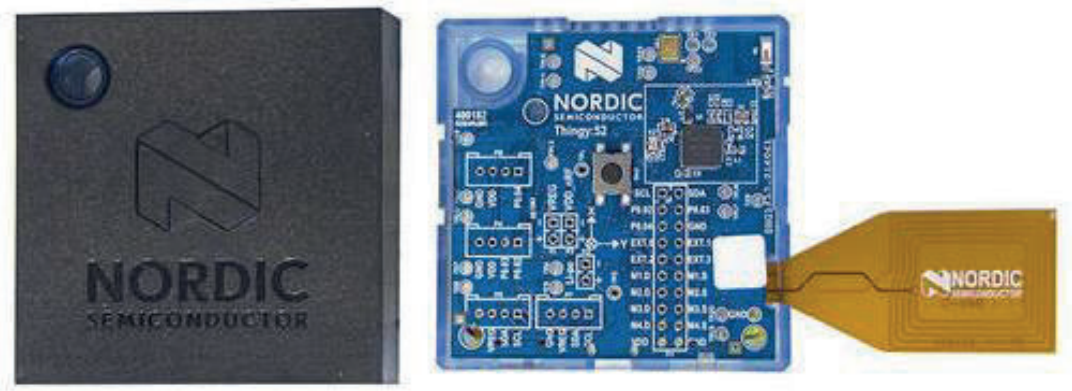

Figure 25: Thingy 52 device.

4.3.1.1. Sensors: IMU

Inside the device there are 2 IMUs, one of low precision focused on battery management and low power modes and the second one of high precision, the MPU-9250. This IMU integrates a tri-axis gyroscope, accelerometer, and magnetometer into a single compact package as in the previous case. This sensor module is engineered to provide precise motion tracking and orientation sensing across multiple axes.

The accelerometer is capable of measuring acceleration along three axes: X, Y, and Z. With a selectable full-scale range of ±2g, ±4g, ±8g, and ±16g. The tri-axis gyroscope has full-scale range options of ±250, ±500, ±1000, and ±2000 degrees per second (dps) for accurate tracking of rotational movements and orientation changes. The three-axis magnetometer has a full-scale range of ±4800 microteslas (uT), to provide information about the orientation of the device relative to the earth's magnetic field. The 3-axis represented over the chip are shown in Figure 26.

The MPU-9250 incorporates an integrated Digital Motion Processor (DMP) that implements the sensor fusion algorithms that combine data from the 3 sensors to provide accurate motion tracking and orientation estimation, reducing the computational burden on the host microcontroller and enabling seamless integration into a wide range of embedded systems.

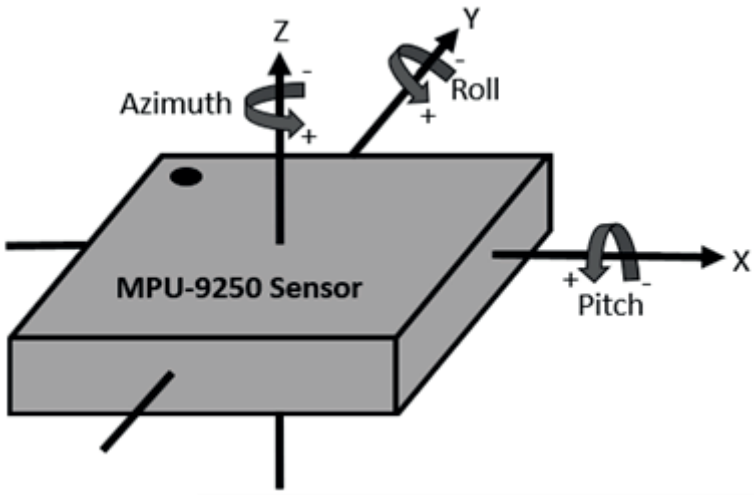

Figure 26: Axis direction on MPU-9250

4.3.1.2. Wireless communications: BLE

Two main Body Area Network (BAN) protocols for device-to-edge communications to smartphones are BLE and ANT+. ANT+ was initially utilized as it was the protocol associated with the first platform under development. However, upon realizing that the initial device did not meet the data capture requirements, it was replaced by the definitive device introduced earlier, which operates using BLE as its communication protocol.

BLE

Communication via Bluetooth Low Energy is facilitated through a custom GATT service designed to transmit information from the axes of the IMU, battery status, gravity vector, and quaternions using multiple characteristics.

Each component within the system operates with its unique characteristics. For the IMU data, a structure of 18 bytes is transmitted, with each axis encoded in specific formats: 16 bits are allocated in a 6Q10 fixed-point format for the accelerometer, 11Q5 for gyroscope data, and 12Q4 for the magnetometer. The gravity vector is packaged into a 12-byte data structure, with 4 bytes dedicated to each axis. Quaternion data is conveyed in 16 bytes, while battery information is encapsulated within 1 byte.

In total, 47 bytes of data are transmitted with each communication cycle, at a frequency of 33MHz or 33 messages per second.

4.3.1.3. SoCs

The system-on-chip (SoC) of Thingy 52 is the Nordic nRF52832, designed specifically for wireless connectivity and IoT applications, and powered by a 32-bit ARM Cortex-M4 processor, clocked at up to 64MHz. It integrates a Bluetooth Low Energy (BLE) radio that supports Bluetooth 5.2 specifications, enabling seamless communication with a wide range of devices and peripherals. This SoC also includes a large set of peripherals including GPIOs, UART, SPI, I2C, PWM, and ADC interfaces and security features such as AES encryption and a secure bootloader. The SoC also supports firmware updates OTA.

4.3.1.4. Belt 3D support

The device must be worn by the patient while performing various tests, so a 3D bracket has been designed to attach the Thingy device to the patient's belt. By placing the sensor device on the waist, we are measuring the patient's center of gravity during the different tests. Figure 27 (a) depicts the created 3D model and Figure 27 (b) shows the actual printed support with the device.

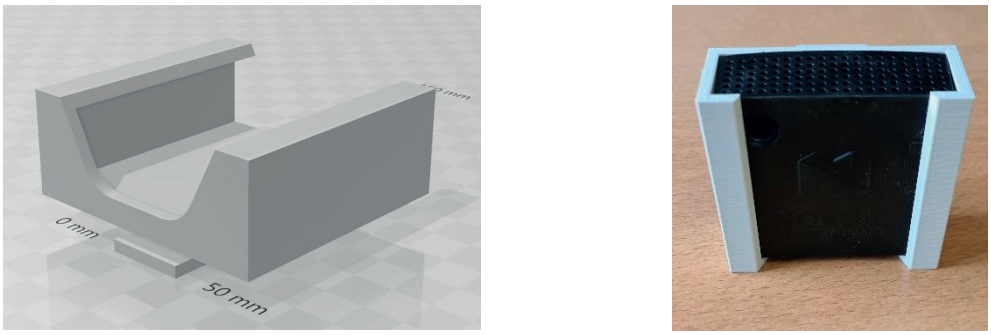

(a) (b)

Figure 27: Belt support (a) 3D model; (b) printed with Thingy device attached.

4.3.2. Edge

An Android-based device serves as the edge component. The application's design is tailored to ensure usability across both smartphones and tablets, accommodating a diverse range of user preferences and device types. For it use in primary care, we decided to use a tablet.

The primary function of the edge within the platform is to oversee and track the tests conducted by the patient. For each test, a dedicated screen is provided where the specific exercise being performed can be selected, along with the corresponding duration required to complete it. While the focus initially centers on a single test, Romberg, the application's architecture is flexible enough to support the integration of multiple tests seamlessly. This versatility ensures that the platform can adapt to evolving clinical requirements and incorporate diverse assessment protocols as needed.

4.3.2.1. User APP

The first version of the application is focused on a clinical test and has been designed so that the collected data are anonymous. Therefore, each patient is assigned a unique code provided by the clinical staff. Once the code is entered, the system starts storing sensor data, which are labeled based on the exercise indicated from the application. Figure 28 (a) Shown the initial screen with different test to perform, Balance (Romberg), SPPB, Tinetti, etc. On the left side the actual data captured in real time from the sensors. Figure 28 (b) depicts the screen with the Romberg test options to select from.

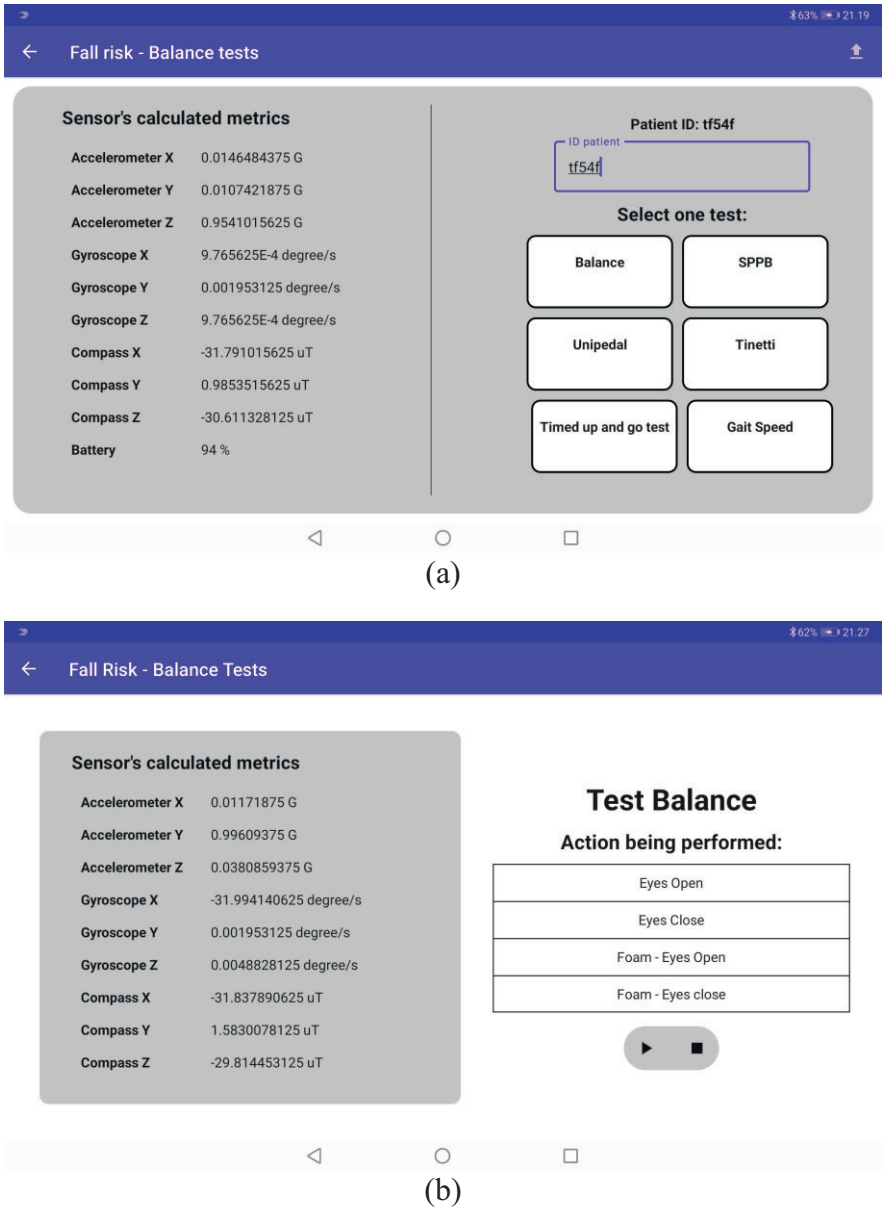

Figure 28: Test app (a) Initial screen with test menu; (b) Romberg test screen with 4 actions to select.

4.3.3. Cloud

The cloud server is responsible for analyzing the data received from the mobile application and performing an analysis. In order to receive data, the system has a web client listening to POST requests that come through an API. When a new request is handled, the client uploads the file with the data, and they are stored on the server's disk awaiting analysis.

To visualize the data, a module has been implemented for a desktop application, as shown in the Figure 29, which allows loading test data for a client and visualizing its graphical

representation. These images correspond to the data obtained from the same test conducted both on the posturograph (right) and using the IMU device (left). We can clearly observe that the first provides only two-dimensional data while the second can draw 3D.

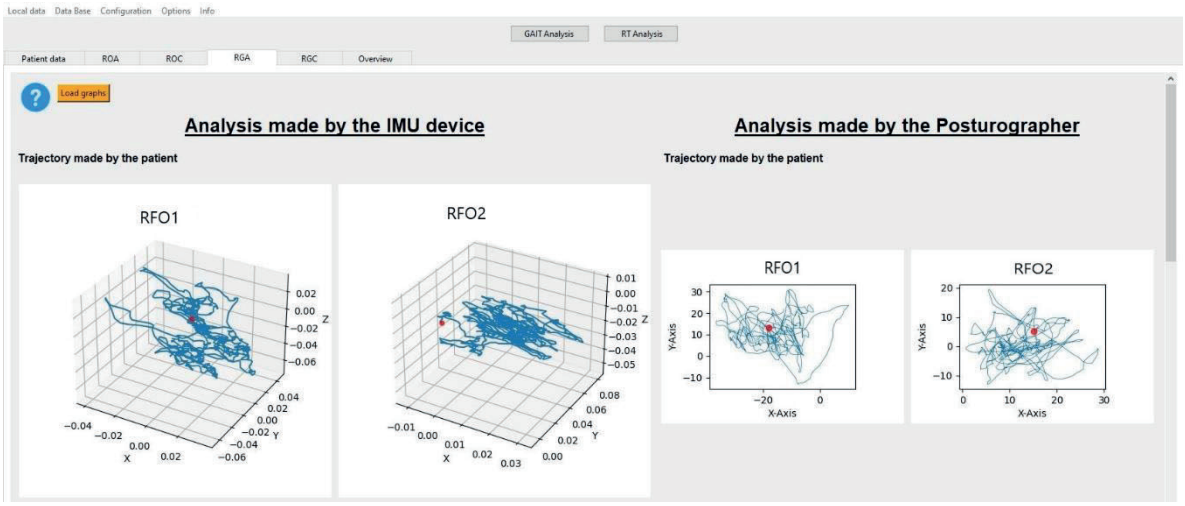

Figure 29: Viewer tool for clinicians showing IMU and Posturograph data.

4.4. Experimentation in a Clinical Study

To validate the MIoT platform we had the opportunity to link our research to a clinical study from Institut Universitari d'Investigació en Atenció Primària (IDIAP) Jordi Gol, Unitat de Suport a la Recerca Metropolitana Nord. The clinical trial was conducted at the primary care center in Mataró with 70 patients aged between 68 and 72 years. Each patient undergoes a series of tests to assess their balance. A posturograph device from IBV is used for this purpose, performing the Romberg test. This device provides scores that assess visual, vestibular, and proprioceptive impulses. In order to evaluate the IoT solution proposed in this chapter, the device is placed at the patient's waist to capture the test data and assess them, comparing them with the data obtained from the posturograph.

4.4.1. Posturograph data

The posturograph measures the displacement experienced by the patient while standing on the platform for 30 seconds. Figure 30 shows a patient performing one of the Romberg tests on a foam. These data are used by the proprietary software to perform calculations and provide patient assessment by capturing 40 values per second, providing 1200 values for each test conducted. With these values, it calculates for each displacement, angle, area, and movement speed.

Figure 30: Patient on posturograph device during Romberg Foam test.

From the patient's displacement points, we can extract all the resulting values. To do this, we need to find the formulas that determine each of the values we want to calculate. In our case we are calculating Total displacement, Medio-Lateral (ML) and Antero-Posterior (AP) dispersion and displacement, Area, and Angle.

Total displacement

During the test, the points by which the patient's center of gravity moves on the platform are stored. The total displacement refers to the displacement from the center of the platform to the center of the point cloud (displacement vector) resulting from the test. First the center of the point cloud (Cx, Cy) is calculated by adding all the points X (p_x) or Y (p_y) divided by the number of points (#p) and then the Pythagoras theorem is applied to find the distance (D_{total}).

$$C_x = \frac{\sum p_y}{\#p}, C_y = \frac{\sum p_y}{\#p}$$

$$D_{total} = \sqrt{c_x^2 + c_y^2}$$

Total angle

The total angle has been calculated as the angle between the displacement vector calculated previously and the x-axis.

$$\alpha = \arctan\left(\frac{c_x}{c_y}\right)$$

ML and AP dispersion

The dispersion is calculated by the standard deviation of the points in the x (ML) and y (AP) directions relative to the center of the point cloud.

$$D_{ML} = \frac{\sqrt{\sum((p_x - c_x)^2}}{\#p}$$

$$D_{AP} = \frac{\sqrt{\sum((p_y - c_y)^2}}{\#p}$$

ML and AP displacement

The ML displacement has been calculated as the displacement between the maximum and minimum values of the first component of the points, while for the AP displacement, the same calculation has been performed but with the second component.

$$D_{ML} = \max\ (p_x) - \min(p_x)$$

$$D_{AP} = \max\ \left(p_y\right) - \min\left(p_y\right)$$

Area

The swept area is approximate area in which the subject swings, calculated from the instant the test starts until the end of the test. To calculate it, first it is necessary to find the eigenvalues ($\lambda_{1,2}$) of the covariance matrix of the centered point cloud, and then calculate the square root of the product of the eigenvalues multiplied by 4.

$$\lambda_{1,2} = eigenvalues(Cov(p - \overline{p}))$$

$$Area = 4\sqrt{\lambda_1 \lambda_2}$$

4.4.2. IMU data

To capture the data to compare with the medical device, the MIoT platform device proposed and detailed in section 4.3.1 has been used. This device is placed on the patient's belt to capture the test data simultaneously with the performance on the posturograph.

The device has collected data from each patient. The obtained data is 3 axis accelerometer, 3 axis gyroscope and 3 axis magnetometers, as well as quaternion and gravity vector from fusion data.

4.4.3. Data analysis

First, an analysis of the displacement results is conducted. As can be observed, the initial differences arise when only analyzing the values without foam with eyes open (Figure 31 a) or closed (Figure 31 b). When closing the eyes, the patient loses reference from one of the three systems involved in balance, and the other two systems must compensate for this loss. If the patient experiences dizziness (vestibular system) or has a leg injury (proprioceptive system), losing vision would quickly disrupt balance.

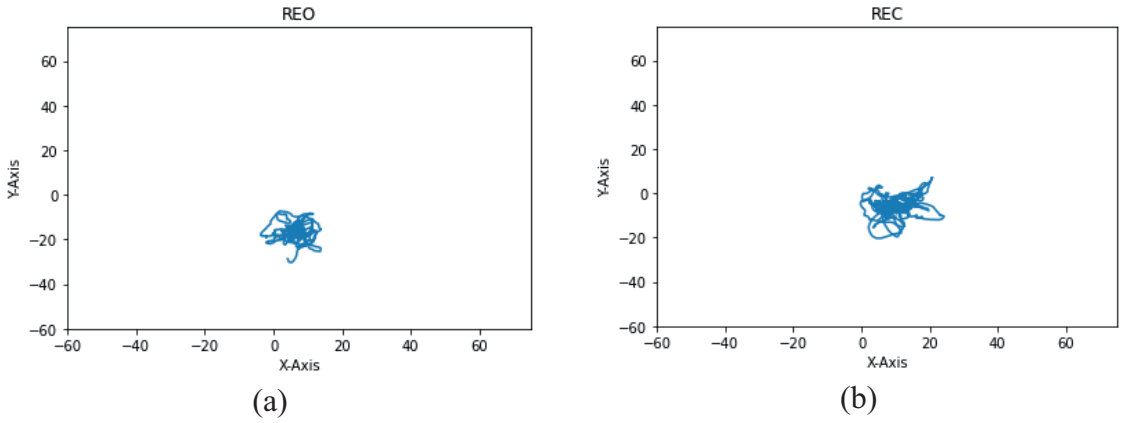

Figure 31: Results from posturograph device after Romberg test with (a) Eyes open; (b) Eyes closed.

Analyzing the difference between tests without foam and with foam, we notice that the patient begins to make wider displacements. This is because introducing the foam affects the proprioceptive system, making the surface unstable and requiring the patient to rely on the visual and vestibular systems to maintain balance. When closing the eyes while using foam, the visual component is lost, allowing for the analysis of proprioceptive behavior, and especially the vestibular system.

Figure 32 (a), shows how the patient on the foam begins to make more pronounced displacements than without the foam, but the visual system provides more reference for stabilization. At the moment when he closes his eyes, as shown in the Figure 32 (b), it is easy to appreciate how his balance is affected by the visual loss, and his displacements are much more pronounced.

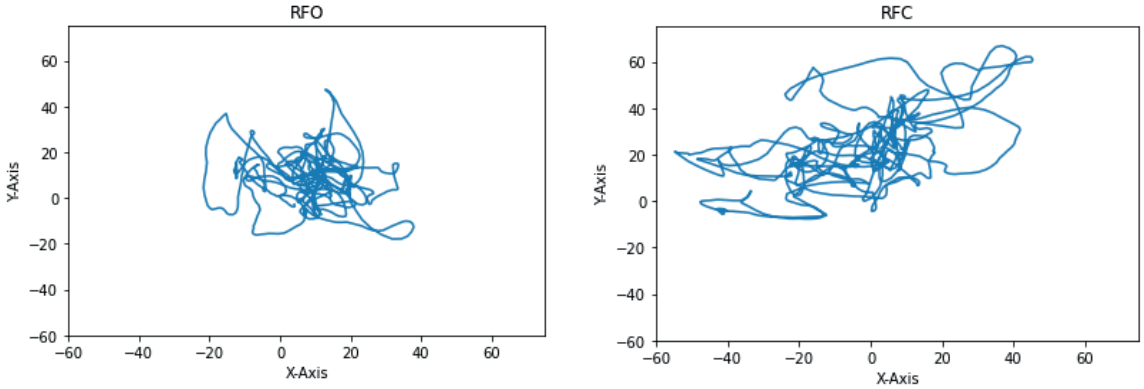

Figure 32: Result from posturograph device after Romberg test over Foam with (a) Eyes open; (b) Eyes close.

Analyzing the data obtained from each test, focusing on acceleration, in Figure 33 (a) we observe that the patient performs the test without the system detecting any issues. However, if we look at Figure 33 (b), we can see how, towards the end of the test, the patient makes a sudden movement that is reflected in the accelerometer. The peaks in the X and Y acceleration axis indicate that the person has experienced imbalance in that direction.

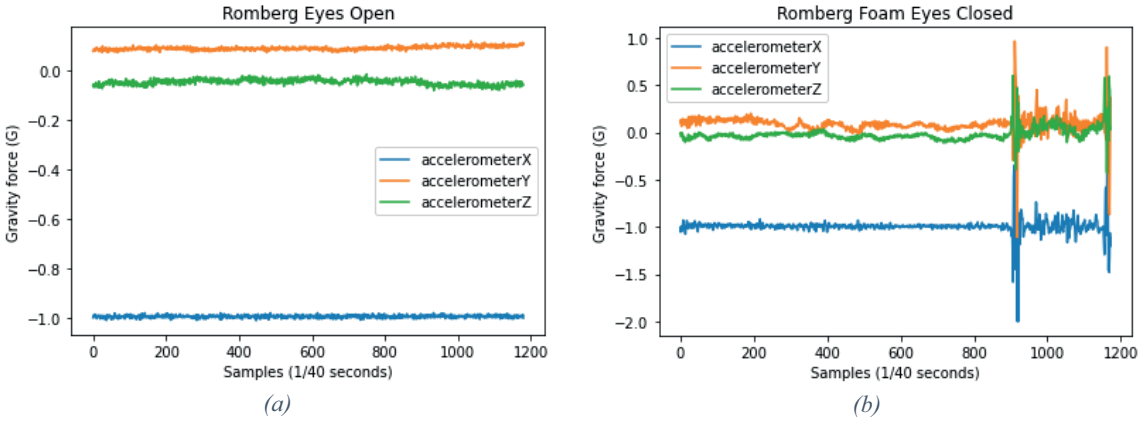

Figure 33: IMU Acceleration output of the Romberg test (a) Eyes open; (b) with Foam Eyes close.

4.5. Results

In this section we are trying to mimic the results obtained by the Posturograph, as a golden reference, with our MIoT device. The model must obtain the final values for the vestibular index. We tried two different models: (1) a mathematical model and (2) and AI algorithm using recurrent neural networks.

Recurrent Neural Networks (RNNs) are suitable for processing data sequences with temporal dependencies. RNNs are capable of capturing hidden correlations and trends present in trajectory data, making them an optimal choice for processing sequences of three vectors

representing trajectory points at different time instants. The RNN is a neural network that incorporates data feedback, allowing outputs from a previous time step to be used as input for the current time step. This mechanism enables the network to store and process long sequences with temporal dependencies.

4.5.1. Posturograph mathematical model

The posturograph device obtains 1200 values for each one of the tests, with these values calculations are made to calculate different parameters of the test results such as total displacement, swept area, angle. Being a closed software it is not possible to access the data used to perform the final assessment for the 3 indices: visual, vestibular, and somatosensory, which indicate the patient's condition. We extracted the mathematical formulas used by the proprietary software of the posturograph to calculate the parameters.

Model fit can be assessed by calculating and averaging the coefficient of determination (R-squared) for each participant and metric. As can be seen in Table 4, the values are calculated correctly except for mean velocity. Analyzing the velocity parameter, there are a few patients' data with a 0 in that field. This produces an error in the calculation.

Metric	R^2
Total Displacement	0.997
Angle	0.999
ML Dispersion	0.978
AP Dispersion	0.994
Area	0.994
Mean Velocity	0.829
ML Displacement	0.949
AP Displacement	0.999

Table 4: Coefficient of determination for posturograph data.

The results of each index have not been possible to calculate mathematically as there is no relationship found between the calculated values and the outcome of each test. It has been concluded that they use a database to estimate the result of each test based on the age and intermediate values calculated for each patient.

4.5.2. Posturograph AI model

The dataset consists of tests conducted on 70 individuals, each of whom has the result of the 3 indices calculated by the posturograph system, which we aim to replicate using neural

networks. As shown in Figure 34 , both the (a) somatosensory and (b) visual indices have ~85% of results at 1, with hardly any results below 0.9. However, in the (b) vestibular index, we can see that patients with values of 0 appear. We will use this index to attempt to replicate the posturograph results and subsequently do the same with the data obtained from the IMU.

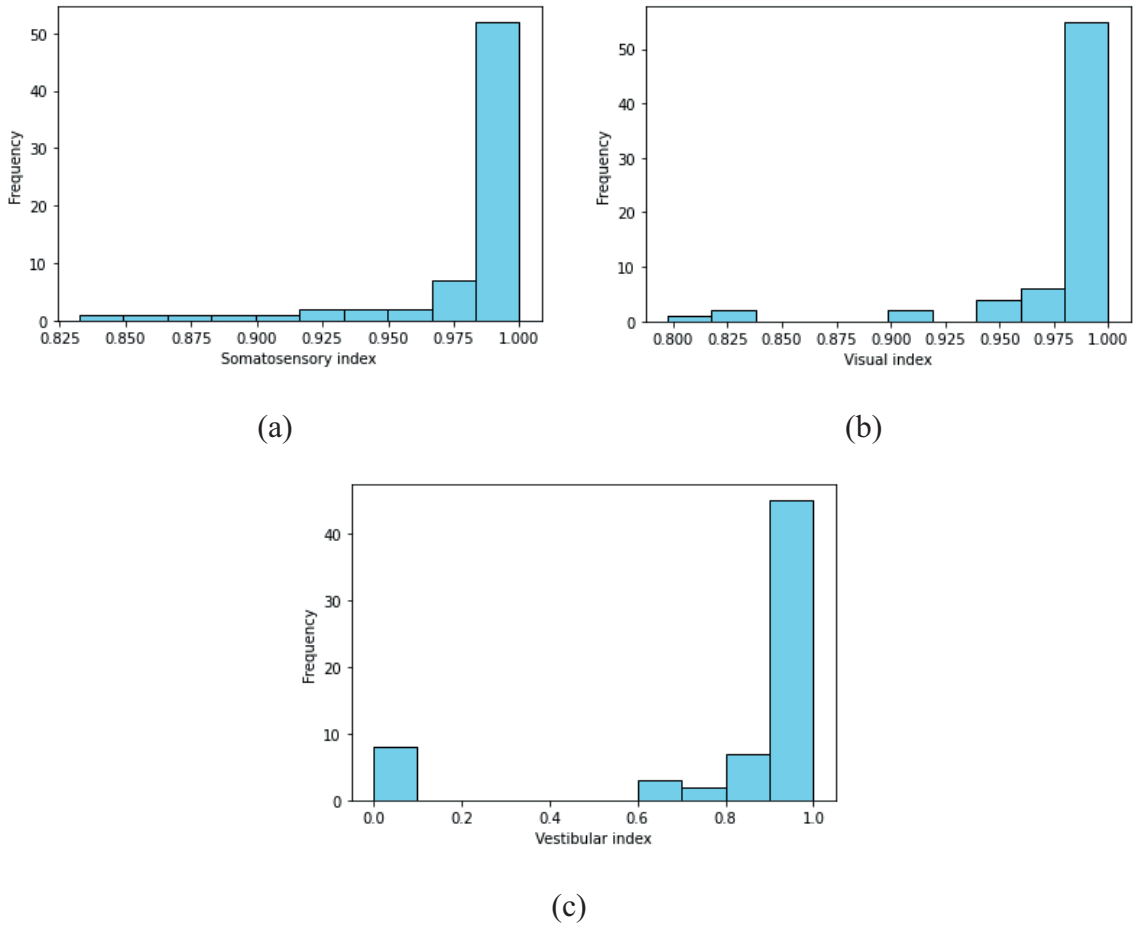

Figure 34: Frequency of occurrence for each index (a) Somatosensory; (b) Visual; (c) Vestibular.

We divide the patients into two groups, one for training where 80% of the data will be assigned, and another for testing to verify the prediction of our model. This results in 38 samples with a value of 1 and 6 samples with a value of 0 for the training group, and 10 samples with a value of 1 and 2 samples with a value of 0.

We decided to use a recurrent neural network to obtain a model of the posturograph algorithm. The model uses Gated Recurrent Units (GRU) as shown in Figure 35. In a first approach we used raw data, employing 1200 values for each axis, while we tried to improve it by using an autoencoder to reduce the dimensionality of the data sequence.

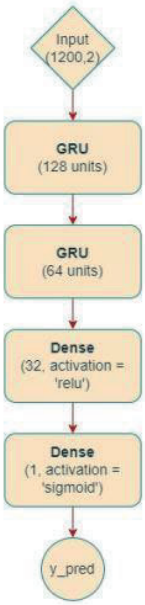

Figure 35: Architecture of AI models for the posturograph data.

Considering only the values of the mean absolute error and loss, Figure 36 shows that the algorithm seems to achieve good performance since the values are small and a slight decrease is observed. However, when we make predictions with samples from the test set (Table 5), we observe that the network only learned to generate almost always the same output and does not deviate much from any of the most repeated values. Same behavior happens with the model trained with data from the autoencoder, shown in Figure 37. The results from prediction are not as good as the previous case (Table 6).

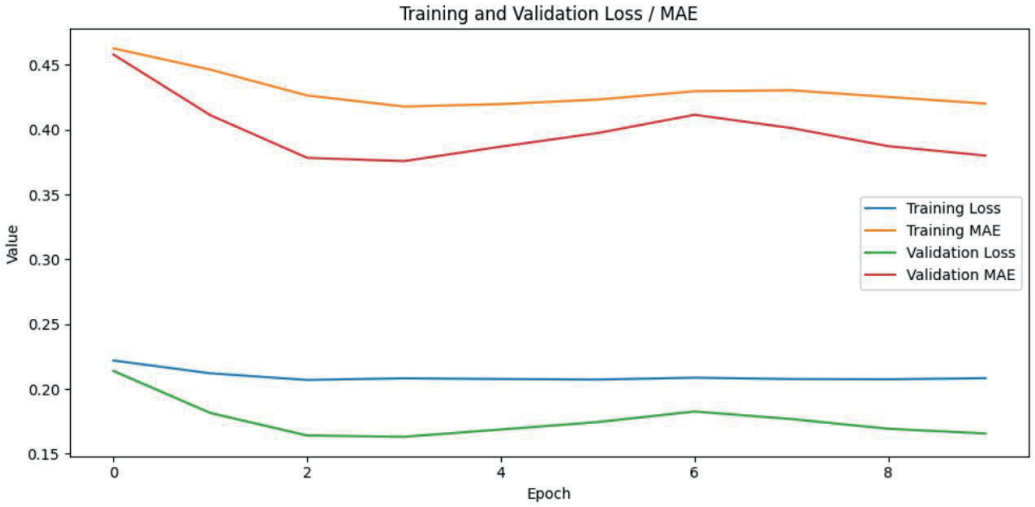

Figure 36: Evolution of the loss and the average of the absolute error during the training and validation of the network trained with the raw data from posturograph on the GRU.

Prediction	Dataset
0.6626099	1
0.62722147	1
0.84453857	1
0.66952425	1
0.660738	1
0.64422446	0.95
0.6469535	1
0.6113506	0
0.65072644	0
0.6452255	0.63
0.6572629	0.83
0.63271946	1
0.67229617	0.98
0.64583224	1

Table 5: Results from the test set compared with posturograph values using RAW data on a GRU.

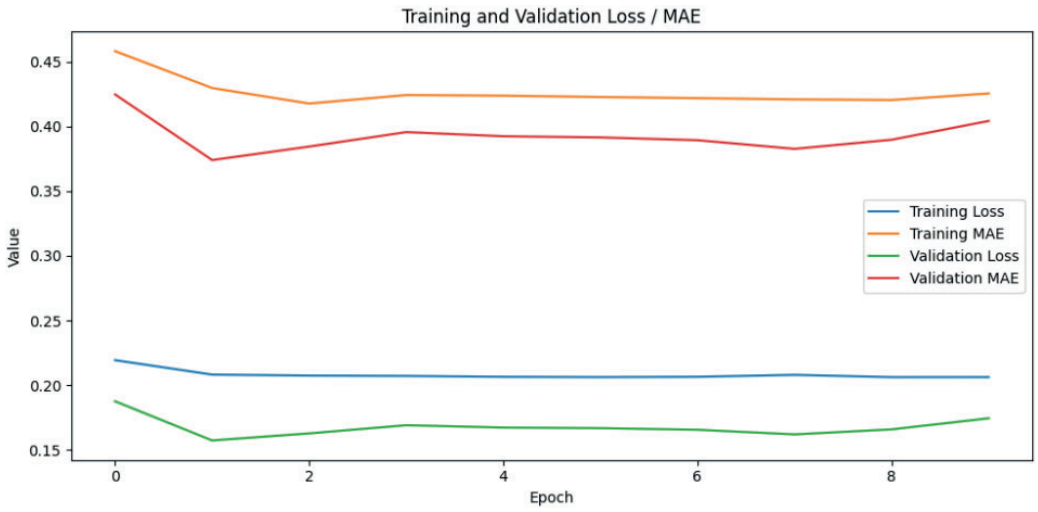

Figure 37: Evolution of the loss and the average of the absolute error during the training and validation of the network trained with the reduced autoencoder data from posturograph.

Prediction	Dataset
0.6135	1
0.6798	1
0.6289	0
0.6028	0
0.5856	1

Table 6: Results from the test set compared with posturograph using reduced autoencoder data.

4.5.3. IMU

Another approach has been based on LSTM recurrent networks. The first approach uses a simple implementation of LSTM to calculate the value of one of the output indices reported by the posturograph with IMU data as inputs. Figure 38 shows that the neural network memorizes the training samples, and when exposed to the validation samples, it is unable to correctly predict those samples where the score is below 90 (Table 7).

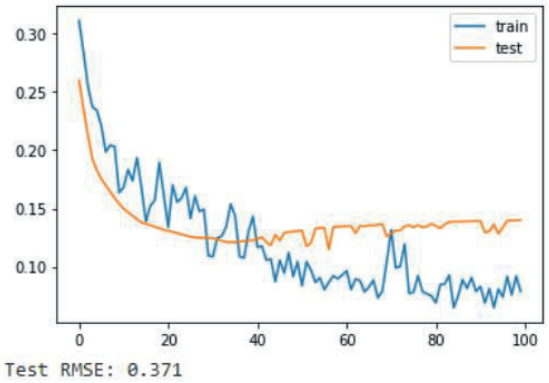

Figure 38: RMSE in the trained LSTM.

Prediction	Dataset
0.9853	0.85
0.9838	1
0.9844	0.98
0.9851	0.95
0.9802	0.63

Table 7: Result LSTM model.

A second model have been built to attempt to predict the VEST index using the IMU data. The model consists of the union of four LSTM-type networks, each designed to process one

of the features collected by the IMU: acceleration, gyroscope, magnetometer, and gravity vector, Figure 39.

To ensure that both data and features are on the same scale and dimensionality, a function was used to map three-dimensional data, into the two-dimensional planar format used by the posturograph by applying min-max scaling normalization with the MinMaxScaler function.

Therefore, in the first LSTM modeling attempt, we used raw data with normalization. The four networks consist of a Long Short Term Memory layer that receives the three feature vectors (one for each axis), a Dropout layer to regularize the model and prevent overfitting, with a dropout probability of 30% for each neuron, and finally, a fully connected layer with a single neuron (Dense layer). This last layer provides the individual model output, a value between 0 and 1, as sigmoid activation is used. Once the four networks are trained individually, the LSTM layers are concatenated and create a deeper and more complex neural network.

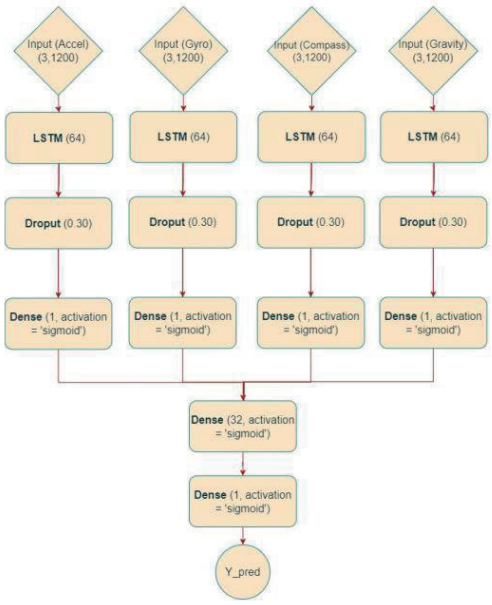

Figure 39: Combined LSTM.

This network has been trained with custom initial weights that give more weight to samples with index 0, as it is the minority class in the datasets. The results (Table 8) give a worse result than the simpler method explained previously.

Prediction	Dataset
0.3388	1
0.3388	1
0.3389	0
0.3388	1
0.3388	0.63

Table 8: Results combination of 4 LSTM networks.

Before training the network, it can be anticipated that obtaining good performance will not be easy due to the small data sets available and highly unbalanced classes. Therefore, in addition to trying different types of RNN architectures, two approaches will be considered: (i) estimation of the index as a continuous value and (ii) a binary classification considering 2 outputs: class 1 or positive sample (VEST index less than 50), and class 2 or negative sample (VEST index greater than 50).

Finally, four different neural networks have been created: (1) GRU for regression, (2) GRU for binary classification, (3) LSTM for regression and (4) LSTM for binary classification.

The main architecture of the four networks is very similar. The first layer is an LSTM/GRU layer with 32, 64, or 128 units, the second layer is again an LSTM/GRU layer with 16, 32, or 64 units, the output of this layer is fully connected to a Dense layer with 8, 16, or 32 neurons, and finally, depending on whether it is regression or binary classification, the last layer consists of a Dense layer with 1 or 2 units, respectively. In the case of regression, the activation function of this last layer is the Sigmoid function, and in the case of binary classification, the SoftMax function is used as it provides probabilities. Figure 40 shows the scheme of the GRU-type network performing (a) binary classification (b) regression.

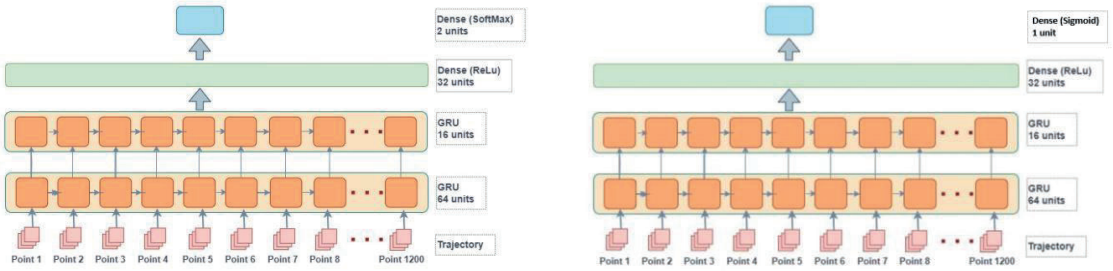

(a) (b)

Figure 40: GRU multilayer network diagram (a) Binary classification; (b) Regression.

The number of units in the layers and the learning rate (LR), and the number of epochs has been defined for each network through an exhaustive search using the Cross Validation

technique. To find the best combination, the training samples are divided into a specified number of groups (3 in this case). The model is trained for each value of the hyperparameters on n-1 subsets of the samples, and the result is validated with the remaining subset. In this type of Cross Validation, only certain random combinations of the specified hyperparameters are tried. The winner parameters in cross validation are shown in Table 9.

Model	gru_units	gru_units2	dense_units	LR
GRU reg.	32	16	32	0.01
GRU class. bin.	64	16	8	0.01
LSTM reg.	32	64	32	0.01
LSTM class. bin.	128	32	32	0.001

Table 9: Winner parameters in CrossValidation.

The 4 neural networks with the calculated parameters had different behavior, as shown in Table 10. The model GRU regression seems to be the best implementation, but the prediction results are not good as seen in Table 11.

Model	Loss	Metric
GRU regression	0.2044	0.3966 (MAE)
GRU Binary classification	0.8424	0.6666 (Accuracy)
LSTM regression	0.2179	0.4138 (MAE)
STM Binary classification	0.6997	0.6190 (Accuracy)

Table 10: Model results with found parameters.

Prediction	Dataset
0.6151087	0
0.66758496	1
0.7172315	0.98
0.7013795	0.63
0.54390967	1
0.69071686	0
0.67489606	1
0.62560946	0.97
0.6653189	0

Table 11: Prediction results GRU regression.

4.6. Summary of the chapter

In this chapter, we delve into the MIoT platform for balance assessment. Again, we initially introduce the tests commonly employed in healthcare settings to assess and monitor an individual's balance status. These tests serve as essential tools in evaluating overall physical health and identifying potential risk factors for falls and other mobility-related issues.

In this case, we start from a clinical study before building the MIoT platform. That study is based on the use of a posturograph as a medical device that will be considered the golden reference for evaluating the effectiveness of our platform's balance analysis capabilities.

Next, we detail the components that make up that specific MIoT platform, shedding light on the underlying technology and architecture that enable balance analysis and data processing.

As we capture data along the clinical study, we delve into the data collected during the balance assessment tests, examining key metrics and variables that offer valuable insights into an individual's balance and stability. During the study, it was not possible to capture many patients' data due to the duration of the different phases of the test, resulting in few participants in each session. Additionally, since participants were voluntary, the number of people taking the test each week varied, sometimes resulting in no patients during certain times of the year.

Finally, we present the findings of the clinical study, highlighting the outcomes and implications of our platform's balance analysis capabilities. Through an analysis and interpretation of our results, we conclude that neither the mathematical models nor the AI algorithms that we tried can reproduce the results provided by the posturograph. A key issue is the reduced number of patients that show balance problems (8 out of 70) what let into a poor data set. Given these data considerations, the idea of applying Data Augmentation to the dataset was not shown useful due to the limited variability in the output data. Engaging in such a task would have resulted in the creation of numerous synthetic data points, yet it would have replicated the same minimal variability observed in the patient data with balance issues.

After assisting the clinicians in their clinical trials, we believe that the tridimensional capability of the IMUs should at the end provide a more complete balance index. For that, in depth study should be carried out together with a clinician research team.

5. Technoeconomic impact of MIoT platforms in Catalonia

One of the main conclusions of the technological developments linked to clinical medical trials, is the different time scales of both engineering and medical disciplines that led to a complex and long iterations. This is reflected in the typical time-to-market duration of startups. It is said that ICT engineering startups crossing point (time to bet benefits) is 5 years while in medical ones is 10 years, mostly due to the duration of clinical trials and certifications. That misalignment indicates the complexity of joint research between engineers and clinicians.

After experiencing those problems for fall prediction, surgery rehabilitation and balance assessment detailed in previous chapters, this chapter introduces the research done for the estimation of the economic impact of our medical IoT platforms on a given population. The study aims to quantify the costs and benefits associated with the deployment of medical IoT platforms, providing valuable information on their financial viability and potential return on investment (ROI). Leveraging economic methodologies, this study seeks to elucidate the direct and indirect costs incurred throughout the platform lifecycle, along with social benefits and care outcomes. That should provide the criteria to support the decision of investing or not on those platforms. The chapter focuses on the public health provisioning models present in the European Union, much different than private systems more popular in other countries such as the United States, provided by medical insurance companies.

The technoeconomic analysis refers to the process of evaluating the economic aspects of technological developments or innovations. It involves assessing the costs, benefits, risks, and overall economic implications associated with adopting, implementing, or investing in specific technologies. Typically considers factors such as capital investment requirements, operational costs, potential revenue generation, cost savings, market demand, competition, regulatory constraints, and the broader economic impact on various stakeholders. The goal is to provide decision-makers with insights and information to make informed choices regarding the deployment or utilization of technology, ensuring that investments are economically viable and aligned with strategic objectives [100], [101].

The methodology used for this study starts from a global estimation of the impact of three health monitoring that our MIoT platforms for gait analysis can cover: equilibrium assessment, monitoring of fall risk for fall prevention and surgery rehabilitation. The technoeconomic analysis will be different for the three cases since they have different requirements in terms of usage and duration. Furthermore, for equilibrium assessment, we will be based on data obtained through a clinical study while the fall prevention and surgery recovery we will perform an estimation based on developed MIoT prototypes. The cost

model depends on the (public) health service model. Our results refer the Catalan region for which we collected the corresponding cost and patients' data.

5.1. MioT Platform cost model

Currently in the market, there are different business models in the IoT domain that account for different assets (device, communication, smartphone app, cloud storage and analytics, service, etc.). When restricted to MIoT there are mainly two main models that roughly depend on the public health model: private or public. In countries with mostly private health systems, companies offer services directly to consumers (patients). An ex-ample of those are panic buttons with fall detection that rely on monthly fees for an emergency service. In countries with mostly public health systems (like Catalonia), is the administration who provides, directly or through a third-party, the service to the users/customers. Most panic buttons are provided by the social services, nowadays being integrated in the health systems. There is also a rising private initiative linked to home security providers.

In both health system scenarios, these services encompass the IoT device, communication (directly to the cloud or through another provider), and services associated with the cloud infrastructure housing user data. As mentioned, our focus lies on this latter model, as we intend to apply the analysis to our public health service.

We consider that the public health system purchases the MIoT platform through a public tender that includes: (i) providing devices and smartphone apps to users during the period of time required for every procedure; (ii) cloud data collection, storage, computation, access to users and clinicians, and interoperability to the public health platforms; (iii) the information technology (IT) personnel costs related to the training for patients, professionals, as well as the telehealth service for patients, support for health centers, maintenance of devices, etc.

Different cases will involve varying devices based on parameter monitoring requirements and usage models regarding frequency and placement. Consequently, these devices will incur differing costs. Edge costs will remain consistent across cases, requiring a smartphone to monitor the device and bridge data to the cloud. Cloud expenses depend on factors like connectivity, storage, and computational needs, varying across cases based on the number of monitored patients, data volume, and computation requirements.

Security and privacy are pivotal aspects ensured by ICT technologies at all levels. The platform also addresses accessibility concerns through various means. Although a significant portion of the elderly population may not use smartphones or have usage limitations, societal trends indicate a reduction in this barrier. Additionally, current device and smartphone app designs help mitigate other accessibility issues related to visual or mechanical impairments.

5.2. Healthcare figures for Catalonia

As previously stated, our objective is to enhance access to a system that enables medical tests to be conducted easily at home, thereby eliminating the need for patients to travel to primary health centers or for clinicians to visit patients' homes. Population demographics are crucial for assessing the costs associated with any technological implementation. Catalonia, situated in northeastern Spain, boasts a population of 7.8 million individuals distributed unevenly: the metropolitan area of Barcelona is home to 5.5 million residents, while the other three provincial capital cities accommodate 1.5 million inhabitants. Approximately 1 million people reside in rural areas, small towns, or villages, with a significant proportion inhabiting mountainous regions. Across the region, there are 420 primary care centers, primarily concentrated in densely populated areas, necessitating travel for medical attention. According to statistics from the regional government [102], roughly 20% of this population is aged over 65 years old.

5.3. Fall prevention case

In a recent study carried out in Spain [103] with 770 participants, it was found that 28.4% (CI 24.9-32.1) experienced at least one fall annually. Additionally, 9.9% (CI 7.4-11.4) reported multiple falls. One third of all falls were attributed to accidental extrinsic causes. Among those who fell, 9.3% sustained fractures (including 3.1% with hip fractures), and 55.4% required medical assistance, with 29% visiting hospital emergency rooms and 7.3% being admitted. The overall incidence rate of falls was 0.64%, and it increased with age (mean age: 71.06 years). Patients in medical care areas exhibited the highest percentage of falls (63.7%). Men had a 1.33 times higher likelihood of falling compared to women. Variations in age, fall risk type, and circumstances were noted based on the type of hospitalization. Multivariate analysis revealed that patients undergoing other medical treatments experienced falls with more severe consequences (7.01%, CI 1.34-36.79) compared to those classified as "low risk" (2.40%, CI 1.02-5.65) [104].

As reported in [105], on average, 8% of the population aged over 65 years are at high risk of falling (experiencing more than one fall per year). We adopt this estimation as applicable to Catalonia for calculating the expenses associated with implementing an autonomous system designed to prevent falls among the elderly. The average cost per fall is estimated at 473€ per person annually [106]. This figure encompasses the expenses related to emergency services, medical care (ranging from minor injuries to surgery or fatalities), and social services.

The monitoring MIoT system discussed in this case analysis is built upon the platform outlined in Chapter 3 of this thesis. This platform comprises a pair of insoles housing an IMU and a pressure sensor surface for extracting gait parameters from patients, a smartphone

application, and a cloud infrastructure where a fall risk index is computed. Additionally, a user interface enables clinicians to customize the index based on the patient's health status.

The objective of our analysis is to identify the threshold at which the cost savings resulting from the reduction in falls offset the expenses associated with deploying the MIoT solution. Given the absence of any other method for continuous monitoring of fall risk, our aim is to determine the point of financial equilibrium.

As explained within the platform development, specifically detailed in section 3.3, the projected cost of the MIoT device is approximated at 150 euros, while the cloud expenses are estimated at 3€ per individual. This higher cloud cost reflects the escalated demands for data storage and computational resources, particularly in the context of its utilization within activities of daily living (ADL). Furthermore, we posit that the remaining costs, encompassing the smartphone application, training, service provision, among others, align closely with those observed in preceding cases.

Figure 41 illustrates that, in this framework, the deployment costs associated with the MIoT platform offset the costs associated with falls when its effectiveness results in a 45% reduction in falls. Moreover, the potential for economies of scale in this context remains significant. Figure 42, shows the decrease in this break-even point according to the cost of the MIoT device.

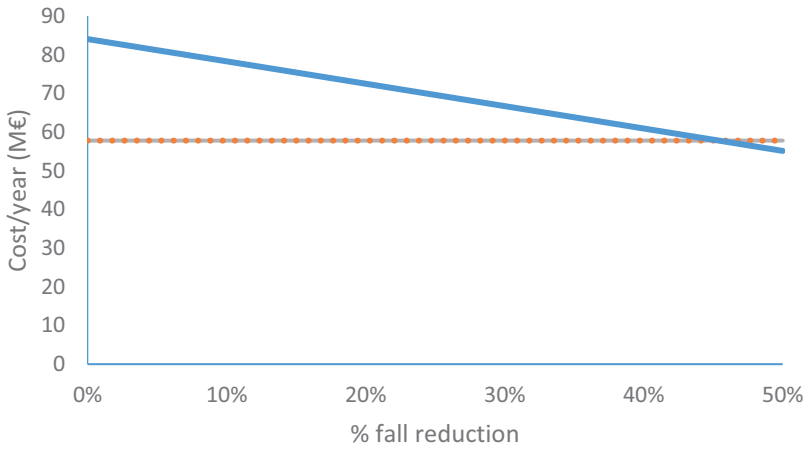

Figure 41: Cost of the fall to the health system using the proposed MIoT solution (blue) according to the reduction of the number of falls compared with the cost without reduction (dotted orange).

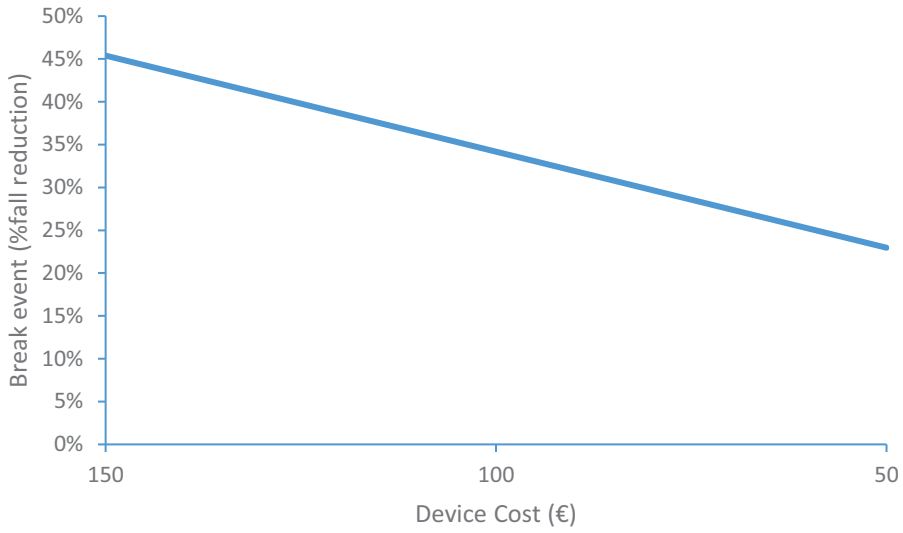

Figure 42: Reduction of the break event (% of fall reduction) depending on the MIoT device cost.

5.4. Surgery recovery case

In Catalonia, Cancio et al. [107] provided a comprehensive study on the impact of femur fractures on the population. Among the conclusions, we extracted that the average cost per patient during the 12 months post-fracture is estimated as 10,797 euros, contrasting with 4,076 euros in the year preceding the fracture. This results in a 6,721 euro increase per patient. Hospital admissions account for 62% of the costs, with 31% attributed to social-health resource utilization, and 80% incurred within the initial 6 months. Among 905 women and 337 men with initial fractures, 253 women and 71 men experienced subsequent fractures, with a relative risk (RR) of 1.95 (95% confidence interval -CI-, 1.70-2.25) for women and 3.47 (95% CI, 2.68-4.48) for men [108]. As said in Chapter 3, we propose employing the gait-analysis MIoT platform utilized in the fall prevention scenario, limited to the duration of rehabilitation.

Therefore, in the Catalan context, the combined expense of surgery and subsequent rehabilitation amounted to 6,721 € per patient in 2015 [107], covering both hospital-based and home-based rehabilitation initiatives. According to public data provided by the Spanish National Statistics Institute (INE) for Catalonia, the Consumer Price Index experienced a 20.0% increase between 2015 and 2023. Based on this report, the Health Department asserts that 50% of the total cost per patient is attributable to hospital expenses, encompassing surgery and initial rehabilitation, while the remaining 50% accounts for a series of rehabilitation sessions conducted at primary care facilities. Considering the inflation rate from 2015 to 2023, the projected cost of post-hospitalization rehabilitation stands at 165 million euros.

Besides, the publication estimates the population afflicted with femur fractures in Catalonia at 38,208 in 2015. Given that the population increased from 7,443,140 to 7,970,433 inhabitants during the same period, it is estimated that by 2023, the number of individuals affected by femur fractures reached 40,915.

The implementation of the MIoT platform is estimated to yield various enhancements with distinct cost implications: Firstly, there will be a reduction in the average duration of rehabilitation sessions, as treatments will be scheduled based on patient progress rather than adhering to fixed timeframes. Secondly, there is an anticipated enhancement in the final outcomes of rehabilitation, specifically in terms of augmenting the degree of independence in instrumental ADL. Lastly, the adoption of the MIoT platform is expected to mitigate transportation expenses for patients, although clinical costs may remain similar due to the need for supervised monitoring sessions and clinician oversight of unsupervised measurements accessible through the cloud.

We consider that the patient will use the same MIoT platform the same platform than in the previous case, section 3.4, but only during the rehabilitation process, with a mean duration of 6 months. The cost per surgery rehabilitation of the MIoT platform considers that the patient holds one device during the whole recovery duration. A part or the duration, unitary costs of the MIoT solution are on the same order than in the previous cases.

Two distinct application models are considered for monitoring rehabilitation progress: The first model entails remote supervision of tests typically conducted at primary care centers, akin to the equilibrium measurement scenario. Conversely, the second model involves patients wearing their insoles during ADLs to continuously capture walking data, with cloud software identifying test scenarios and computing rehabilitation recovery indices accessible to clinicians at any time. The disparity between both models lies in the volume of data storage and computational requirements, with the test-oriented supervised model incurring a cloud cost of 1 euro per month per patient, while the ADL-oriented unsupervised model entails a higher cost of 3 euros per month per patient.

With those models, there will be a large difference between supervised and unsupervised models- The estimation of the costs of the deployment of the MIoT platform for this case is 181 million euros for the test-oriented supervised model and 94 million euros for the ADL-oriented unsupervised one, being this one much lower than the cost of the current rehabilitation model. In the supervised case, an 8.7% decrease on the duration of mean rehabilitation compensates the MIoT system deployment costs. This dependency is illustrated in Figure 43.

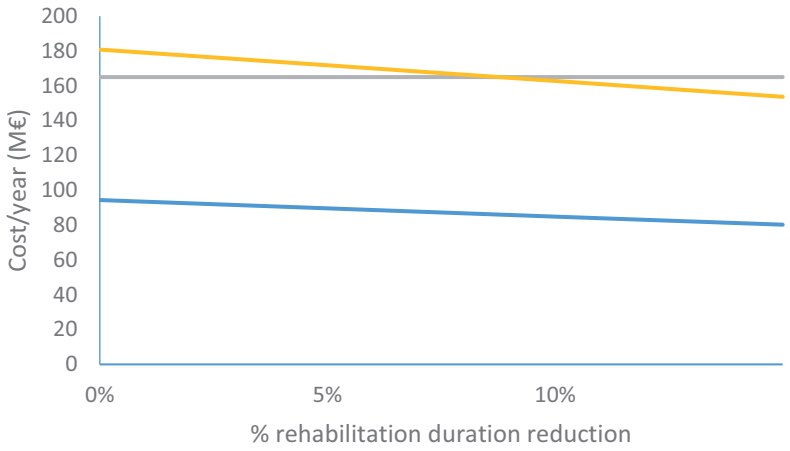

Figure 43: Cost per year of the proposed MIoT solution for the test-oriented supervised model (yellow) and ADL-oriented unsupervised model (blue) according to the reduction of the duration of the rehabilitation compared with the cost estimation with the current.

5.5. Equilibrium Measurement Case

Diving into the details of the conducted study, identified as clinical method, to carry out this analysis, we consider that the health center had to acquire a posturograph, with an approximate cost of 30,000 €. Besides the price, which is unaffordable for an average person, one must also consider the size and complexity of the equipment, not designed for domestic use. Additionally, we account for the time dedicated by the medical staff to conduct the clinical test: one nurse with an hourly cost of around 30 euros [109].

The clinical study presented in section 4.4 will be used as a basis for cost calculations. It turns out that each patient spent approximately 1hour undergoing the test. The cost per patient for the posturograph measurements does not include any app nor cloud costs and data is handled using USB sticks while it required one hour of nurse support. Considering the cost of the posturograph, if we divide it by the number of patients who perform the test and add the cost per hour of a nurse, we obtain a cost per patient of 468 euros.

The MIoT platform, as outlined in section 4.3, serves as the basis for cost estimation. Each device costs 37.5 euros, with the same device utilized for all 70 patients. Consequently, the cost per patient for the MIoT amounts to 254 euros, primarily influenced by the development cost of the application.

At present, our analysis focuses on a group of just 70 individuals at a single primary care facility, where we have already identified significant savings of 55% with the MIoT compared to traditional clinical tests. Expanding our perspective to the entire population aged above 65 in our region, which comprises approximately 1.5 million individuals requiring the test, becomes essential.

Installing posturographs at each primary care center would incur a total cost of approximately 12.5 million euros, along with an annual clinical staff expense estimated at 45.8 million euros. Consequently, the total expenditure would reach 58.5 million euros. On the other hand, deploying the proposed MIoT platform across the entire region to conduct tests for the same number of patients comes with an estimated cost of around 60 million euros. Thus, for the initial year, the implementation costs of both systems are comparable.

The clinical procedure for measuring balance or equilibrium, which significantly reduces the incidence of falls, must remain in use autonomously throughout the patients' lives. When projecting estimates over a span of 5 years, the population above 65 years is expected to increase by 400 thousand people. Over a 10-year period, this increase is projected to reach 1 million individuals, aligning with population aging and increased life expectancy trends.

The cost of conducting one balance test per person annually using posturographs is estimated to amount to 64 million euros in the fifth year and 90 million euros in the tenth year. The cumulative cost over 11 years is projected to reach 668 million euros.

Regarding the MIoT platform, factoring in an additional 20% of devices for repair purposes, the cost breakdown includes the following elements: (i) the purchase cost of 3 million devices at 37.5 euros per unit; (ii) the implementation of the mobile application and cloud system, along with expenses for training and support, totaling 2 million euros; (iii) the cloud storage cost per patient (1€/month); and (iv) a 6% business benefit for the deployment company as part of the public tender. Additionally, we have accounted for a 2% inflationary increase in salary costs during this period.

Figure 44 illustrates a comparison between the cost evolution of the existing health model (utilizing posturographs) and the MIoT solution for equilibrium assessment over the years for the population aged 65 and above. In the initial year, deploying the posturograph system is nearly three times less expensive than implementing the MIoT platform, primarily due to the initial device purchase costs. The breakeven point occurs around the third year.

If we consider cost reductions attributed to economies of scale, particularly impacting electronic devices, we find that if the device cost falls below 11.5 euros per unit, the MIoT platform becomes more cost-effective than the health model using posturographs in the first year. This assumption is reasonable for high-volume device production, aligning with the current costs of activity band manufacturers with a comparable level of complexity to our device. However, such downscaling cannot be applied similarly to posturographs, given their significantly lower numbers.

Additionally, given the presence of 420 posturographs and accounting for 240 operational days per year, with 10 patients attended daily, individuals aged 65 and above can undergo a test at most once every 1.5 years, without factoring in the annual increase in the population

over 65. In contrast, with the MIoT solution, they have the flexibility to undergo testing at any desired frequency.

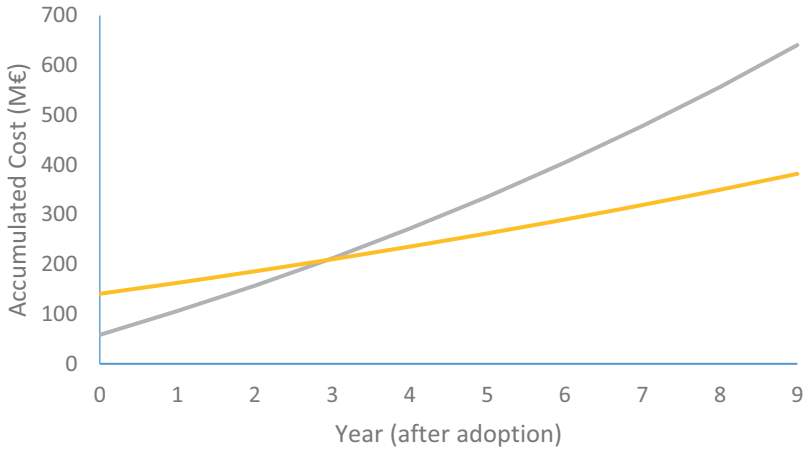

Figure 44: Cost comparison among the evolution of the traditional model using a posturograph (gray line) and the MIoT solution (yellow line) for equilibrium assessment along the years for the 65+ population.

5.6. Summary of the chapter

In this chapter, various aspects related to the implementation and cost analysis of the MIoT platform have been explored in the framework of a technoeconomic analysis.

The chapter begins with an examination of the costs suffered by healthcare services as a result of falls within the inhabitants, with particular emphasis on individuals aged 65 and older. It underscores the comprehensive cost of falls within this demographic stratum, followed by a comprehensive analysis of the expenses linked to post-surgery rehabilitation and studies affecting to balance, delineating their direct correlation with falls.

The economic implications of deploying the MIoT platform requires considering factors such as device costs, cloud infrastructure, and service expenses. We provide detailed cost breakdowns and comparisons between traditional healthcare models and the MIoT solution. Moreover, we discuss the evolution of costs over time, projecting potential savings and efficiencies gained through the adoption of the MIoT platform. We considers scenarios where the MIoT platform can lead to reductions in rehabilitation time and overall healthcare expenses.

As well, we discuss different application models for monitoring rehabilitation progress, supervised and unsupervised during ADLs, emphasizing the flexibility and adaptability of the MIoT platform to diverse healthcare settings and patient needs. We also demonstrate that the deployment cost will reduce with the reduction (absolute or relative) of the costs of device compared with human resources, especially in the unsupervised models. Overall, underscores

the pointed potential of the MIoT platforms in updating healthcare delivery, improving patient outcomes, and optimizing resource utilization in the healthcare system.

6. Conclusions

This research introduces a comprehensive MIoT platform model designed to address critical aspects of long-term healthcare monitoring and management beyond traditional clinical environments in the framework of the digital health paradigm that flourished after the COVID-19 pandemics, where health had to be provided at patient's home.

By integrating a range of inertial sensors in wearable devices, a mobile application, and a cloud-based infrastructure, our platform offers a versatile approach to monitoring patients' daily live activities and providing valuable insights to healthcare professionals on gait related clinical evaluations such as fall prevention, surgery rehabilitation and equilibrium assessment.

The initial component of our platform consists of specialized insole templates embedded with pressure and inertial motion sensors. These sensors enable continuous monitoring of the patient's gait patterns and movements, allowing for early detection of abnormalities and prediction of fall risk. This aspect of the platform is particularly valuable for enhancing patient safety, especially for individuals at risk of falls or those undergoing rehabilitation following hip and femur surgeries. In the technical aspect, has been implemented LoRaWAN to add a long-range communication to send alerts in case of emergency, such as a fall, and extending the battery life. Finally, the cost of the pair of insoles has been reduced to 150€. In terms of software, a new application has been developed to communicate with the insoles, adding video call functionality to enable medical tests while the clinician monitors. Regarding the cloud, the system has been made more secure and can now be installed in hospital environments. During the research, the insoles were to be tested in a clinical study to verify their usefulness in a medical setting and to be able to conduct a more in-depth study of the recovery rate. Because of the emergence of the COVID-19 pandemics, this study was impossible to carry out at the Grenoble University Hospital, as all clinical research activity was stopped.

In addition to gait monitoring, we implemented a MIOT platform solution for assessing balance using an inertial motion sensor integrated into the patient's belt. This feature enables clinicians to conduct balance tests remotely, eliminating the need for patients to visit medical facilities for routine assessments. By facilitating remote testing and monitoring, our platform enhances accessibility to healthcare services and promotes patient-centered care at a much higher frequency (weeks or months) that currently monitored (more than a year).

One of the distinguishing features of our platform is the utilization of artificial intelligence (AI) models for analyzing and interpreting patient data. These AI algorithms enable advanced data processing and pattern recognition, allowing clinicians to derive meaningful insights from the amount of sensor data collected by the platform. By leveraging AI-driven analytics,

healthcare professionals can make informed decisions regarding patient care and treatment strategies, ultimately improving patient outcomes and quality of life.

To test the platform and obtain patient data, we have participated in a clinical study of balance where we have been able to capture data and compare them with a posturography device that has served as a gold standard. Using the data captured by our device, different neural networks have been applied to try to replicate the same assessment results as those offered by the posturograph platform. Due to the limited data available, the results have not been entirely satisfactory, but we believe that by increasing the number of data it will be possible to train a model that offers the same results as the current system while reducing the cost of implementation.

The referred experiences of our MIoT platforms on clinical studies allows us to affirm that joining engineering and clinical research takes much longer than usually planned. In order to provide arguments towards this long-term research model, we did an in-depth technoeconomic analysis of the MIoT platforms implementation and operational costs in the Catalonia region. By comparing these costs with existing healthcare expenditures, we provide a vision into the potential cost-effectiveness and financial viability of integrating our platform into the public health system. The results show that, after few years of deployment, the use of MIoT platforms will compensate the costs of the current clinical model. The downscaling of device costs compared with salaries due to the economies of scale, can further facilitate this adoption. The drawback is related to the usually slow adoption by the public health systems.

From the results obtained from the analysis, it is inferred that with the current cost of our MIoT platform, a 45% fall prevention would be necessary to be profitable. Applying economies of scale, if the manufacturing cost of the insoles could be reduced to 50€, the platform would be profitable with a 23% fall prevention rate. For the case of rehabilitation, applying a supervised model, the system would be profitable if it managed to reduce the duration of rehabilitation by 8.7%, and it would be profitable from the start in a non-supervised model. Finally, for the balance assessment, by the third year, the return on investment is achieved, and the costs are lower than the system currently used to measure balance.

At large, this analysis underscores the importance of investing in innovative digital health solutions to optimize resource utilization and enhance the delivery of healthcare services and include continuous monitoring to provide quick reactions and decisions to the changes on the health and wellbeing state of patients.

6.1. Open Research

In future works, expanding the patient dataset holds importance to enhance the efficacy of artificial intelligence models. By acquiring a more extensive and diverse range of patient data, the models can be trained to capture a wider spectrum of health outcomes and complexities.

Moreover, the acquisition of unbiased result data presents an opportunity to enrich the dataset and mitigate the limitations associated with biased data. With that data at hand, implementing data augmentation techniques becomes feasible, thereby enabling the generation of synthetic data that can further augment the training process.

Additionally, diversifying the dataset can lead to a more comprehensive understanding of patient profiles and health conditions, facilitating the development of more robust and accurate predictive models. This bigger dataset could involve various demographic factors, medical histories, and health parameters, enabling the models to account for a broader range of scenarios and patient characteristics.

Bibliography

[1] M. Arefin, M. M. Rahman, M. Hasan, R. Ahmed, and M. Mahmud, "A Topical Review on Enabling Technologies for Internet of Medical Things: Sensors, Devices, Platforms and Applications," Sep. 2023, doi: 10.20944/PREPRINTS202309.0189.V1.

[2] H. De Man, "Ambient intelligence: gigascale dreams and nanoscale realities," *ISSCC. 2005 IEEE International Digest of Technical Papers. Solid-State Circuits Conference, 2005.*, pp. 29–35, 2005, doi: 10.1109/ISSCC.2005.1493857.

[3] R. Ghosh, T. Majumder, A. Bhattacharjee, and R. Debbarma, "FinFET Advancements and Challenges: A State-of-the-Art Review," *Nanoelectronics Devices: Design, Materials, and Applications (Part I)*, p. 208, 2023.

[4] V. Pachkawade, "NEMS Based Actuation and Sensing," *Authorea Preprints*, Oct. 2023, doi: 10.36227/TECHRXIV.22771271.V1.

[5] S. P. Patro, N. Padhy, and R. D. Sah, "Heart Rate Monitoring Using IoT and AI for Aged Person: A Survey," *The Role of IoT and Blockchain: Techniques and Applications*, pp. 39–59, 2022.

[6] J. Wilden, A. Chandrakar, A. Ashok, and N. Prasad, "IoT based wearable smart insole," *2017 Global Wireless Summit, GWS 2017*, vol. 2018-January, pp. 186–192, Jul. 2017, doi: 10.1109/GWS.2017.8300466.

[7] S. Subramaniam, S. Majumder, A. I. Faisal, and M. Jamal Deen, "Insole-Based Systems for Health Monitoring: Current Solutions and Research Challenges," *Sensors 2022, Vol. 22, Page 438*, vol. 22, no. 2, p. 438, Jan. 2022, doi: 10.3390/S22020438.

[8] M. Hashem, A. A. Al Kheraif, and H. Fouad, "Design and development of wireless wearable bio-tooth sensor for monitoring of tooth fracture and its bio metabolic components," *Comput Commun*, vol. 150, pp. 278–285, Jan. 2020, doi: 10.1016/J.COMCOM.2019.11.004.

[9] B. Gao, Z. He, B. He, and Z. Gu, "Wearable eye health monitoring sensors based on peacock tail-inspired inverse opal carbon," *Sens Actuators B Chem*, vol. 288, pp. 734–741, Jun. 2019, doi: 10.1016/J.SNB.2019.03.029.

[10] F. Zafari, A. Gkelias, and K. K. Leung, "A Survey of Indoor Localization Systems and Technologies," *IEEE Communications Surveys and Tutorials*, vol. 21, no. 3, pp. 2568–2599, 2019, doi: 10.1109/COMST.2019.2911558.

[11] M. Codina *et al.*, “Augmented Reality for Emergency Situations in Buildings with the Support of Indoor Localization,” *Proceedings 2019, Vol. 31, Page 76*, vol. 31, no. 1, p. 76, Nov. 2019, doi: 10.3390/PROCEEDINGS2019031076.

[12] M. P. R. S. Kiran, P. Rajalakshmi, K. Bharadwaj, and A. Acharyya, “Adaptive rule engine based IoT enabled remote health care data acquisition and smart transmission system,” *2014 IEEE World Forum on Internet of Things, WF-IoT 2014*, pp. 253–258, 2014, doi: 10.1109/WF-IOT.2014.6803168.

[13] G. Botilias, A. Papoutsis, P. Karvelis, and C. Stylios, “Track My Health: An IoT Approach for Data Acquisition and Activity Recognition,” *Stud Health Technol Inform*, vol. 273, pp. 266–271, Sep. 2020, doi: 10.3233/SHTI200654.

[14] S. R. Durgekar, S. A. Rahman, S. R. Naik, S. S. Kanchan, and G. Srinivasan, “A Review Paper on Design and Experience of Mobile Applications,” *EAI Endorsed Transactions on Scalable Information Systems*, vol. 11, no. 3, Jan. 2024, doi: 10.4108/EETSIS.4959.

[15] R. Schnall *et al.*, “A user-centered model for designing consumer mobile health (mHealth) applications (apps),” *J Biomed Inform*, vol. 60, pp. 243–251, Apr. 2016, doi: 10.1016/J.JBI.2016.02.002.

[16] G. Molina-Recio, R. Molina-Luque, A. M. Jiménez-García, P. E. Ventura-Puertos, A. Hernández-Reyes, and M. Romero-Saldaña, “Proposal for the user-centered design approach for health apps based on successful experiences: Integrative review,” *JMIR Mhealth Uhealth*, vol. 8, no. 4, p. e14376, Apr. 2020, doi: 10.2196/14376.

[17] T. McCurdie *et al.*, “mHealth consumer apps: the case for user-centered design,” *Biomed Instrum Technol*, vol. Suppl, pp. 49–56, 2012, doi: 10.2345/0899-8205-46.S2.49.

[18] M. Pasha and S. M. W. Shah, “Framework for E-Health Systems in IoT-Based Environments,” *Wirel Commun Mob Comput*, vol. 2018, 2018, doi: 10.1155/2018/6183732.

[19] P. Tsiachri Renta, S. Sotiriadis, and E. G. M. Petrakis, “Healthcare Sensor Data Management on the Cloud,” *ARMS-CC 2017 - Proceedings of the 2017 Workshop on Adaptive Resource Management and Scheduling for Cloud Computing, co-located with PODC 2017*, pp. 25–30, Jul. 2017, doi: 10.1145/3110355.3110359.

[20] A. Bader, H. Ghazzai, A. Kadri, and M. S. Alouini, “Front-end intelligence for large-scale application-oriented internet-of-things,” *IEEE Access*, vol. 4, pp. 3257–3272, 2016, doi: 10.1109/ACCESS.2016.2580623.

[21] WHO, “Step Safely: Strategies for preventing and managing falls across the life-course,” Geneva, 2021. Accessed: Mar. 11, 2024. [Online]. Available: https://www.who.int/about/accountability/governance/constitution

[22] C. A. Meier, M. C. Fitzgerald, and J. M. Smith, “eHealth: Extending, Enhancing, and Evolving Health Care,” *https://doi.org/10.1146/annurev-bioeng-071812-152350*, vol. 15, pp. 359–382, Jul. 2013, doi: 10.1146/ANNUREV-BIOENG-071812-152350.

[23] R. Panadés Zafra, N. Amorós Parramon, M. Albiol-Perarnau, and O. Yuguero Torres, “[Analysis of the challenges and dilemmas that bioethics of the 21st century will face in the digital health era].,” *Aten Primaria*, vol. 56, no. 7, pp. 102901–102901, Mar. 2024, doi: 10.1016/J.APRIM.2024.102901.

[24] C. M. Rutledge, K. Kott, P. A. Schweickert, R. Poston, C. Fowler, and T. S. Haney, “Telehealth and eHealth in nurse practitioner training: current perspectives,” *Adv Med Educ Pract*, vol. 8, pp. 399–409, Jun. 2017, doi: 10.2147/AMEP.S116071.

[25] T. Reed, V. Tuckson, M. Edmunds, and M. L. Hodgkins, “Telehealth,” *https://doi.org/10.1056/NEJMsr1503323*, vol. 377, no. 16, pp. 1585–1592, Oct. 2017, doi: 10.1056/NEJMSR1503323.

[26] I. T. Platform, “Open or closed: A project proposal for investigating two different EHR platform approaches,” *Context Sensitive Health Informatics: Sustainability in Dynamic Ecosystems*, vol. 265, p. 207, 2019.

[27] V. Mishra, K. Gupta, D. Saxena, and A. K. Singh, “A Global Medical Data Security and Privacy Preserving Standards Identification Framework for Electronic Healthcare Consumers,” *IEEE Transactions on Consumer Electronics*, 2024, doi: 10.1109/TCE.2024.3373912.

[28] S. Tyagi, A. Agarwal, and P. Maheshwari, “A conceptual framework for IoT-based healthcare system using cloud computing,” *Proceedings of the 2016 6th International Conference - Cloud System and Big Data Engineering, Confluence 2016*, pp. 503–507, Jul. 2016, doi: 10.1109/CONFLUENCE.2016.7508172.

[29] K. D. Mandl *et al.*, “The SMART Platform: early experience enabling substitutable applications for electronic health records,” *Journal of the American Medical Informatics Association*, vol. 19, no. 4, pp. 597–603, Jul. 2012, doi: 10.1136/AMIAJNL-2011-000622.

[30] “The International Patient Summary – key health data, worldwide.” Accessed: Mar. 12, 2024. [Online]. Available: https://international-patient-summary.net/

[31] A. Ullah, H. Aznaoui, D. Sebai, L. Abualigah, T. Alam, and A. Chakir, “Internet of Things and Cloud Convergence for eHealth Systems: Concepts, Opportunities, and Challenges,” *Wirel Pers Commun*, vol. 133, no. 3, pp. 1397–1447, Dec. 2024, doi: 10.1007/S11277-023-10817-2/METRICS.

[32] S. Ryu, “mHealth: New Horizons for Health through Mobile Technologies: Based on the Findings of the Second Global Survey on eHealth (Global Observatory for eHealth Series, Volume 3),” *Healthc Inform Res*, vol. 18, no. 3, p. 231, 2012, doi: 10.4258/hir.2012.18.3.231.

[33] S. P. Rowland, J. E. Fitzgerald, T. Holme, J. Powell, and A. McGregor, “What is the clinical value of mHealth for patients?,” *npj Digital Medicine 2020 3:1*, vol. 3, no. 1, pp. 1–6, Jan. 2020, doi: 10.1038/s41746-019-0206-x.

[34] H. Oh, C. A. Rizo, M. Enkin, and A. Jadad, “What is eHealth? A systematic review of published definitions,” 2014, Accessed: Feb. 19, 2024. [Online]. Available: https://www.researchgate.net/publication/7858958

[35] R. E. Scott and M. Mars, “Telehealth in the developing world: current status and future prospects,” *Smart Homecare Technol Telehealth*, p. 25, Feb. 2015, doi: 10.2147/SHTT.S75184.

[36] P. Pérez Sust *et al.*, “Turning the Crisis Into an Opportunity: Digital Health Strategies Deployed During the COVID-19 Outbreak.,” *JMIR Public Health Surveill*, vol. 6, no. 2, p. e19106, May 2020, doi: 10.2196/19106.

[37] C. Occhiuzzi, C. Vallese, S. Amendola, S. Manzari, and G. Marrocco, “NIGHT-Care: a passive RFID system for remote monitoring and control of overnight living environment,” *Procedia Comput Sci*, vol. 32, pp. 190–197, 2014, doi: 10.1016/j.procs.2014.05.414.

[38] C. Raj, C. Jain, and W. Arif, “HEMAN: Health monitoring and nous: An IoT based e-health care system for remote telemedicine,” *Proceedings of the 2017 International Conference on Wireless Communications, Signal Processing and Networking, WiSPNET 2017*, vol. 2018-January, pp. 2115–2119, Jul. 2017, doi: 10.1109/WISPNET.2017.8300134.

[39] J. Y. Wu, Y. Wang, C. T. S. Ching, H. M. D. Wang, and L. De Liao, “IoT-based wearable health monitoring device and its validation for potential critical and emergency applications,” *Front Public Health*, vol. 11, p. 1188304, 2023, doi: 10.3389/FPUBH.2023.1188304/FULL.

[40] A. Lakhan *et al.*, “Smart-Contract Aware Ethereum and Client-Fog-Cloud Healthcare System,” *Sensors 2021, Vol. 21, Page 4093*, vol. 21, no. 12, p. 4093, Jun. 2021, doi: 10.3390/S21124093.

[41] A. Sajid and H. Abbas, “Data Privacy in Cloud-assisted Healthcare Systems: State of the Art and Future Challenges,” *J Med Syst*, vol. 40, no. 6, pp. 1–16, Jun. 2016, doi: 10.1007/S10916-016-0509-2/METRICS.

[42] A. Pundziene *et al.*, “Value capture and embeddedness in social-purpose-driven ecosystems. A multiple-case study of European digital healthcare platforms,” *Technovation*, vol. 124, p. 102748, Jun. 2023, doi: 10.1016/J.TECHNOVATION.2023.102748.

[43] G. Bergen, M. R. Stevens, and E. R. Burns, “Falls and Fall Injuries Among Adults Aged ≥65 Years - United States, 2014,” *MMWR Morb Mortal Wkly Rep*, vol. 65, no. 37, pp. 993–998, Sep. 2016, doi: 10.15585/MMWR.MM6537A2.

[44] A. F. Ambrose, G. Paul, and J. M. Hausdorff, “Risk factors for falls among older adults: a review of the literature,” *Maturitas*, vol. 75, no. 1, pp. 51–61, May 2013, doi: 10.1016/J.MATURITAS.2013.02.009.

[45] C. S. Florence, G. Bergen, A. Atherly, E. Burns, J. Stevens, and C. Drake, “Medical Costs of Fatal and Nonfatal Falls in Older Adults,” *J Am Geriatr Soc*, vol. 66, no. 4, pp. 693–698, Apr. 2018, doi: 10.1111/JGS.15304.

[46] J. C. Davis, M. C. Robertson, M. C. Ashe, T. Liu-Ambrose, K. M. Khan, and C. A. Marra, “International comparison of cost of falls in older adults living in the community: a systematic review,” *Osteoporos Int*, vol. 21, no. 8, pp. 1295–1306, Aug. 2010, doi: 10.1007/S00198-009-1162-0.

[47] J. A. Stevens, P. S. Corso, E. A. Finkelstein, and T. R. Miller, “The costs of fatal and non-fatal falls among older adults,” *Inj Prev*, vol. 12, no. 5, pp. 290–295, Oct. 2006, doi: 10.1136/IP.2005.011015.

[48] M. E. Tinetti and C. S. Williams, “Falls, injuries due to falls, and the risk of admission to a nursing home,” *N Engl J Med*, vol. 337, no. 18, pp. 1279–1284, Oct. 1997, doi: 10.1056/NEJM199710303371806.

[49] K. Wang *et al.*, “The Incidence of Falls and Related Factors among Chinese Elderly Community Residents in Six Provinces,” *Int J Environ Res Public Health*, vol. 19, no. 22, Nov. 2022, doi: 10.3390/IJERPH192214843.

[50] K. Peng *et al.*, “Incidence, risk factors and economic burden of fall-related injuries in older Chinese people: a systematic review,” *Inj Prev*, vol. 25, no. 1, pp. 4–12, Feb. 2019, doi: 10.1136/INJURYPREV-2018-042982.

[51] S. Turner, R. Kisser, and W. Rogmans, “Falls among older adults in the EU-28,” Policy briefing 20 (EuroSafe). Accessed: Mar. 05, 2024. [Online]. Available: https://www.eurosafe.eu.com/uploads/inline-files/POLICY BRIEFING 20_Facts on falls in older adults in EU.pdf

[52] K. A. Hartholt *et al.*, “Societal consequences of falls in the older population: injuries, healthcare costs, and long-term reduced quality of life,” *J Trauma*, vol. 71, no. 3, pp. 748–753, Sep. 2011, doi: 10.1097/TA.0B013E3181F6F5E5.

[53] M. Mansoor, R. Amin, Z. Mustafa, S. Sengan, H. Aldabbas, and M. T. Alharbi, “A machine learning approach for non-invasive fall detection using Kinect,” *Multimed Tools Appl*, vol. 81, no. 11, pp. 15491–15519, May 2022, doi: 10.1007/S11042-022-12113-W/METRICS.

[54] X. Kong, X. Kong, Z. Meng, L. Meng, and H. Tomiyama, “Three-States-Transition Method for Fall Detection Algorithm Using Depth Image,” 2096, doi: 10.20965/jrm.2019.p0088.

[55] X. Xi, M. Tang, S. M. Miran, and Z. Luo, “Evaluation of Feature Extraction and Recognition for Activity Monitoring and Fall Detection Based on Wearable sEMG Sensors,” *Sensors 2017, Vol. 17, Page 1229*, vol. 17, no. 6, p. 1229, May 2017, doi: 10.3390/S17061229.

[56] G. Fortino and R. Gravina, “Fall-MobileGuard: A smart real-time fall detection system,” *BodyNets International Conference on Body Area Networks*, 2015, doi: 10.4108/EAI.28-9-2015.2261462.

[57] T. Shi, X. Sun, Z. Xia, L. Chen, and J. Liu, “Fall Detection Algorithm Based on Triaxial Accelerometer and Magnetometer”.

[58] K. H. Chen, Y. W. Hsu, J. J. Yang, and F. S. Jaw, “Evaluating the specifications of built-in accelerometers in smartphones on fall detection performance,” *Instrum Sci Technol*, vol. 46, no. 2, pp. 194–206, Mar. 2018, doi: 10.1080/10739149.2017.1363054.

[59] S. Jacob, G. Fernie, and A. R. Fekr, “A novel wearable biofeedback system to prevent trip-related falls,” *Heliyon*, vol. 10, p. 26291, 2024, doi: 10.1016/j.heliyon.2024.e26291.

[60] Y. Tang, Z. Peng, and C. Li, “An experimental study on the feasibility of fall prevention using a wearable K-band FMCW radar,” *2017 United States National Committee of URSI National Radio Science Meeting, USNC-URSI NRSM 2017*, Mar. 2017, doi: 10.1109/USNC-URSI-NRSM.2017.7878303.

[61] M. Li, G. Xu, B. He, X. Ma, and J. Xie, “Pre-Impact Fall Detection Based on a Modified Zero Moment Point Criterion Using Data from Kinect Sensors,” *IEEE Sens J*, vol. 18, no. 13, pp. 5522–5531, Jul. 2018, doi: 10.1109/JSEN.2018.2833451.

[62] “GAITRite | World Leader in Temporospatial Gait Analysis.” Accessed: Mar. 18, 2024. [Online]. Available: https://www.gaitrite.com/

[63] S. Blades, H. Marriott, S. Hundza, E. C. Honert, T. Stellingwerff, and M. Klimstra, “Evaluation of Different Pressure-Based Foot Contact Event Detection Algorithms across Different Slopes and Speeds,” *Sensors 2023, Vol. 23, Page 2736*, vol. 23, no. 5, p. 2736, Mar. 2023, doi: 10.3390/S23052736.

[64] “Human Gait Analysis | Tekscan.” Accessed: Mar. 18, 2024. [Online]. Available: https://www.tekscan.com/products-solutions/human-gait-analysis

[65] “XSENSOR | Gait & Motion Research.” Accessed: Mar. 18, 2024. [Online]. Available: https://www.xsensor.com/solutions-and-platform/human-performance/gait-motion-insoles

[66] “Physilog - physilog | Digital motion analysis platform.” Accessed: Mar. 18, 2024. [Online]. Available: https://www.gaitup.com/

[67] N. Al Abiad, K. S. van Schooten, V. Renaudin, K. Delbaere, and T. Robert, “Association of Prospective Falls in Older People With Ubiquitous Step-Based Fall Risk Parameters Calculated From Ambulatory Inertial Signals: Secondary Data Analysis,” *JMIR Aging*, vol. 6, no. 1, Jan. 2023, doi: 10.2196/49587.

[68] “SENSE4CARE - ANGEL4 FALL DETECTION · Accent Systems.” Accessed: Mar. 17, 2024. [Online]. Available: https://accent-systems.com/project/sense4care/

[69] R. Harte, B. Broderick, L. Glynn, and G. O. Laighin, “The Wireless Insole for Independent and Safe Elderly Living (WIISEL),” *Research Day 2013 Schedule*, p. 26.

[70] H. Arndt *et al.*, “Real-Time Constant Monitoring of Fall Risk Index by Means of Fully-Wireless Insoles.,” in *pHealth*, 2017, pp. 193–197.

[71] V. Stara *et al.*, “Does culture affect usability? A trans-European usability and user experience assessment of a falls-risk connected health system following a user-centred design methodology carried out in a single European country,” *Maturitas*, vol. 114, pp. 22–26, 2018.

[72] R. Harte *et al.*, “A Human-Centered Design Methodology to Enhance the Usability, Human Factors, and User Experience of Connected Health Systems: A Three-Phase Methodology,” *JMIR Hum Factors*, vol. 4, no. 1, Jan. 2017, doi: 10.2196/HUMANFACTORS.5443.

[73] R. Harte *et al.*, “Human-Centered Design Study: Enhancing the Usability of a Mobile Phone App in an Integrated Falls Risk Detection System for Use by Older Adult Users.,” *JMIR Mhealth Uhealth*, vol. 5, no. 5, p. e71, May 2017, doi: 10.2196/mhealth.7046.

[74] R. Harte *et al.*, “A Multi-Stage Human Factors and Comfort Assessment of Instrumented Insoles Designed for Use in a Connected Health Infrastructure,” *J Pers Med*, vol. 5, no. 4, pp. 487–508, Dec. 2015, doi: 10.3390/JPM5040487.

[75] M. Di Rosa *et al.*, “Concurrent validation of an index to estimate fall risk in community dwelling seniors through a wireless sensor insole system: A pilot study.,” *Gait Posture*, vol. 55, pp. 6–11, Jun. 2017, doi: 10.1016/j.gaitpost.2017.03.037.

[76] G. Talavera *et al.*, “Fully-wireless sensor insole as non-invasive tool for collecting gait data and analyzing fall risk,” *Lecture Notes in Computer Science (including subseries Lecture Notes in Artificial Intelligence and Lecture Notes in Bioinformatics)*, vol. 9456, pp. 15–25, 2015, doi: 10.1007/978-3-319-26508-7_2/COVER.

[77] World Health Organization, “Step Safely - Strategies for preventing and managing falls across the life-course,” *Step Safely*, pp. 4–38, 2021, Accessed: Mar. 11, 2024. [Online]. Available: https://www.who.int/teams/social-determinants-of-health/safety-and-mobility/step-safely

[78] A. Aboutorabi, M. Arazpour, M. Bahramizadeh, S. W. Hutchins, and R. Fadayevatan, “The effect of aging on gait parameters in able-bodied older subjects: a literature review,” *Aging Clin Exp Res*, vol. 28, no. 3, pp. 393–405, Jun. 2016, doi: 10.1007/S40520-015-0420-6/TABLES/3.

[79] J. Magaziner, E. M. Simonsick, T. M. Kashner, J. R. Hebel, and J. E. Kenzora, “Predictors of functional recovery one year following hospital discharge for hip fracture: a prospective study,” *J Gerontol*, vol. 45, no. 3, 1990, doi: 10.1093/GERONJ/45.3.M101.

[80] L. Hutchings, R. Fox, and T. Chesser, “Proximal femoral fractures in the elderly: how are we measuring outcome?,” *Injury*, vol. 42, no. 11, pp. 1205–1213, Nov. 2011, doi: 10.1016/J.INJURY.2010.12.016.

[81] M. E. Tinetti, “Performance-Oriented Assessment of Mobility Problems in Elderly Patients,” *J Am Geriatr Soc*, vol. 34, no. 2, pp. 119–126, 1986, doi: 10.1111/J.1532-5415.1986.TB05480.X.

[82] J. M. Guralnik *et al.*, “A Short Physical Performance Battery Assessing Lower Extremity Function: Association With Self-Reported Disability and Prediction of Mortality and Nursing Home Admission,” *J Gerontol*, vol. 49, no. 2, pp. M85–M94, Mar. 1994, doi: 10.1093/GERONJ/49.2.M85.

[83] R. H. Dolin *et al.*, “The HL7 clinical document architecture,” *Journal of the American Medical Informatics Association*, vol. 8, no. 6, pp. 552–569, Nov. 2001, doi: 10.1136/JAMIA.2001.0080552/2/M_JAMIA0080552.APP2F.JPEG.

[84] D. Kalra, T. Beale, and S. Heard, “The openEHR foundation,” *Stud Health Technol Inform*, vol. 115, pp. 153–173, 2005.

[85] “Smart Sensor BNO055 | Bosch Sensortec.” Accessed: Mar. 11, 2024. [Online]. Available: https://www.bosch-sensortec.com/products/smart-sensor-systems/bno055/

[86] “TTN Coverage.” Accessed: Mar. 11, 2024. [Online]. Available: https://ttnmapper.org/heatmap/

[87] “STM32WB - Bluetooth, Wireless Microcontrollers (MCU) - STMicroelectronics.” Accessed: Mar. 11, 2024. [Online]. Available: https://www.st.com/en/microcontrollers-microprocessors/stm32wb-series.html

[88] “Dual-Band Antenna for DSRC, V2V, WiFi, and BLE | Flexible PCB Antenna | FXP831.” Accessed: Mar. 12, 2024. [Online]. Available: https://www.taoglas.com/product/freedom-fxp831-2-44-9-6-0ghz-flex-pcb-antenna-ipex-mhfi/

[89] “Antennas Part - 2067640050 | Molex.” Accessed: Mar. 12, 2024. [Online]. Available: https://www.molex.com/en-us/products/part-detail/2067640050

[90] “3.7 V 180mAh Ultra Thin Battery 014461 | Ufine Battery.” Accessed: Mar. 12, 2024. [Online]. Available: https://www.ufinebattery.com/products/3-7-v-180mah-ultra-thin-battery-014461/

[91] “History of the Qi Specifications | Wireless Power Consortium.” Accessed: Mar. 12, 2024. [Online]. Available: https://www.wirelesspowerconsortium.com/knowledge-base/specifications/history-of-the-qi-specifications/

[92] “Qi Receiver click - a wireless power receiver | MikroElektronika.” Accessed: Mar. 12, 2024. [Online]. Available: https://www.mikroe.com/qi-receiver-click

[93] “Máquina láser de corte PC1390 – PEREZCAMPS.” Accessed: Mar. 12, 2024. [Online]. Available: https://laser.perezcamps.com/index.php/portfolio/maquina-laser-de-corte-pc1390/

[94] D. R. Noll, “Management of Falls and Balance Disorders in the Elderly,” *Journal of Osteopathic Medicine*, vol. 113, no. 1, pp. 17–22, Jan. 2013, doi: 10.7556/JAOA.2013.113.1.17.

[95] L. Z. Rubenstein and K. R. Josephson, “The epidemiology of falls and syncope,” *Clin Geriatr Med*, vol. 18, no. 2, pp. 141–158, 2002, doi: 10.1016/S0749-0690(02)00002-2.

[96] F. B. Horak, D. M. Wrisley, and J. Frank, “The Balance Evaluation Systems Test (BESTest) to differentiate balance deficits,” *Phys Ther*, vol. 89, no. 5, p. 484—498, May 2009, doi: 10.2522/ptj.20080071.

[97] N. Miranda-Cantellops and T. K. Tiu, “Berg balance testing,” 2021.

[98] A. Khasnis, R. M. Gokula, and others, “Romberg’s test.,” *J Postgrad Med*, vol. 49, no. 2, p. 169, 2003.

[99] Dinascan P600 Posturograph, “P600.” Accessed: Mar. 17, 2024. [Online]. Available: https://analisisbiomecanico.ibv.org/productos/tecnicas-de-registro/dinascan-ibv/p600.html

[100] S. Y. W. Chai, F. J. F. Phang, L. S. Yeo, L. H. Ngu, and B. S. How, “Future era of techno-economic analysis: Insights from review,” *Frontiers in Sustainability*, vol. 3, p. 924047, Aug. 2022, doi: 10.3389/FRSUS.2022.924047/BIBTEX.

[101] Z. Barahmand and M. S. Eikeland, “Techno-Economic and Life Cycle Cost Analysis through the Lens of Uncertainty: A Scoping Review,” *Sustainability 2022, Vol. 14, Page 12191*, vol. 14, no. 19, p. 12191, Sep. 2022, doi: 10.3390/SU141912191.

[102] “Statistical Institute of Catalonia. Short-term economic indicators.” Accessed: Mar. 07, 2024. [Online]. Available: https://www.idescat.cat/indicadors/?id=conj&lang=en

[103] A. Rodríguez-Molinero *et al.*, "Caídas en la población anciana española: Incidencia, consecuencias y factores de riesgo," *Rev Esp Geriatr Gerontol*, vol. 50, no. 6, pp. 274–280, 2015, doi: 10.1016/J.REGG.2015.05.005.

[104] M. Aranda-Gallardo, J. M. Morales-Asencio, J. C. Canca-Sanchez, and J. C. Toribio-Montero, "Circumstances and causes of falls by patients at a Spanish acute care hospital," *J Eval Clin Pract*, vol. 20, no. 5, pp. 631–637, 2014, doi: 10.1111/JEP.12187.

[105] M. K. Appeadu and B. Bordoni, "Falls and Fall Prevention in Older Adults," *Geriatric Emergency Medicine: Principles and Practice*, pp. 343–350, Jun. 2023, doi: 10.1017/CBO9781139250986.033.

[106] R. Busutil, D. O'Boyle, X. Puig, C. Perez Vives, O. Planas, and H. Cheng, "PIT9 IMPACT OF FALLS IN THE ELDERLY POPULATION FOR THE SPANISH NATIONAL HEALTH SYSTEM," *Value in Health*, vol. 22, pp. S666–S667, Nov. 2019, doi: 10.1016/j.jval.2019.09.1405.

[107] J. Cancio Trujillo, M. Clèries, M. Inzitari, D. Ruiz Hidalgo, S. Santaeugènia Gonzàlez, and E. Vela, "Impacte en la supervivència i despesa associada a la fractura de fèmur en les persones grans a Catalunya," Barcelona, 2015. Accessed: Mar. 06, 2024. [Online]. Available: https://scientiasalut.gencat.cat/bitstream/handle/11351/3577/supervivencia_fractura_femur_2015.pdf

[108] J. R. Center, D. Bliuc, T. V. Nguyen, and J. A. Eisman, "Risk of subsequent fracture after low-trauma fracture in men and women," *JAMA*, vol. 297, no. 4, pp. 387–394, Jan. 2007, doi: 10.1001/JAMA.297.4.387.

[109] "Catalan Health Institute (ICS). Payment book 2023. ICS statutory staff." Accessed: Mar. 07, 2024. [Online]. Available: https://ics.gencat.cat/web/.content/Documents/transparencia/personal/Llibre-de-retribucions-gener-2023.pdf

Annexes

Annex A

- **Cadence**: is the number of steps a person takes in 1 minute.
- **Gait Symmetry:** Is distinguished by the nearly identical movement patterns exhibited by both limbs on each side during a gait cycle.
- **Step length:** distance covered from the heel strike of one foot to the heel strike of the opposite foot during a single gait cycle.
- **Gait cycle:** sequence of events that occur from the initial contact of one foot with the ground through to when the same foot contacts the ground again.
- **Pressure mapping (Heel, Toe, Sum):** measure the distribution of pressure and forces exerted by the foot during standing, walking, or running.
- **Stride time:** time interval between two consecutive heel strikes of the same foot during walking or running.
- **Gait Speed:** velocity at which a person walks or runs over a specified distance.
- **Double support:** phase of the gait cycle during walking where both feet are in contact with the ground simultaneously.
- **Single Support:** phase of the gait cycle during walking or running where only one foot is in contact with the ground while the other foot is in swing phase.
- **Acceleration Amplitude:** magnitude or strength of acceleration experienced by an object or a system.
- **Heel Strike Force Slope**: rate of change of the force applied at the heel during the initial contact phase of the gait cycle.
- **Number of steps:** count of individual steps taken by a person during a specific period or activity, typically measured within a given timeframe, such as per minute, per hour, or over a certain distance.
- **Activity time:** duration or period during which an individual engages in physical activity or performs a specific task or exercise.
- **Distance:** measurement of the amount of space between two points or locations.
- **Average acceleration amplitude:** mean or average magnitude of acceleration experienced by an object or system over a specified period of time.
- **Lateral shift:** movement or displacement occurring in a sideways direction, typically perpendicular to the primary axis or orientation of an object or system.
- **Frontal shift:** movement or displacement that occurs in the frontal plane, which is typically perpendicular to the sagittal plane and divides the body into front and back portions.
- **Maximum movement angle:** greatest angular deviation or rotation achieved by a joint or body segment during a specific movement or activity.
- **Swept area:** total area covered or swept by a moving object or system over a specified period.

- **Total displacement:** overall distance and direction traveled by an object or system from its initial position to its final position.
- **Maximum lateral force:** greatest amount of sideways or lateral force exerted on an object or system during a specific activity or event.
- **Maximum frontal force:** highest magnitude of force exerted in the forward direction during a specific activity or event.
- **Average velocity:** overall displacement of an object or system divided by the total time taken to cover that distance.

Annex B

In Annex A we introduce more screens of the cloud solution. Rights/roles administration application (RAA) manage user roles, their access rights and user interfaces. Figure 45 shows the section, where roles can be edited.

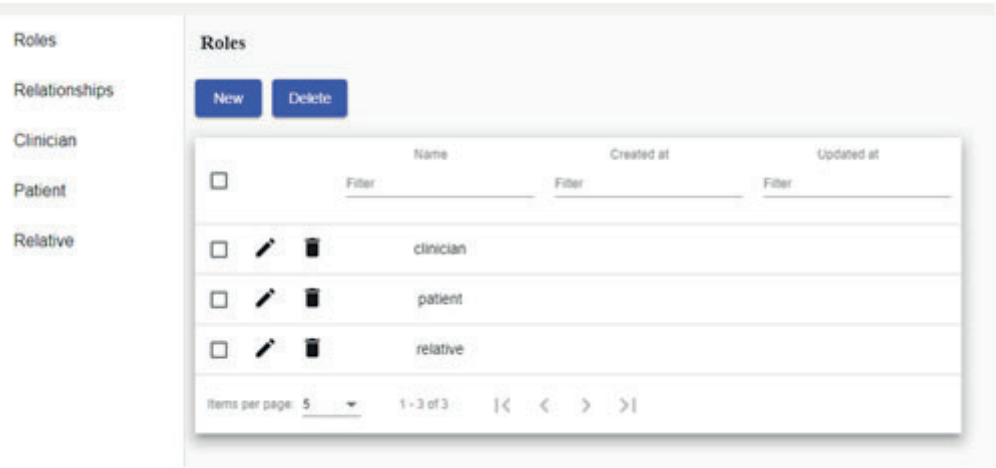

Figure 45: Role creation.

The clinician section starts with the visualization of a list of all the patients associated to the clinician. When the clinician logs into the system with his credentials, he gets the screen shown in the snapshot in Figure 46. Clinician can visualize a list of all his patients. Here, the clinician can create a new patient entry or delete an existing one; he can edit patient related information, can access reports, can access the gait analysis editor, and can set the notification status. An email address and or a phone number can be set. In case of a fall of the patient, an alarm email/SMS is sent to the recipients.

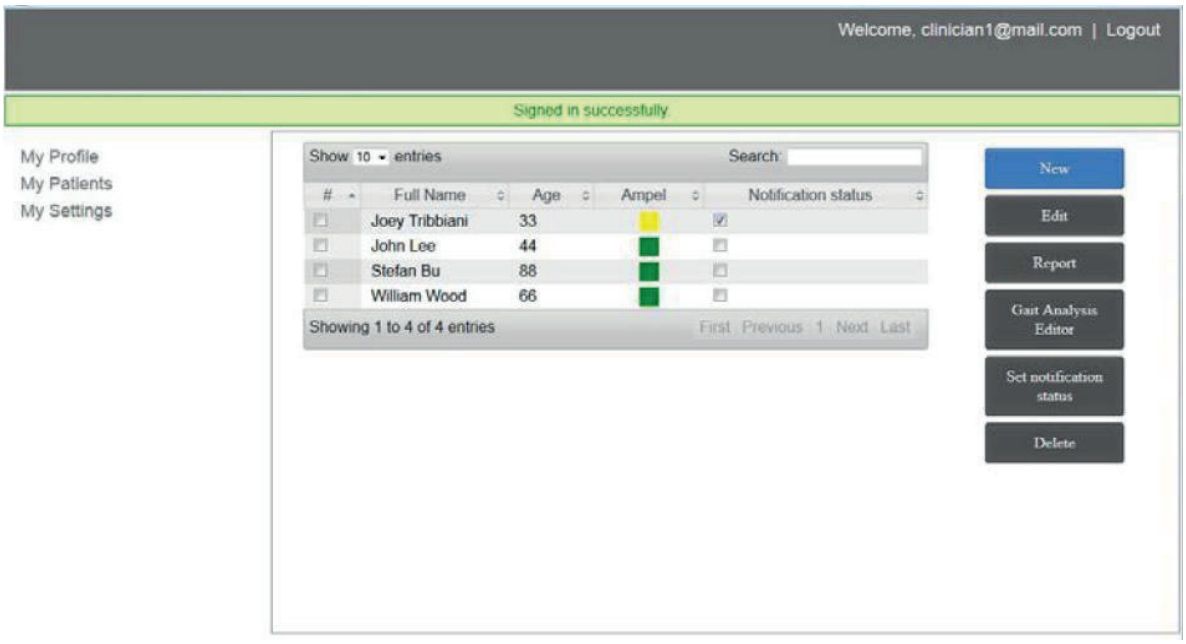

Figure 46: Web app: Patient list from clinician view.

The entry point of the patient section of the web application is the patient information page shown in Figure 47. The page visualizes the personal information of the patient and provides a navigation menu from which the patient can access several functionalities, such as profile, reports, clinicians' information, technicians' information, and relative's information.

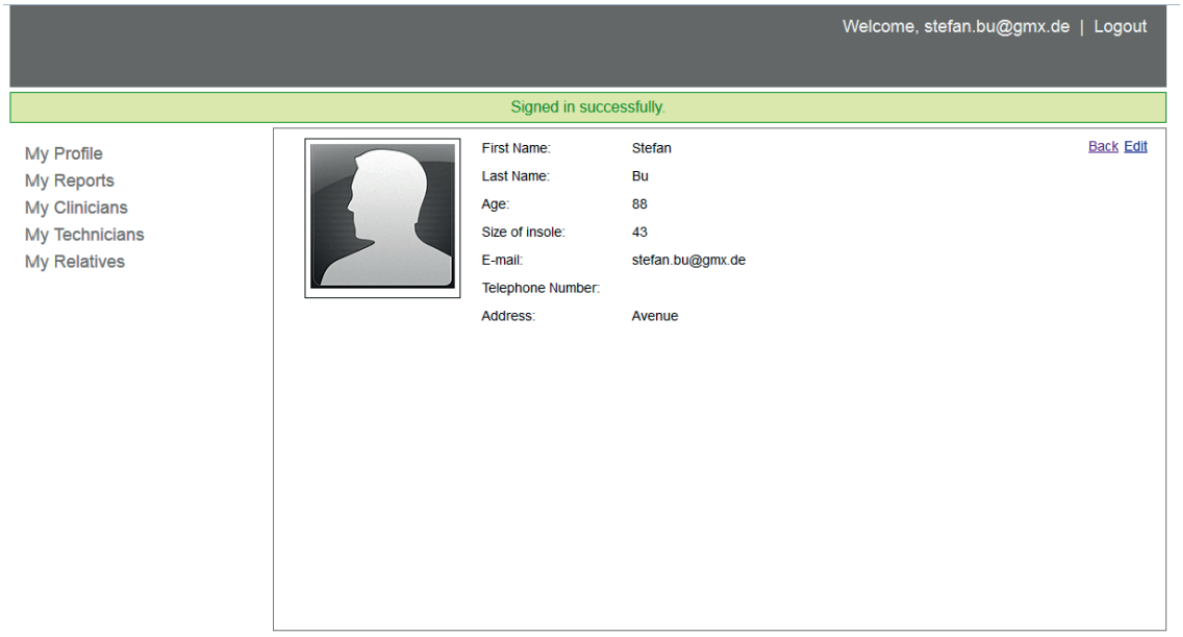

Figure 47: Patient information.